Design and Characterization of UHF-RFID Tag Antennas for Sensor & IoT Applications

Abstract: The objective of this thesis is to develop new configurations of RFID-UHF tag antennas for traceability applications, as well as the realization of a characterization bench and performance measurements at low cost. The performance of the proposed RFID-UHF tag antennas was evaluated by electromagnetic simulation using the commercial software 'CST Microwave Studio' and by measurements. In this thesis, we also focused our attention on extending the field of application of this technology to the field of sensors. The main idea of this study is based on the fact, that the RFID tag antenna (which plays here the role of a sensor) is sensitive to its environment, which modifies the properties of the antenna, and thus the matching. The measurement of the variation in the concentration of the solutions (Sugar, NaCl, and Alcohol) was carried out in this part by measuring the activation power of the tag. This measurement system, we propose in this thesis, has several advantages such as low cost, non-invasive, rapid, and the possibility of sending measurements over a long distance using a repetitive cycle of measurements.

In this thesis, we propose three contributions. The first one consists of the UHF RFID antennas characterization bench we propose to measure the performances of this antenna with an automated low cost measurement platform. In the second contribution, we propose a new configuration of RFID-UHF tag antennas for a range of industrial traceability applications. The performances of the proposed RFID-UHF tag antennas were evaluated by electromagnetic simulation using 'CST Microwave Studio' commercial software and by measurements. Finally, in the third contribution, we focused our attention on extending the field of application of this technology to the field of RFID-UHF food product sensors. The main idea of this study is because the RFID tag antenna (which plays here the role of a sensor) is sensitive to its environment, which modifies its properties. The measurement of the variation in the concentration of the solutions (Sugar, NaCl, and Alcohol) was carried out in this section by measuring the activation power of the tag.

The measurement system proposed in this thesis has several advantages. For instance, this is a low cost, noninvasive and rapid measurement system, which has the possibility of sending measurements over a long distance using a repetitive cycle of measurements.

Keywords: RFID-UHF, TAG Sensors, Antennas, Flexible Antenna, IC-Chip, Matching, Platform, Characterization, IoT

Mohammed Ali ENNASAR

Design and Characterization of UHF-RFID Tag Antennas for Sensor & IoT Applications

Année : 2020 N° thèse : 190/ST2I

Année : 2020 **Thèse N° : 190/ST2I**

École Nationale Supérieure d'Informatique et d'Analyse des Systèmes
Centre d'Études Doctorales en Sciences des Technologies de l'Information et de l'Ingénieur

THÈSE DE DOCTORAT

DESIGN AND CHARACTERIZATION OF UHF-RFID TAG ANTENNAS FOR SENSOR & IoT APPLICATIONS

Présentée par

Mohammed Ali ENNASAR

Le 16/12/2020

Formation doctorale : Sciences de l'Ingénieur-Génie électrique
Structure de recherche : Smart Systems Laboratory (SSL)

JURY

Professeur Hassan BERBIA PES, ENSIAS, Université Mohammed V de Rabat	**Président**
Professeur Mohamed ESSAAIDI PES, ENSIAS, Université Mohammed V de Rabat	**Directeur de thèse**
Professeur Ahmed OULAD SAID PES, Ecole Royale de l'Air, Marrakech	**Rapporteur**
Professeur Jamal EL AOUFI PH, AIAC, Casablanca	**Rapporteur**
Professeur Faissal EL BOUANANI PH, ENSIAS, Université Mohammed V de Rabat	**Rapporteur**
Professeur Ahmed HABBANI PES, ENSIAS, Université Mohammed V de Rabat	**Examinateur**
Professeur Otman EL MRABET PH, FS, Université Abdelmalek Essaadi, Tétouan	**Examinateur**

DEDICATION

To my uncle, aunt, my parents, sisters, and brothers for their unconditional love and endless support.

ACKNOWLEDGEMENTS

Most of all, I am grateful to God, the Almighty, for His blessings and strength to endure the rough journey of my Ph.D. thesis.This doctoral work could not be done without the support, assistance, and consultation of a large number of people. First of all, I would like to thank my thesis director Dr. Mohamed ESSAAIDI, for agreeing to supervise this doctoral work, for his trust and believe on competences to achieve expected goals of this thesis, for his many informative and outstanding instructions and for all the hours, he dedicated to supervising this work. He may find here my deep gratitude and appreciation for his remarkable personal and professional qualities.

I am very grateful to my co-advisor, Dr. Otman EL MRABET who guided me throughout my research and discussed my results in order to expand the scope of my thesis. This cannot overlook his helpful suggestions, encouragement, moral support and his endless guidance. I was lucky to have him on board this thesis and looking forward to developing a new research project with him in the near future. I would like also to thank Dr. Abdellatif El AFIA for his personal qualities and for his unconditional and effective support during my Ph.D. preparation. He may find here my gratitude and compassion for his support.

Likewise, I would like to thank the Director of Information and Telecommunication System Laboratory (LaSiT) of Tetuan, Dr. Mohcine KHALLADI, for his full cooperation and support, and for allowing me to use the measurement devices, and for providing the warm welcoming conditions for me to prepare my Ph.D. Thanks also go to all members of (LaSiT). I had the opportunity and honor to work with Dr. Ikram AZNABET, Mohamed KANJAA, Mohamed EL KHAMLICHI, Mohammed Larbi MOUTIS, Mohamed EL BAKKALI, and Reda MAOUHOUB; they may find here my particular gratitude for their friendship and high professionalism.

Thank also goes to all my family, who have supported and assisted me throughout my Ph.D., I am warmly grateful for all their time, exchanges and advices.

ABSTRACT

The objective of this thesis is to develop new configurations of RFID-UHF tag antennas for traceability applications, as well as the realization of a characterization bench and performance measurements at low cost. The performance of the proposed RFID-UHF tag antennas evaluated by electromagnetic simulation using the commercial software 'CST Microwave Studio' and by measurements. In this thesis, we also focused our attention on extending the field of application of this technology to the field of sensors. The main idea of this study based on the fact, that the RFID tag antenna (which plays here the role of a sensor) is sensitive to its environment, which modifies the properties of the antenna, and thus the matching. The measurement of the variation in the concentration of the solutions (Sugar, NaCl, and Alcohol) carried out in this part by measuring the activation power of the tag. This measurement system, we propose in this thesis, has several advantages such as low cost, non-invasive, rapid, and the possibility of sending measurements over a long distance using a repetitive cycle of measurements.

In this thesis, we propose three contributions. The first one consists of the UHF RFID antennas characterization bench we propose to measure the performances of this antenna whi an automated low cost measurement platform. In the second contribution, we propose a new configuration of RFID-UHF tag antennas for a range of industrial traceability applications. The performances of the proposed RFID-UHF tag antennas evaluated by electromagnetic simulation using 'CST Microwave Studio' commercial software and by measurements. Finally, in the third contribution, we focused our attention on extending the field of application of this technology to the field of RFID-UHF food product sensors. The main idea of this study is because the RFID tag antenna (which plays here the role of a sensor) is sensitive to its environment, which modifies its properties. The measurement of the variation in the concentration of the solutions (Sugar, NaCl, and Alcohol) carried out in this section by measuring the activation power of the tag.

The measurement system proposed in this thesis has several advantages. For instance, this is a low cost, noninvasive and rapid measurement system, which has the possibility of sending measurements over a long distance using a repetitive cycle of measurements.

Keywords: **RFID-UHF, TAG Sensors, Antennas, Flexible Antenna, IC-Chip, Matching, Platform, Characterization,IoT**

RESUME

L'objectif de cette thèse est de développer de nouvelles configurations d'antennes de tag RFID-UHF pour les applications de traçabilité, ainsi que la réalisation d'un banc de caractérisation et des mesures de performances à faible coût. Les performances des antennes de tag RFID-UHF proposées ont été évaluées par simulation électromagnétique à l'aide du logiciel commercial 'CST Microwave Studio' et par des mesures. Dans cette thèse, nous avons également focalisé notre attention à étendre le champ d'application de cette technologie vers le domaine des capteurs. L'idée principale de cette étude repose sur le fait que l'antenne de tag RFID (qui joue ici le rôle d'un capteur) est sensible à son environnement qui modifie les propriétés de l'antenne comme l'adaptation. La mesure de la variation de la concentration des solutions (Sucre, NaCl , et Alcool) a été réalisée dans cette partie en mesurant la puissance d'activation de tag. Le système proposé dans cette thèse présente plusieurs avantages tels que le faible coût, la non-invasité, la rapidité, et la possibilité d'envoyer des mesures à grande distance à l'aide d'un cycle répétitif de mesures.

Dans le cadre de cette thèse, nous avons développé trois contributions. La première contribution porte sur la conception et la réalisation d'un banc de caractérisation des performances d'antennes RFID Tag UHF, et la création d'une plate-forme automatisée pour mesurer ces performances à faible coût. Dans la deuxième contribution nous avons proposé une nouvelle configuration d'antennes de tag RFID-UHF pour une gamme d'applications dans le domaine de traçabilité industrielle. Les performances des antennes de tag RFID-UHF proposées ont été évaluées par simulation électromagnétique à l'aide du logiciel commercial 'CST Microwave Studio' et aussi par des mesures expérmentales. Finalement, dans la troisième contribution, nous avons focalisé notre attention sur l'extention du champ d'application de cette technologie vers le domaine des capteurs RFID-UHF pour la caractérisation des produits alimentaires. L'idée principale de cette étude repose sur le fait que l'antenne de tag RFID (qui joue ici le rôle d'un capteur) est

sensible à son environnement qui modifie les propriétés de l'antenne. La mesure de la variation de la concentration des solutions (Sucre, sel (NaCl) et Alcool) a été obtenue dans cette partie à partir de la puissance d'activation de tag. Le système proposé dans cette thèse présente plusieurs avantages, par exemple, il est à faible coût, non invasif, rapide, et il permet d'envoyer des mesures à grande distance à l'aide d'un cycle répétitif de mesures.

Mots clés : **RFID-UHF, TAG Capteurs, Antennes, antenne flexible, adaptation. Platform, caractérisation,IoT**

Contents

Chapter 3. Development of Automatic Platform Measurement for RFID Tag Characterization

Chapter 4. Design and Characterization of a Compact Single Layer Modified S-Shaped Tag Antenna for UHF-RFID Applications

Chapter 5. Design and Characterization of a Broadband Flexible Polyimide RFID Tag Sensor for Detection of Liquid Concentration

NOMENCLATURE

IoT	Internet of Things
OCR	Optical Character Recognition
OOK	On-Off Keying
IC	Integrated circuit
FCC	Federal Communications Commission
EPC	Electronic Product Code
DUT	Device under Test
dBm	dB Watt
dBi	Gain Expressed in dB with Respect to an Isotropic Radiator
dB	Decibel
$2D$	Two-Dimensional
$1D$	One- Dimensional
ISO	International Organization for Standardization
PEC	Perfect Electric Conductor
BP	Bandwidth
S_{11}	Reflection Coefficient
ε_r	Relative Dielectric Constant
$\mathbf{S}$	Poynting Vector
λ	Wavelength in Free Space
Z_A	Input Impedance of the Tag Antenna
PNA	Programmable Network Analyzer
P_{ERP}	Effective Radiated Power
P_{EIRP}	Standardized Radiation Power Compared to An Isotropic Antenna
LF	Low Frequency
HF	High Frequencies
h	Dielectric Thickness
FDX	Full-Duplex
$Gtag$	Gain of the Tag Antenna
f	Frequency
EU	European
CP	Near Field
CL	Far Field
ASK	Amplitude-Shift Keying
VNA	Vector Network Analyzer
UHF	Ultra-High Frequency
SER/	Surface Equivalent Radar Differential
SER	Surface Equivalent Radar
RFID	Radio Frequency Identification
RADAR	Radio Detection And Ranging
IFF	Identification Friend Or Foe
EIRP	Equivalent Isotropic Radiated Power
ERP	Equivalent Radiated Power
ETSI	European Telecommunications Standards Institute

List of Figures

List of Tables

General Introduction

Introduction and Motivation

Radio Frequency Identification (RFID) is a rapidly developing technology that uses electromagnetic waves to automatically identify or track people and objects. This technology is effectively used in several sectors such as inventory control and management, logistics operations, bioengineering operations, and manufacturing. Worldwide, the RFID system operates in four slots of frequencies: low frequency (LF, 125 KHz), high frequency (HF, 13.56 MHz), ultra-high frequency bands (UHF, 860-960 MHz) and microwave (MW, 2.45 GHZ, and 5.8 GHz). Recently, UHF identification technology has gained a lot of attention due to its longer range and higher data transfer rate, compared to LF and HF.

The development and widespread use of RFID technology allow the emerging of sensors tags (antenna) due to its passivity, and cost-effectiveness. Therefore, numerous antenna-based RFID analyzes have been reviewed in many literature. However, until now, this technology is only limited to tracking information and identifying objects in different supply chains.

On the other side, today cities are rapidly expanding with an increasing population. According to the United Nations, 55% of the world's population lives in urban areas in 2020, and this number likely to increase by 2050 to reach 68% .This prediction represents real economic challenges and can deteriorate the quality of the world's population livelihood. Therefore, cities must start applying some transformations to their development models to enhance or at least maintain a decent life quality. The concept of a smart city, which based on IoT, is one of the proposed solutions to overcome the upcoming challenges.

To this end, monitoring and tracking all activities in smart cities become primordial to serving and optimizing everyday services such as solid waste management, traffic, healthcare, and food quality production and distribution.

This later service (food quality production and distribution) is vital for human health and for the foods industry as well. In this thesis, RFID technology was used to detect the changing concentration of sucrose and NaCl in aqueous solutions that can be found in many consumer products (foods and beverages industry).

Thesis Contributions

The research work developed in this thesis aims mainly (i) to build a low cost automated platform that allows the experimental characterization and performance estimation of RFID-UHF tag; (ii) to gain a comprehensive background on RFID tag antennas for UHF band, by proposing a new configuration of RFID-UHF tag antennas suitable for a range of industrial tracking applications; and (iii) to extend the implementation of RFID tag antennas in particular to food products sensing, by detecting small changes in the characteristics of the space surrounding the RFID tag antenna.In our case, the measurement of the concentration of two aqueous solutions (Sugar, NaCl and Alcohol) was carried out.

The system proposed in this thesis allows the possibility to send measurements over a long distance using a repetitive cycle of measurements, in addition to its several advantages including low cost, non-invasive, and rapidity.

Dissertation outline

This thesis dissertation is articulated into five consolidated chapters that cover automatic identification techniques; RFID technology; description of the experimental platform; a single-layer modified S-shaped tag antenna; and challenges to measuring the concentration of biomolecules in liquid solutions using UHF-RFID technology.

Thus, the first chapter presents a review of automatic identification techniques such as code bar and quick response code. We have also given a brief history of RFID technology, applications, standards, and regulations.

The second chapter provides a detailed definition of RFID technology, with a focus on passive UHF architecture. A survey was conducted to classify existing RFID systems into classes (passive, semi-passive and active), bands (LF, HF, UHF,). In this chapter, different coupling mechanisms (communication links) were discussed.

The third chapter describes a new platform for experimentally characterize the performance of the RFID–UHF tags. This platform is based on the Thing Magic Micro (M6e-M) reader connected to a single circularly polarized patch antenna having a gain of 6 dBi at the frequency range of 800–1000 MHz. The RFID reader is aconnected to the polarized patch antenna via 1.8 m of 50 coaxial cable model CNT-195-FR to generate 36 dBm at 915 MHz. The whole system is controlled by a homemade software (installed in a computer) to plot the measured results such as activation power, radiation pattern, read a pattern, and read range. The developed system is completely different from the commercial systems (Voyantic Tag Performance Lite), both in terms of cost and simplicity/complexity.

The fourth chapter proposes a new compact single-layer modified S-shaped tag antenna for UHF-RFID applications. To achieve a compact size of 51×34 mm2 for this tag antenna, the technique of using an S-shaped strip was applied adding a pair of equilateral triangular stubs into this structure. A good impedance matching can be obtained at 915 MHz, which is the average frequency of the North-American UHFRFID band (902 to 928 MHz). The performance of this RFID S-shaped tag antenna was tested on different materials. The obtained simulated results were compared to experimental measurements.

The fifth chapter addresses the challenge of measuring the concentration of biomolecules (in our case sucrose, NaCl and Alcohol) in liquid solutions using UHFRFID technology. To this end, an RFID S-shaped tag antenna with sensing

ability printed on a flexible substrate operating at the UHF band (860–960 MHz) was designed and fabricated. The sensing mechanism is based on the change in the characteristics of the medium (or liquid) surrounding the RFID tag. Results are presented for tested biomolecules (sucrose and NaCl) in aqueous solutions with concentrations ranging from 0% to 80%. This system has among other advantages, the possibility to send on time measurements over a long distance.

Finally, this thesis is wrapped up with a consolidated conclusion highlighting the main contributions and perspectives for further researche.

Chapter 1

Automatic Identification and Application

1.1 Introduction

In this chapter, we will discuss the concept of automatic identification, which operates radio frequency identification (RFID) technologies. We will look at some important examples of RFID technologies that will enable us to understand the work of RFID systems. RFID systems have already many ranges of applications in our life, as they are expected in the near future. To be everywhere. Moreover, well integrated into the very day such integration is achieved by new protocol and infrastructures including readers and RFID Tags. In this chapter, we will present the technological evolution of the RFID Technologies for simple tracking and identification application to more innovative sensing technology involving the RFID as support very flexible.

1.2 Automatic Identification Systems

1.2.1 Barcode Systems

The Barcodes is the first successful commercial application in automated supermarket checkout systems in 1974 and since then have become widespread, simple, and cost-effective, but have limited identification capabilities [1]. Is represents the graphic coding of the information. It is a standard visual identification system for a product. It allows instant and automated data capture for significant increases in productivity and consumption.

It stamped in the distribution chain at the product, package and pallet level, but also in countless systems of flow traceability and inventory management. It consists of a group of bars and juxtaposed spaces, whose color and size are variable (Figure 1).

Figure 1: Barcode

The combination of the barcode obtained provides information on the origin, reference, type and producer of the product. It allows a linear optical reading by laser beam, to make the identification automatic, allowing, for example, the consideration of the price of the article as well as easier computer management of stocks[1] [2] . The Americans Joseph Woodland and Bernard Silver filed the first barcode patent, on October 7, 1952. The first commercial use dates back to 1966, but the American engineer, George Laurer, conceived the first UPC code with 10 digits in 1973 [3] . This system is unobtrusive, reliable and economical. It is able to capture accurate data and move goods quickly in all types of automation.

Whether at the point of sale, at the hospital or in a manufacturing environment, there are many barcode symbol [4]. Each symbol has its own rules for encoding / decoding and printing characters (letter, number, and punctuation), as shown in (Figure 2).

Figure 2: Example of Barcode

Linear or one-dimension (1D): All code information organized horizontally as bars and spaces of different thicknesses for right-to-left reading. It is also the most common optical recognition technology.

Two-dimension (2D): There are two types of common 2D bar codes: stacked codes and matrix codes. They can perform the same function while taking up much less space. They can also function as the database itself.

Finally, the main advantages of the barcode include low cost and the presence of wellestablished standards. However, a bar code can only contain limited and fixed information. In addition, it requires direct optical visibility to read it. To overcome these defects, this technique has been developed to communicate via electromagnetic waves and RFID chips.

1.2.2 Magnetic Stripe Card

The magnetic stripe card is another method used in identification. It stores data by altering the magnetism of the iron-based magnetic particles on a plastic-like film band of magnetic material on the card. The magnetic stripe card as shown on the back of a card (Figure 3) , is in theory very similar to a piece of cassette tape fastened to a card where data can be written or read. However, its operation requires a physical contact by swiping the card past a reading head. In most cards, the magnetic stripe contains three tracks which are typically recorded at 210 bits per inch (8.27 bits per mm) or 75 bits per inch (2.95 bits per mm), which may contain diverse data such as personal information, an identification number, an expiration date, and other information depending on the nature of the application [5]. This technique is commonly used in credit cards; identity cards, transportation tickets, electronic

benefit transfer cards (such as food stamps), gift cards, and so forth. Some magnetic stripe cards like credit cards may contain an RFID tag as well for electronic payments.

Figure 3: Magnetic Stripe Card

1.2.3 Smart Cards

There are two types of smart cards: contact smart cards and contactless smart cards. Defined as an electronic data storage system, the smart card embeds an integrated circuit, which has the capability of processing data.

The contact smart card is battery-less and is powered by the reader, which requires mechanical contact with the smart card for its transaction. The smart card became widely used through mobile phone usage in 1990s [5]. The dimensions of contact smart cards are usually credit card size (85.60 mm x 53.98 mm). Ones used in SIM cards

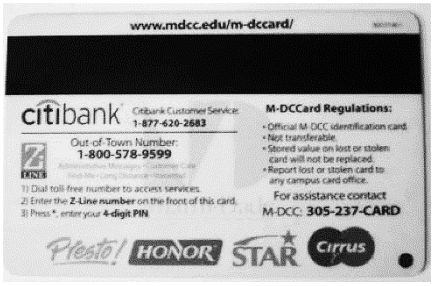

Figure 4: Smart Cards

The several pads shown on the SIM card (Figure 4) are used for functions like clocking, ground, power supply, I/O, and reset. Two types of contact smart cards exist: memory cards and microprocessor cards.

Memory cards are characterized by a nonvolatile memory Electronically Erasable Programmable Read Only Memory (EEPROM), which is accessed through sequential logic states.

Microprocessor cards are characterized by volatile memory (ROM, RAM, and EEPROM) segments and incorporated microprocessor components.

In contactless smart cards, the chip communicates with the reader using a built in inductor that captures the incident radio frequency interrogator signal from the reader. These readers are normally installed in places where a fast or hands-free transaction is desired, such as convenient stores and public transport networks [6]. A universal contactless smart card reader symbol has been established and is shown in (Figure 5). Examples of commonly used contactless smart cards are South Korea's T-money

(transportation fares, convenient stores), Mumbai bus transportation service, Japan Rail's Suica Card, and London's Oyster Card. RFID is a related technology to that of the contactless smart card. Ampleness of information on RFID is given in the next section.

Figure 5: Example of Smart Card Reader

1.2.4 RFID-UHF Tag Passive

Radio-identification, more commonly referred to as 'RFID' (Radio Frequency Identification) [7], is a specific term used for remotely storing and retrieving data (in the form of a unique serial number) using markers called RFID-Tags. This technology

makes it possible to identify an object, to follow its course and to know its characteristics remotely thanks to a label emitting radio waves, attached or incorporated in the object. It is grouped in the broad category of automatic identification technologies. RFID technology allows the reading of labels even without direct line of sight and can cross a succession of layers of materials (paint, snow, etc.). The RFID tag (or RFID tag) consists of an antenna and an RFID chip, usually attached to the products or objects to be identified (Figure 6).

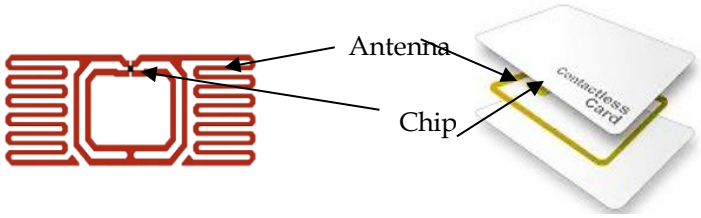

Figure 6: Passive RFID Tag

In a simple way, the RFID tag is a 'smart cart', to read it, we need an RFID reader. The communication between the RFID reader and the RFID tags is done by radio frequency wave. RFID tags may include other components depending on the type of application. Let us mention the contactless smart card as an example of a RFID tag specific to secure applications.

The first principle of RFID technology has been applied during the Second World War, and is directly related to the development of radio propagation and the radar system [8]. To identify / authenticate flying machines in British airspace, allies put transponders in their aircraft to answer interrogations of their radars. This system, known as IFF 'Identify Friend or Foe', represents the first use of RFID (Figure 7) [4]. Today, air traffic control remains based on this principle. The RFID was first studied by Harry Stockman in 1948 [9], followed in particular by the works of F. L. Vernon [6], and those of D.B. Harris [10], who are considered the founders of this technology.

The first patent related to RFID technology was filed in the United States by Mario Cardullo in 1969 for the identification of locomotives [8]. RFID systems during the years 1969 and 1979 remain restricted, mainly for military use for controlling access to sensitive sites, such as the nuclear sector. At the end of the 1970s, technology spread to the private sector. The identification of livestock in Europe remains one of the first commercial applications. This is followed by numerous uses in the same field, particularly in the car manufacturers' production lines. By the early 1980s, RFID tags began to be manufactured by several European and American companies. Technological advances allow the appearance of the passive tag receiving its energy by the signal of the reader [11]. This feature makes the tag less expensive because it allows the absence of on-board power source, and reading distances are a few centimeters.

In the 1990s, it is the beginning of standardization for easy interaction of RFID equipment to accept the services of other systems. In addition, the miniaturization of the RFID system allows its integration into a single chip by IBM.

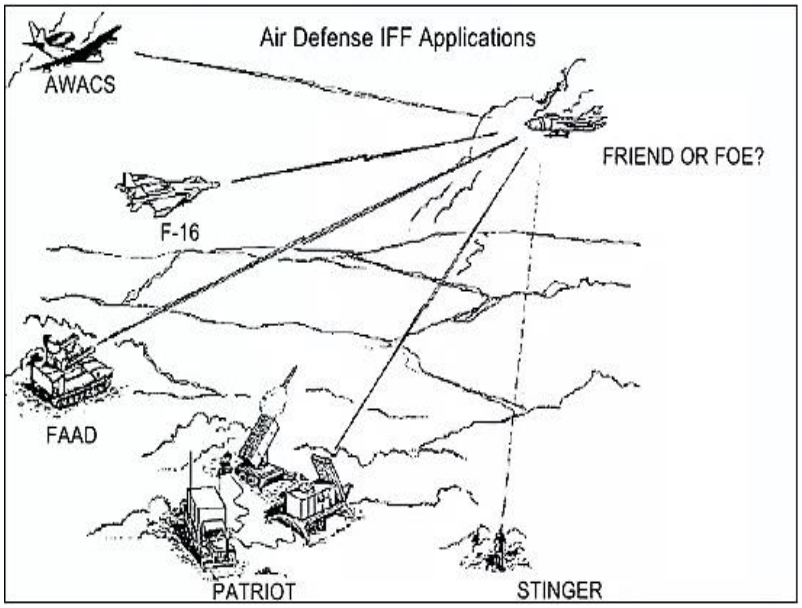

Figure 7: IFF System (Identify Friend or Foe)

During the 2000s, it is the widespread increase in RFID applications thanks to the miniaturization of its technology a few years ago. In 2004, MIT's 'Auto-ID' center becomes an organization known as 'Global EPC', which aims to promote the EPC standard (a kind of super barcode stored in an RFID tag) developed by academics and adopted by industry. In 2007, the professional and international association of electrical and electronic engineers (IEEE) organized the first international conference exclusively on the RFID subjects. Then, in 2010, the IEEE RFID-TA conference is introduced as well as the integration of RFID without chip market.

From a regulatory point of view, RFID is gaining new frequency bands and taking advantage of some extra mill-watts allowed on some frequencies.

1.3 Applications of RFID Technology

1.3.1 RFID as a Payment Tool

As a payment tool, RFID technology has been used as a closed payment system that only works in the specific operational frequency range. Contactless smart cards and transponders can only be used to purchase goods or services from a particular supplier [12]. Among the RFID applications in this field, the Pidion BIP-1300 model (Figure 8) is a PDA (Personal Digital Assistant) device that supports chip, magnetic stripe or contactless payments. Through RFID wristbands, customers have access to convenient payment features: These are mainly prepaid systems, which mean that the card must be charged to a charging terminal with money, credited on the chip card and then debited at the provider's cash desk. Because closed systems are tailored to the needs of the system vendor, wide varieties of RFID standards and data structures are used.

Figure 8: BIP-1300 Barcode Scanner

1.3.2 RFID Applications in Transport and Logistics

RFID is an effective way of limiting the errors inherent in human intervention. In transport areas, the identification, location and monitoring of individuals and vehicles can be carried out using RFID technology [13]. This one allows to regulate the means of transport and the optimization of the management of the flows: In road tolls by means of motorway tickets without stopping of the vehicle. In airports, railway stations, metro and bus stations, the customer passes his card on a base that authenticates it, validates his ticket, and gives him access to the network (Figure 9) and finally in the car parks, it facilitates access and parking of vehicles.

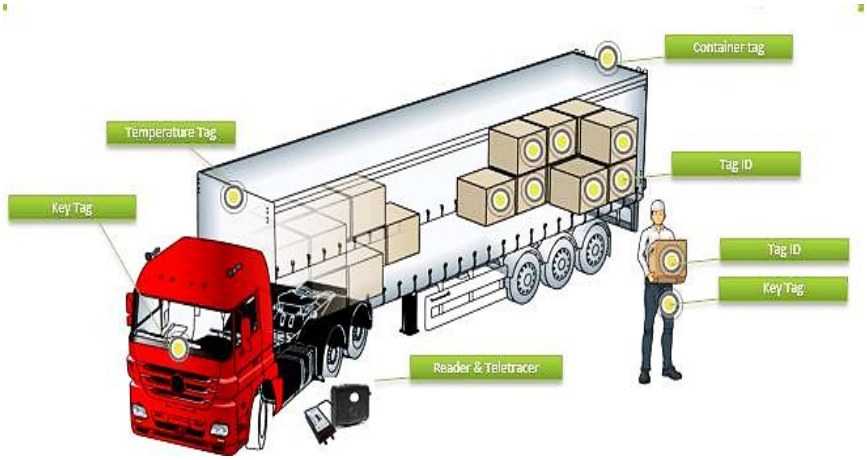

Figure 9: RFID in the Transport and Logistics Sectors

In the field of logistics, RFID ensures the availability of a product in the right place and at the right time, and this at a competitive cost. Indeed, by integrating the supply chain of the distribution, RFID revolutionizes the stages of products transfer, from the

supplier to the distributor until the consumer [14]. It optimizes the flow of goods in the supply chain and simplifies operations at different stages of the supply chain, including tracing, identification, authentication and tracking. It is a response to rising supply chain costs in the face of complex multi-channel marketing.

1.3.3 RFID at the service of individual's identification

In airports, railway stations, metro and bus stations, ports and various public access points, the safety of people is an ongoing issue that grows with their mobility [15]. In these places, sometimes the authentication of the identity papers is essential for the security and the identification of the persons. With RFID technology of readers and IDs, it is possible to meet all the identification needs of people, regardless of the level of security required. For example, the electronic passport consists of a contactless microprocessor chip with antenna integrated into the passport data page or integrated into the passport cover (Figure 10).

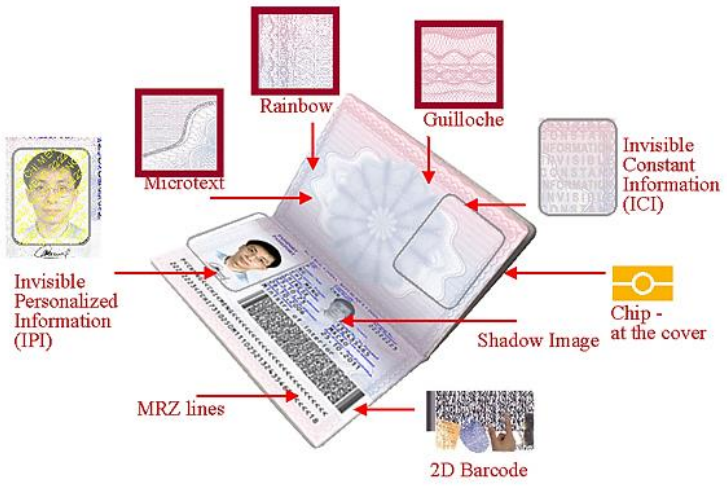

Figure 10: RFID in Identity Documents

The RFID chip can store personal data (name, date of birth, sex) as well as an abstract photograph of the passport. RFID is then a means of ensuring the validity of the documents and information contained in the passport [16]. The purpose of the

contactless chip is to improve the security of passports against forgery. In 2002, before the introduction of ePassports in Germany, 290 completely falsified passports were detected and the contents of 394 passports were forged.

1.3.4 RFID in the Health Sector

RFID technology is less well known in the health sector. However, it allows many advances in the location of patients, the security provided by medical traceability, the monitoring of processes, and the quality of care of patients [17]. This technology offers axes of development for the identification, the authentication, the geo-localization of materials and patients, the security of the follow-up of the patients as well as for the traceability of the health products from the pharmacy to the patient's room. In some hospitals and clinics, emergency department patients are equipped with an RFID wristband that allows doctors and health care personnel with a tablet PC to know in real time the data related to each patient (Figure 11).

Figure 11: RFID Multiple use in Hospitals and Clinics

Another example is the tracking of donations of blood. RFID chips ensure the traceability of the donation and thus allow safer transfusions. The control and monitoring of patients can also be carried out by means of these chips attached or implanted in the human body subcutaneously for ensuring their medical follow-up or during their hospitalization. The RFID also offers a wide range of possible applications for medical device manufacturers [18]. The automatic identification of consumables and accessories using RFID technology simplifies the handling of modern devices and contributes significantly to patient safety.

Finally, RFID technology can play key role in monitoring the collection of infectious risk care activities (DASRI), and thus involves a large number of players in the medical sector.

1.3.5 RFID at the Service of Livestock

RFID is a technology with multiple uses and applications. The official electronic identification of farm animals is an indispensable element of modern breeding. It makes it possible to automatically link the identifier of the animal to an individual measurement recorded by a sensor (sorting of animals, weighing, control of milk production, dosage and composition of food rations, quantity of food ingested, monitoring health, weight of the animal, precise identification of the number of animals and management of vaccination cards, detection of heat) [19]. Above all, RFID ensures food traceability and prevents accidents that cause food shortage in the market.

In addition, the monitoring of domestic animals, remotely via the internet, to know their activity and status, allows them to be supervised, secured and improved their identification (Figure 12).

Beyond these aspects, it reduces the workload of farmers by automating the individual monitoring of animals for sorting or distribution of food. With current labels with memory (Figure 12), it is also possible to track pets (dogs, cats ...) and record medical information (vaccination) or even food.

Figure 12: RFID for Animals

1.4 Global Market for RFID Technology

The ID-TechEx Research has analyzed the RFID market for over 19 years [20]. Their report provides detailed data and analysis of the entire RFID sector based on their extensive research including interviews with RFID adopters and technology providers in the various application of RFID in the markets. The report provides a comprehensive level of insight into the RFID industry.

This comprehensive report from IDTechEx gives the complete picture covering passive RFID (for UHF, HF and LF frequencies), battery assisted passive, active RFID and chipless RFID. It provides detailed and in-depth forecasts. The IDTechEx find that in 2018 (Figure 13), the total RFID market will be worth $11.0 Billion, rising to $13.4 Billion in 2022. This includes tags, readers and software/services for RFID labels, cards, fobs and all other form of factors, for both passive and active RFID.

In retail, the RFID continues to be adopted for apparel tagging above all other applications by volume - that application alone will demand 8 Billion RFID labels in 2018 - which still has some way to go with RFID penetrating only about 10% of the total addressable market for apparel in 2018. RFID in the form of contactless cards will demand 2.2 Billion cards in 2018, driven by contactless payment, transit and secure access applications. In a completely different sector again, the tagging of animals (such as pigs, sheep and pets) is substantial as it continues to be a legal requirement in many more territories, with 540 million tags being used for this sector in 2018.

In total, IDTechEx expects that 16.4 billion tags will be sold in 2018 versus 15.0 billion in 2017. Most of that growth is from passive UHF RFID (RAIN RFID) labels. However, in 2018 UHF (RAIN RFID) tag sales by value will only be 20% of the value of HF tag sales (including NFC), mainly because HF tags where used for security which have a higher price point versus the cheaper ones usually disposable UHF (RAIN) tags used for tagging things [21].

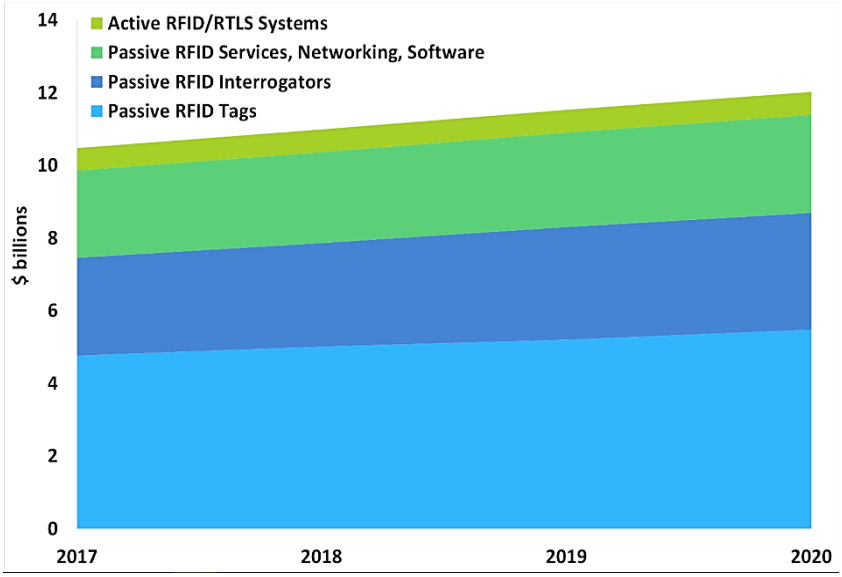

Figure 13: Total RFID Market in US$ Billions (Source: Idtechex)

1.6 Conclusion

This chapter is devoted to the presentation of the generalities on passive RFIDUHF; we have presented a chorological review of the use of RFID technology. The defined the concept of the Automatic Identification and Data Capture (AIDC), which includes a set of systems that facilitate our daily lives, each one, has its own characteristics. We have listed the different areas of application. We also provided a full analysis each market in detail, including in-depth data analysis of the evolution of the RFID technology. One of the promising application of the RFID technology in the field of the RFID –enable sensor, that will support additional and will suppose a disruptive technology is the field of the (IoT) and smart system that will be the topic of our next chapter type of demand from 2017 to 2020. In the following, one of the important applications in the world of technology is RFID-enabled sensors that will support additional functions in determining the ability or operation in sensor applications.

Chapter 2

Fundamentals and Operating Principles for UHF-RFID Tag and Sensors Applications

2.1 Introduction

Thanks to the cutting-edge technology development of the sensors, RFID has become a very suitable alternative for communicating with the sensors and transferring the available data. The first part of this chapter provides a detailed definition of RFID technology, with focus on passive UHF RFID technologies in particular, as these technologies differ according to the type of operating frequency range (LF, HF, UHF ...), the type of use (passive or active), and also depending on the application domain. The second part introduces the technology advances in RFID sensors. Some research papers were presented and compared according the performance of the RFID-UHF sensoroperating mode. Accordingly, these research papers were the basic references to discuss and determine the next steps tackled in chapter 5, regarding the design of RFID sensor that will be used to detect NaCl and Sugar molecules and estimate their concentration in a liquid medium.

2.2 RFID System Operation

The operating mode of RFID system functions as follows [22]:

- The reader transmits a radio signal on a determined frequency to RFID tags located in its reading field,
- The reader emits a signal and establishes a hand shaking according to a predefined communication protocol, thanks to an antenna and a demodulator that translat,

- Analog information into digital data the reader antenna creates an electromagnetic wave (OEM) and transmits a signal to the tags located in its reading range.
- Once the chips of these tags are activated, they send back a signal. The reader, which also functions as a receiver, captures the information contained in the chip (specific code, a unique identification number, a brief description or a batch number for example).
- A dialogue is then established according to a communication protocol and data is exchanged.
- The exchanged data are then saved to a computer database (Figure 14)

In summary, the tag communicates with the reader that transmits the information collected to a computer where it is recorded in a database [23]. On the other hand, the computer can store information in the chip via the reader, which functions as a transmitter and receiver.

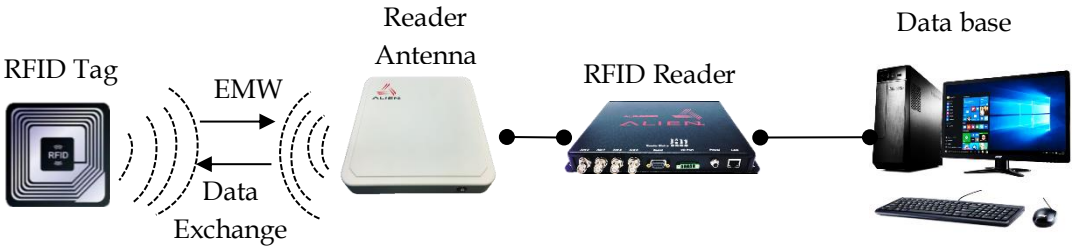

Figure 14: General Operating Principle of an RFID System

2.2.1 RFID Tag Components

All tags RFID contain three basic elements (Figure 15), tag antenna, integrated circuit, and substrate, despite their different shapes, different dimensions, and different capabilities [24].

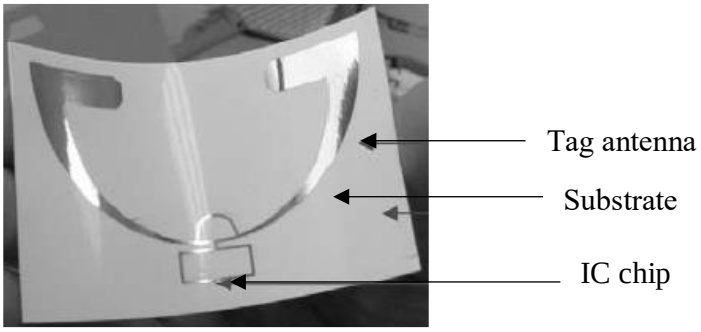

Figure 15: RFID Tag Component

2.2.1.1 Tag Antenna

The size of the antenna tag is often the same as the size of the tag. The antenna is responsible for transmitting and receiving the RF waves, hence enabling the prompt communication. For the passive RFID tags, it also acts as the energy transformer to power up the IC chip from the energy received from the reader's antenna. In passive systems, the information/energy is delivered by the RF wave transmitted from the reader's antennas. The tag's antennas will gather the energy received at its terminals by a coupling mechanism and deliver it to the rectifier inside the IC in order to convert it to DC power [25].

Most of RF devices connected to their load wich have been designed to match 50 ohms or 75-ohm [26]. However, RFID tag antenna is connected directly on the RFID IC-chip, which primarily exhibits a complex input impedance [27]. Therefore, impedance matching between the two components is essential in order to secure maximum power delivery from the antenna reader to the IC chip, to optimize the performance of the reader antenna. On the other hand, we can improve the performance of the RFID tag antenna by matching the impedance between the antenna a nd the IC chip.

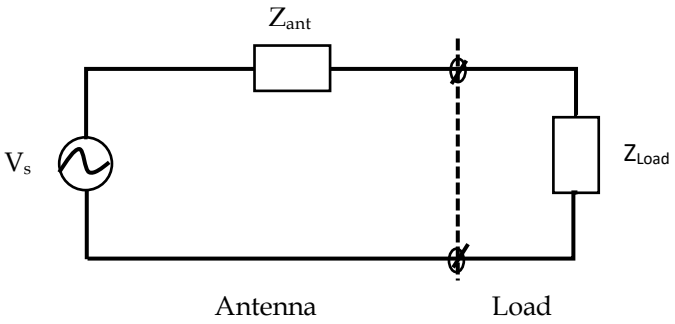

Figure 16: Theequivalent Circuit of the RFID Tag

The equivalent circuit of the loaded antenna shown in (Figure 16). It represents the voltage across the RFID taginducted from the receiving signal. The antenna is modeled by the complex input impedance Zant at its terminal prob. The chip also has a complex impedance Z_{load}, which is frequency dependent [28]. The load's impedance is specific to the design of the IC and may be measured. In order to ensure maximum power transfer from the antenna to the load, the input impedance of the antenna must be conjugate matching to the IC's impedance in the operating frequency of the tag. In simpler terms, the real part of the antenna input impedance must be equal to the real part of the load's impedance, while the imaginary part of the antenna input impedance must be equal to the opposite of the imaginary part of the load's impedance [29].

2.2.1.2 Integrated Circuits

The integrated circuit (IC) is the core of the RFID tag. It is a silicon chip with dimensions usually less than 1.1 mm [30]. The IC chip ofan RFID tag works like aless sophisticated microprocessor. The IC main purpose is to transmit the tag's unique identifier. The unique identifier is stored in the IC memory. When the IC is powered up by the energy flowing from the tag antenna, its logic circuit will retrieve the identifier number stored in the memory, will then modulate the backscatter signal to broadcast this information back. Depending on the type and purpose of the tag, the

IC tag can have extra memory to which the user can write extra information using the reader.

2.2.1.3 Substrate

The substrate is the support that holds the patch antenna tag. The substrate can be rigid or flexible depending on the manufacturing materials. In some special cases, the space to place RFID tags is limited due to the dimensions of the tag antenna. The flexible magnetic composite substrate can help with reducing the dimension of the antenna form [31]. A low-cost fabrication with several design examples will be given in the next chapters. Several types of substrates are considered, while focusing on the sensing applications.

2.2.2 RFID Tag Type

The first classification of RFID tags is based on wether the electronic chip is present on the tag or not [32]. The presence or absence of the radio transmitter and battery of an RFID tag is the basis for a second way of classifying RFID systems (Figure 17). In addition to these physical proprieties, there is a RFID systems classification according to the communication protocol [33]. In this part, different families of RFID systems will be discussed categorized according to the physical proprieties. There are three types of RFID tags: passive, semi-passive and active.

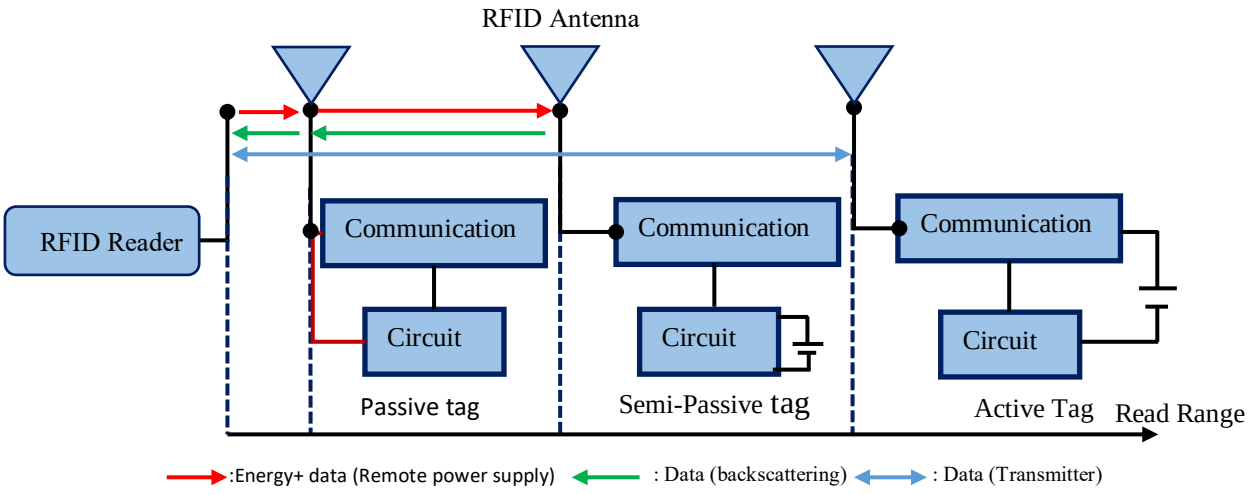

Figure 17: Power RFID Tags Types

2.2.2.1 Passive Tag

Most passive RFID tags operate (without clean energy, without battery or direct current), waiting for radio frequencies sent by transceivers (RFID readers) and using the energy of the received radio signal in order to be activated. This passive tag is composed of an RFID chip that stores the data to be transmitted and an antenna to communicate with the reader that provide the only energy source at the time of interrogation [34]. It is powered from theelectromagnetic energy transmitted by the RFID reader, and uses the principle of the backscattering to power up the IC chip.In fact, the radiated energy out of the reader becomes one of the most important factorsin determining the operating range of the , system.Nevertheless, due to the complexity of theelectromagnetic wave propagation, the first transmission is not sufficient to explain the operating range of an RFID (reader–tag–reader) with short communication range, the transmission will be given in the section as:

$$\frac{P_r}{P_t} = G_t G_r (1 - |\rho|^2) |\hat{\rho}_t . \hat{\rho}_r|^2 (\frac{\lambda}{4\pi d})^2 \qquad (2.1)$$

Where:

Pr: Received power from the receiver antenna;

Pt: Radiated power from the transmitter antenna;

Gr: Gain of the reader antenna;

Gt: Gain Tag antenna;

ρ: Gomplex reflection coefficient at the input of the transmitter ;

ρt: polarization unit vector of the transmitter antenna;

ρr: Polarization unit vector of the receiver antenna;

λ: Wavelength at the transmission frequency in free space;

d: Read range of RFID system (reader-tag distance).

The Friis formula can also be written in a decibel form, as shown in the equation below:

$$P_r = P_t + G_t + L_m - L_p - 20log_{10}\left(\frac{4\pi d}{\lambda}\right) - 20log_{10} \qquad (2.2)$$

The polarization mismatch is given by $|\hat{\rho_t}.\hat{\rho}_r|^2$ equals mismatch loss Lp in decibels between the polarization of the reader and the tag. $(1 - |\rho|^2)$On the other hand, Lm represents the mismatch loss between the impedance of the IC and the antenna of any RFID tag. These terms represent the propagation or the path loss, which depends on the wavelength (and hence frequency) of the operation and the distance traveled.

From (2.2) it can also be noted that the read range is inversely proportional to the square root of the received power at the tag coming from the reader. It is both important and useful to deal with decibels (dB) when talking about communication systems including RFID. At this point, it is also useful to introduce the term sensitivity of the system, as it is a crucial parameter of RFID tags and readers. The sensitivity of a communication electronic device, in our case an RFID tag, defines the minimum magnitude of input signal that is required to produce a specific output signal with a given signal-to-noise ratio. This number is given in dBm (dBm is dB milliwatt where 0 dBm is equivalent to 1 milliwatt) by the manufacturers.

In one scenario, consider a signal being emitted by an RFID reader at a power of 1w, which corresponds to 30 dBm. After a distance d, thePr has to exceed a certain threshold to activate the RFID tag; this commonly known as the tag sensitivity and is given in dBm as well. Sensitivity for passive RFID tags (or sensitivity of their ICs) are typically around negative tens of dBm depending on their design, while sensitivity of RFID readers could go below negative hundreds of dBm. This is due to the low profile of the tag's IC and the complexity of the RFID readers.

2.2.2.2 Semi-Passive Tags

Semi-passive tags technology is similar to passive identification cards, but they have their own battery that works constantly. However, their operating principle is based on the principle of retro-reflection modulation to communicate the data to the readers. These tags are more robust and faster in reading and transmitting data than passive tags, but they are also moreexpensive) [35]. They have other disadvantages that have excluded them from the industry, such as their unreliability and the inability to test the battery level, as well as their environmental impact due to the harmful chemicals contained in the batteries (Figure 18).

Figure 18: UHF RFID Tag Semi Passive

2.2.2.3 Active Tag

Active tags can transmit data autonomously [36]. They have better computing abilities and more memory. Unlike passive tags, they are equipped with internal

battery, and need an onboard power supply. However, they have a shorter shelf life and are bulky, moreexpensive and more complex to produce (Figure 19).

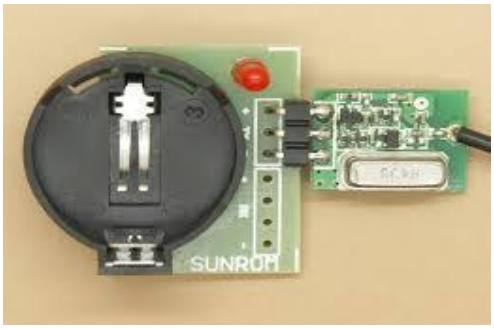

Figure 19: UHF RFID Tag Active

Depending on the different frequencies, the physical principles used are not the same. In the next part, and based on physical criteria, different families of RFID systems will behighlighted.

2.2.2.4 Chipless

RFID tags do not include chipless on the IC chip (Figure 20) [37], but rather transmit data by physical effects and not on any IC memory. This type of transmitter and receiver it often used in reload stores to protect against theft. These devices can use SAW technology and operate on the principle of converting radio frequencies from novelties to a nano surface through sound waves that formed by a digital power transformer (IDT), whichis placed on a balanced substrate such as lithium niobate. The IDT it linked to the antenna to be receive from /sent to the antenna. Once converted into an audio wave, the latter skips some published reactions (it has a unique configuration, thus specifying its identification number) [37]. Meaning that each tag has its own unique identifier (ID) to determine the physical locations of the consumer. Actually, the chipless tags characters are not clear codes for high-level applications, but efforts have been devoted to designing RFID tags without chip

inside. The concept of chipless RFID tags seems to be the lowest cost promising solution.

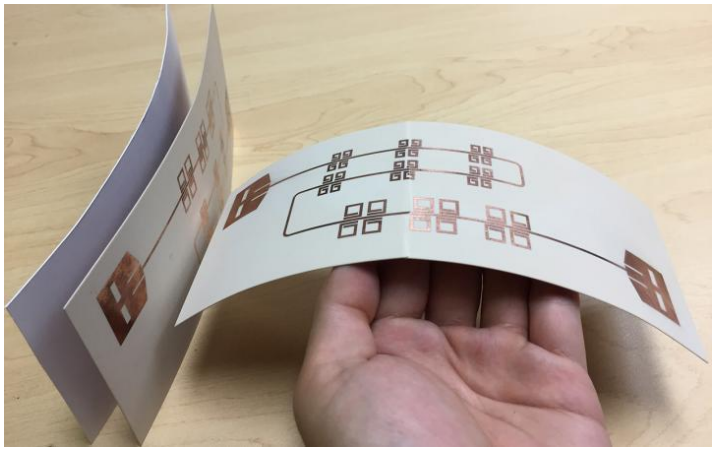

Figure 20: Chipless Tags

2.3 State of the Art Architecture of a Passive UHF RFID System

Passive UHF RFID systems have a very particular operating mode, based on the principle of retro-reflector [38]. Unlike to conventional communication systems, they are powered remotely and have no battery or source of own radiofrequency wave, they reflect the signals that transmitted to them by a reader. The identification is performed by labels consisting of at least one integrated circuit (IC), often known as a silicon chip containing the identifier (ID) of the label, and the logic necessary to navigate the protocol that guides the communication between the label and the reader. The reader may contain theuser interface of its own, but will most often be connected to a particular network or host computer, which interacts with the user to control the reader, and stores and displays the resulting data [39].Figure 21 presents an overview of the general operating principle of a passive UHF RFID system.

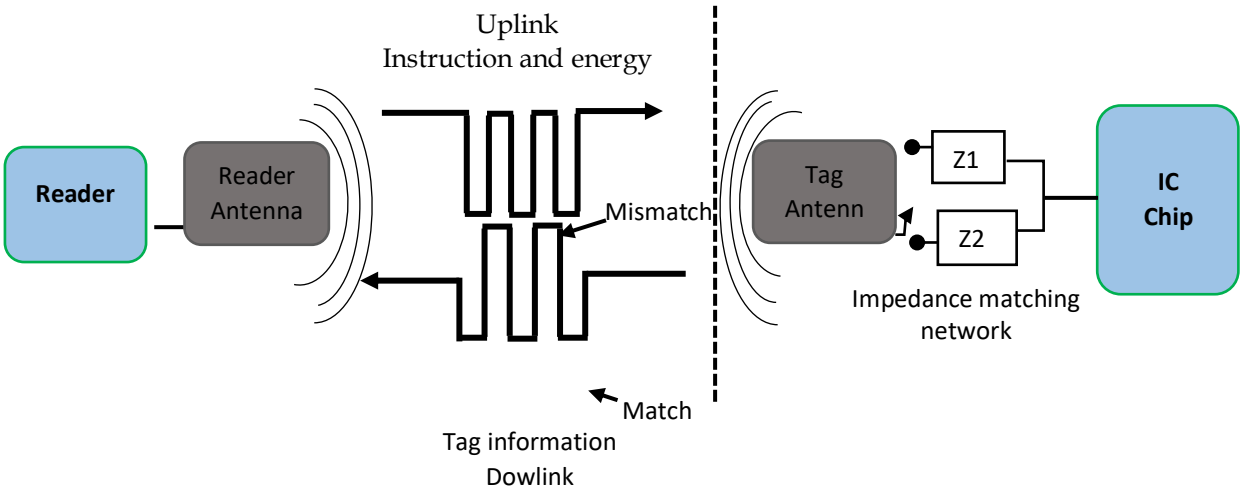

Figure 21: Overview of the General Operating Principle of a Passive UHF RFID System

2.3.1 UHF RFID-Chip Architecture for the Passive Tag

It is areceiver, which is placed on the elements to be traced (object, animal ...). it is provided with a chip containing the information and an antenna to allow the exchange of information [40].(Figure 21) shows an example of UHF RFID tag architecture. The chip consists of a radio frequency RF Frond-End part, a low frequency analog part where the baseband processing and a digital part are done.

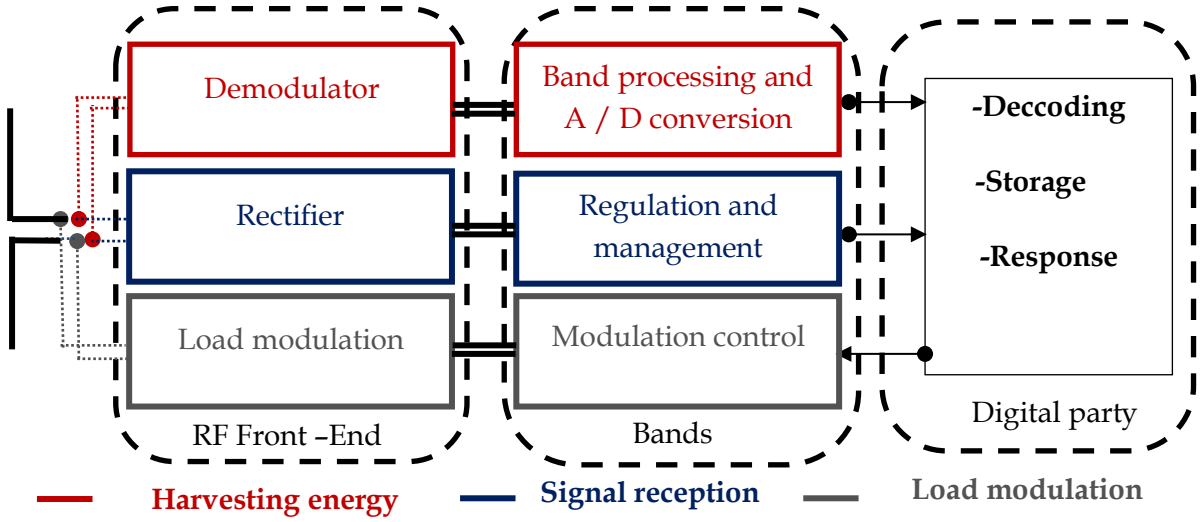

Figure 22: IC-RFID UHF Chip Architecture

The digital part consists of a static device to analyze the received requests, to code/decode the information and to send the responses of these requests to the radio frontend. The digital part is activated by the radio frontend when the antenna receives sufficient energy from [41].

The radio-frequency part is a circuit between the antenna and the first intermediate frequency which assumes three main functions [42].

- The energy recovery function is usually provided by a rectifier that can recover a DC voltage from the RF signal received by the antenna. This voltage must allow the feeding of the tag. Often, the rectifier is followed by an regulator or a voltage limiter to stabilize the voltage and protect the chip from the risk of overvoltage
- Signal receptionor the information signal retrieval function is generally provided by a conventional reception chain comprising a demodulator, a baseband filter and an analog / digital converter.
- Decoding and information processing is done digitally, most often using a simple logic system.Retro-modulation function is provided by a load modulation system at the input of the antenna

2.3.2 Passive UHF RFID Reader

It is an active device. That plays the role of the interface between a host application and RFID tags. It has two main roles: perform communication management with RFID tags and transmit their data to the host application [20].A reader is composed of different functions illustrated in the Figure 23.

- **Numerical part functions** generates and formats the digital signal containing in the information to be transmitted to the tags and processes in return the answer of this one [43]. Thus, in addition to the implementation of the communication

protocol, the digital unit is able to encode / decode signals, possibly encrypt / decrypt or any other function imposed by the required application.

- **An analog front-end partis** finalized by an antenna. (Figure 23) has synchronized modulation / demodulation blocks to a local oscillator. It also has filtering blocks, and amplification, which constitute thee mission hannela nd reception. The Radiofrequency part is thereforeresponsible for generating a carrierable to feed the remote tag, modulatea digital signal generated by the control unit and demodulatethe tag response. The frequency used by the readers depends on the type of targeted application and the desired performances. These are detailed in the frequency band section.

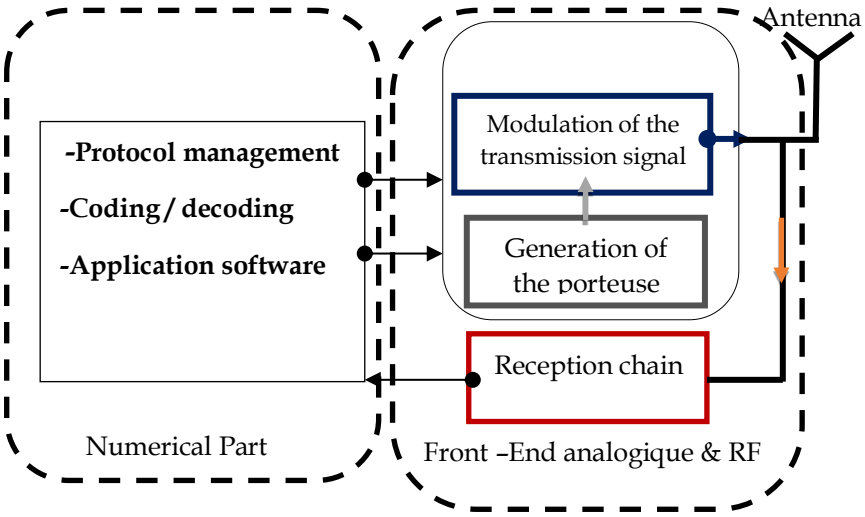

Figure 23: Architecture of a UHF RFID Reader

2.3.3 Principle of the Retro-reflector

The reader transmits the interrogating (ASK: Amplitude Shift Keying) modulated signal to the tag at the operating frequency (Figure 24). The transmitted signal is also used to feed the RFID chip on the tag. The RFID chip contains a energy recovery circuit, which is responsible for transforming the power E.M collected by the tag antenna in DC voltage. The reader continues, after the transmission of its interrogation, to emit unmodulated signal always at the same frequency (CW) to

maintain the power supply of the RFID chip. The response of the tag is the retro modulation of this signal [44]. Indeed, the signal (CW) sent by the reader is reflected by the chip using charge modulation as a variation of the reflection coefficient at the interface between the tag antenna and the chip. Physically, it consists of a variation of the input impedance of the chip, thus creating an impedance mismatch with the antenna. Now, to modify an impedance, one can vary its real part or its imaginary part. Indeed, the RFID chip is seen at the terminals of the tag antenna as an impedance Zc a load adapted to the impedance of the antenna. The impedance of the chip switches between two states to create thetag response. Each state corresponds to areflection level. These two states correspond to the two logical levels (0) and (1), if the modulation relates to the real part of the load (Figure.24 -a), then one carries out a modulation ASK and if c is the imaginary part that is concerned (Figure.24-b), it is a PSK (Phase Shift Keying) modulation [45].

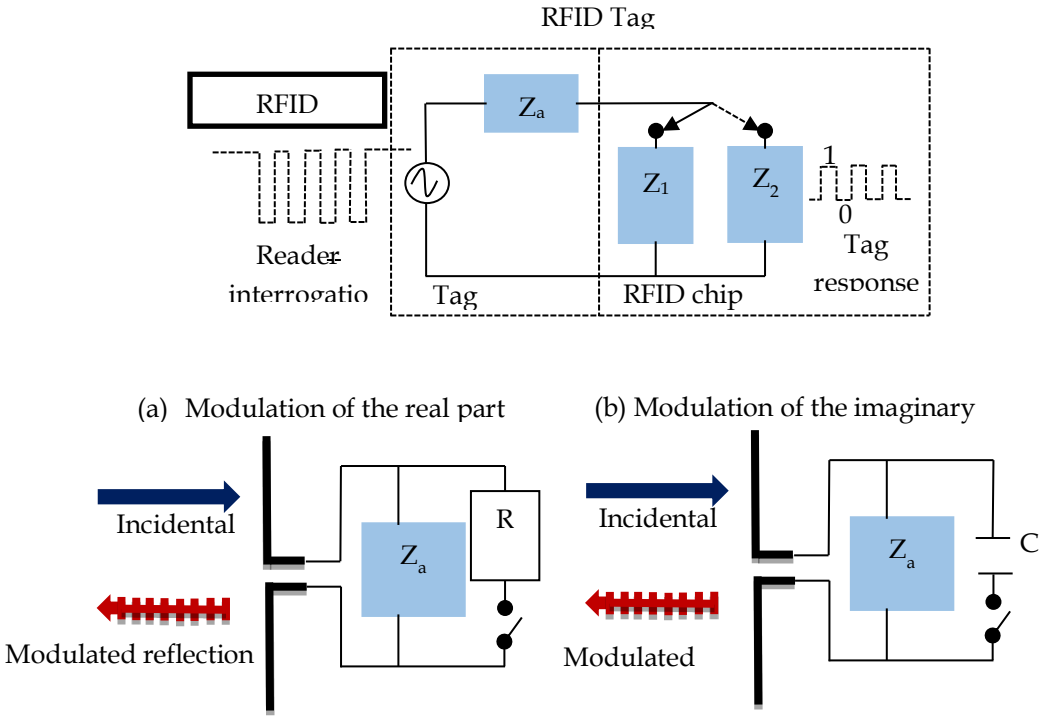

Figure 24: Principal of the Retro-reflector

2.3.4 Middleware

A middleware of an RFIDsystem is a new class of programs that creates a network of information exchange between physical devices - readers and tags - and business applications [46]. The network is implemented by using the same information exchange technique in all the applications involved using software components (Figure 25). The software components of the middleware provide communication between applications regardless of the computers involved and regardless of the hardware and software characteristics of the computer networks, network protocols, operating systems involved. The middleware can therefore be divided into three main components [47], the Figure 14shows theequipment management component, the data management component and the service management component.

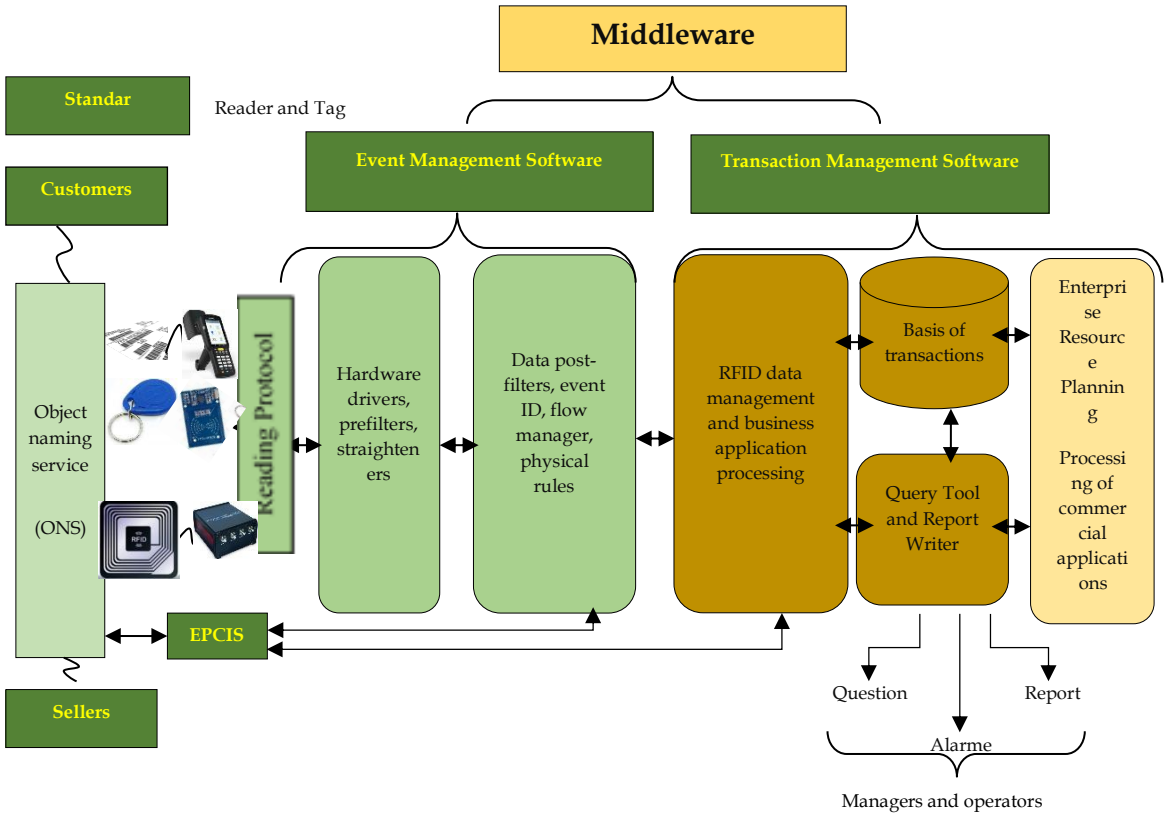

Figure 25: Middleware Architecture

2.4 Frequency Band of RFID Systems

Based on frequencies already allocated and widely used by a multitude of users (Radios, Television, Army, Civil Defense, etc), RFID has been assigned number of frequencies classified into four groups [48]:

- Low Frequency (LF), below 135 KHz, two frequencies are used, the 125 KHz and the 134 KHz;
- High Frequency(HF) : one frequency is used, the 13.56 MHz;
- Ultra High Frequency (UHF): two frequencies are used, the 433 MHz and the band from 860 to 960 MHz;
- Supra High Frequency (SHF): two frequencies were initially reserved, 2.45 GHz and 5.8 GHz. The latter was finally abandoned due to lack of demand but remains at the disposal of RFID.

It should be noted that each frequency has its own characteristics, both from the point of view of the communication parameters (distance, speed of exchange) and theenvironment in which it operates (presence of metal and liquid, electromagnetic activity ...) [49]. Therefore, it isimpossible to consider a single frequency that could solve all thetraceability problems by RFID. To be more specific, each frequency will have its own preferential area of application. On the other hand, certain areas of application may be covered by several frequencies. Thus, RFID systems must obey rules such as the allocation of frequencies and the authorized power. RFID arefundamentally distinguished by the frequency of the radio waves and the means used to feed the labels. This operating frequency is very important since the properties of electromagnetic waves differ greatly between low frequencies and high frequencies. There are currently 5 major RFID technologies: BF, HF, UHF, SHF and without chip.

2.4.1 Low Frequencies (BF) and High Frequencies (HF) in RFID

Low Frequencies (BF) are ranged between 120-135 KHz.In the near magnetic field zone, they make it possible to have a rangein the order of few centimeters to one meter [50]. The physical characteristics of the BF tags make them ideal candidates to be supported by different types of materials: textiles, plastics, etc. On the other hand, the frequency class 13.56 MHz, which belongs to the High Frequencies, also uses the near magnetic field. Often, the labels used in these bands are smart cards, with reading distances of the order of few centimeters to onemeter. They are generally used to trace objects, (e.g. books in bookstores and libraries, and the location of baggage at airports), control access, and personnes identification.

2.4.2 Ultra High Frequencies (UHF)

The 0.86-0.96 GHz and 2.4-2.5 GHz frequency bands belong to the UHF family. However, in order to distinguish them, it is usual to use the term UHF for systems operating around 0.9 GHz and to call microwaves frequencies near 2.4 GHz. Since the application requires large reading distances or a large information rate, RFID systems operating in UHF or micro-waves are chosen. The communication between the antennas of the transmitter and the receiver is then no longer by magnetic coupling but by electromagnetic propagation. The disadvantage with the principle of propagation of electromagnetic waves (OEM) is that the system becomes more sensitive to disturbances (proximity of liquid or metals) than with the magnetic coupling phenomenon [51]. There are also other less used frequency bands, for example the frequencies ranging from 5.7 to 5.8 GHz or the frequency 0.433 GHz. (Figure 26) shows some of the common and less common frequency bands in which RFID systems operate. We also find the corresponding wavelength - the distance between the points at which the field has a fixed value when the signal moves at the speed of light.

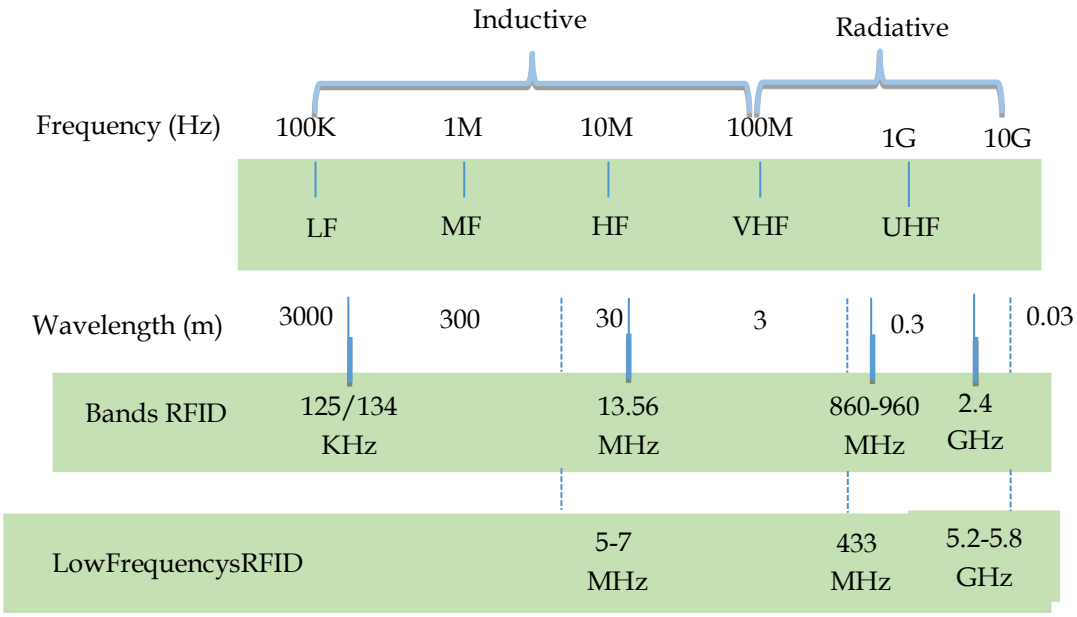

Figure 26: RFID Frequency Band

2.5 Authorized Power RFID

As regards the power, the coupling between labels and reader is different according to the frequency range for the BF and HF up to 13.56 MHz, the inductive couplingis used with the RFID system operating in "near field". We will then speak of maximum intensity of the field. This intensity is expressed in dBµA/m (decibel-microampere per meter) [52]. We give the different regulations given by theETSI (European Telecommunications Standards Institute) Table 1.

For other frequencies, the coupling is electromagnetic and the RFID system operates in 'far field' mode. We will speak of maximum transmission power. This power is expressed in Watts. However, the unit differs according to geographical areas and the power is not calculated in the same way. In Europe, the unit is the Watt calculated in ERP (Effective Radiated Power), in America, this power is normalized compared to an isotropic reference antenna and the unit is still the Watt but this time calculated in EIRP (Equivalent Isotropic Radiated Power). The ratio between the two units is 1W

ERP = 1.62 W EIRP. Thus theEuropean standard allowing 2 Watts ERP actually corresponds to 2x1.62 = 3.24 Watts EIRP, equivalent to the 4 Watts EIRP eligible in the USA for example [53].

Table 1: Permissible RFID Powers in Near-Field and Far-Field

Region	Operation Band	Authorized power
Europe	13.56 MHz	42 dBµA / m @ 10 m
Europe	865-865,6 MHz	100mW ERP
	865,6-867,6 MHz	2 W ERP
	867,6-868 MHz	500 mW ERP
United States	902-928 MHz	4 W EIRP
Asia and Oceania	Japan 952-954 MHz	4 W EIRP
	Korea 908.5 to 914 MHz	4 W EIRP
	Australia 915 to 928 MHz	1 W EIRP

2.6 Characteristics of RFID System Types

The different RFID systems can be classified according to the frequency with which they operate, the nature of the tags, the range, the bit rate, the storage capacity and the type of reader-tag coupling [54] - [55] (Table 2).

Table 2: Characteristics of Types RFID Systems

Near field RFID system			Far field RFID system		
Technologies	LF	HF	UHF	SHF	chipless
Frequency	125 Khz	13,56 Mhz	433.92Mhz 860 Mhz ˜ 960Mhz	2,45 Ghz 5,8 Ghz	3.2Ghz ˜ 10Ghz
Read range	0,5 m	1m	10 to 100m depend the application	10 to 150m	Less than 1
Memory capacity	<256 bits	Until 2048 bits	Until 8 kbits	Until 32 kbits	estimated <256 bits
security	Strong	Strong	Low	Low	Strong
Cost	˜0.1€-0.2€	˜0.1€- 1€-	˜0.2€- 2€	˜0.2€- 5€-	˜0.1€
Tags types	Passif	Passif	Active /Passif	Active	Chipless
Application	animal	Access control	Inventory	medical	……..

2.7 IEC Standards/ ISO Norms

The International Organization for Standardization (ISO) is an independent, international non-governmental organization whose 164 members are the national standards bodies, ISO's central secretariat is located in Geneva, Switzerland. It provides ISO members with administrative, and technical support, coordinates the decentralized program for the development of international standards in the various fields and publishes them. The ISO / IEC standards for the identification and management of objects or equipment have written in the series of ISO 18000 interface protocols designed for logistics operations, the ISO participates in the allocation of standards covering the full frequencies, that are used worldwide in RFID.

Table.3 provides the main technical standards developed by ISO that regulate communication parameters such as operating frequency bandwidth, and maximum transmit power, modulation type, coding, bit rate and protocol, communication application standards include animal identification and antitheft systems [56]

Table 3: ISO / IEC Standards Governing The Operation of RFID

standards	Objective
ISO/IEC18000-1	General architecture and parameters to be standardized
ISO/IEC 18000-2	Parameters for air interface communications up 125 KHz
ISO/IEC 18000-3	Parameters for air interface communications at 13,56 MHz
ISO/IEC 18000-4	Parameters for air interface communications at 2,45 GHz
ISO/IEC 18000-6	Parameters for air interface communications between 0,86-0,96 GHz
ISO/IEC 18000-7	Parameters for air interface cosmmunications at 0,433 GHz

2.8 Technological Progress of the RFID-UHF Tag Sensors

2.8.1 Use of Sensors

The main basic principle of the sensor established in 1982 by a German-Estonian Thomas Johann, when any conductor is subjected to a constant temperature [57], it witnesses a change in the conductor's component and its internal properties. is called the thermoelectric effect or Seebeck effect. From attaching it to another conductor to eventually, "hot". Thus, this conductor will also know a shift in its internal properties via thermal sharing, or magnetic exchange [58].

The sensor can identified as a tool converts a material quantity into a signal, which can observed with a programmable and adjustable tool. The main goal of the sensors is to create a system, for not only monitoring but also for adapting to a changing environment and these changes converted into readable signals or variable-rate determination [59]. This RFID technology works in this mode at low cost, long-time exploitation, the sensor data is transmitted alongside EPC, using signs that operate in the bands (UHF), where data can be transferred over relatively large distances (More from 10 meters), where we will focus in this study on negative UHF RFID technology and its effectiveness in sensitive industrial applications [60].

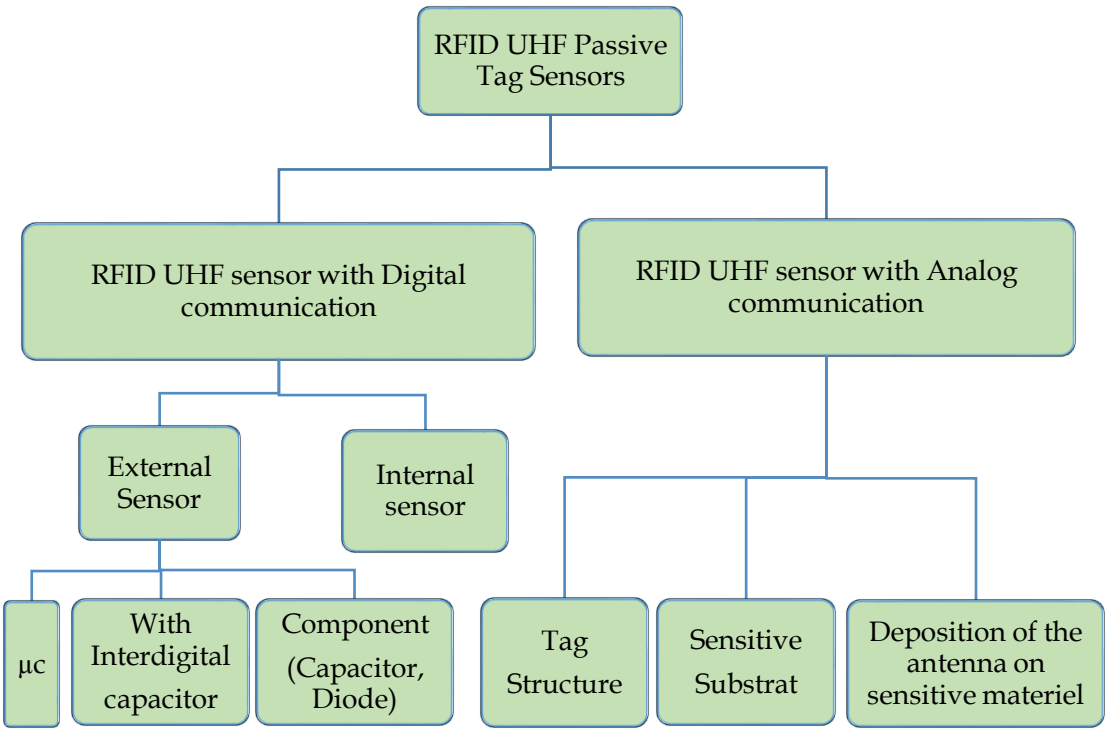

Figure 27: Different Types of Passive UHF RFID Sensor

Figure 27 summarized all types of RFID UHF tag sensor, which will allow us to develop the way this sensor made and its working principle. In this regard, we have focused on method of making RFID antennas and combining them with the work of

non-invasive sensors, based on matchingof the RFID tag withsensitive materiel, were largely dedicated to specific applications.

2.8.2 Types of RFID-UHF Sensors

There are numerous RFID UHF sensors available for different applications and various physical quantities. It is necessary to classify sensors in order to study them. Based on different criterion, the RFID UHF tag sensors can be divided into different classified categories such us:

- Digital communication RFID sensor:
  - Internal RFID sensor
  - External RFID sensor
- Analog communication RFID sensors.

2.8.2.1 RFID Sensor with Digital Communication

2.8.2.1.1 Internal Sensor RFID UHF Tag Antenna

Many RFID chip manufacturers do not incorporate a sensor directly into their products. In Table 4, we included RFID chips with an internal temperature sensor.

Table 4: RFID Chip with Internal Temperature Sensor

Referance	Manufacturer	Activation power	Detection range	Resolution sensor
PE3001 [61]	Producctivity Engineering	0 dBm	-20°C to 50 °c	± 1°c
Magmus83 [62]	RPMicron	-16 dBm	-40 °c to 85 °c	± 1 °c
EM4325 [63]	EM Microelectronic	-8.3 dBm	-40°c to 65 °c	……..
SL900A [64]	AMS	-7 dBm	-29°c to 58°c	± 0.5 °c

Figure 28 present example related to a system which an evolution of the concept of an epidermal wireless temperature sensor with the goal of size miniaturization and characterizing the achievable thermal and communication performance in realistic operative conditions, comprising a reader antenna placed on the wrist and an RFID tag placed at the arm [65].

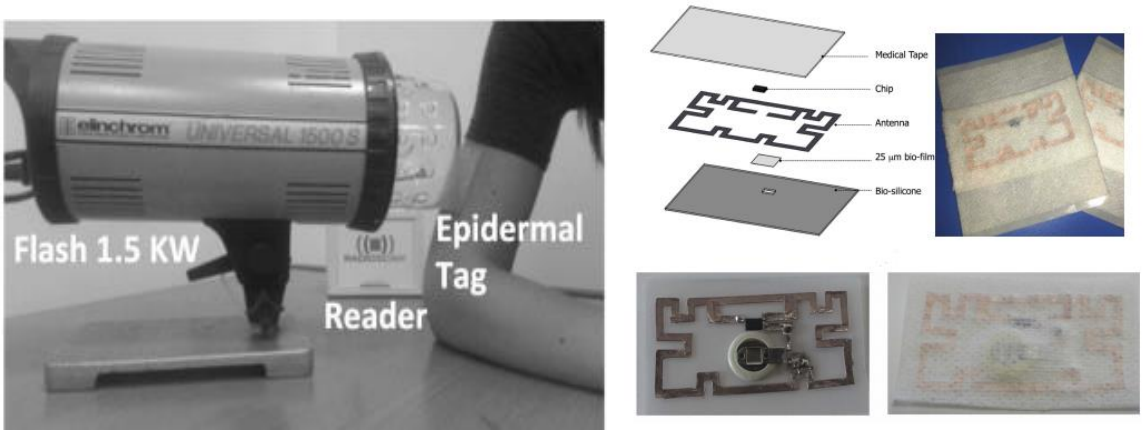

(b) (a)

Figure 28:(a) Set-Up for the Flash-Method. (b) Various Layers RFID of Epidermal Thermometer and Prototype

This sensor-RFID tag is presented, which uses the temperature sensor of the EM4325 chip. The challenge of this study, in which the antenna is put in direct contact with the human body with lossesfor the direct placement over the skin. After uniform recalibration, the accuracy of the IC sensor satisfies the target value for standard thermometers (ear 0.2°C, underarm 0.5°C). The capability of wirelessly reading the sensor up to a distance of 0.7 m (battery-less mode) and 2.3 m (battery-assisted mode).

In another study [66], we also see a temperature sensor (using the EM4325 chip). This study focused on the use of these sensors in medical applications, by observing the wound, some surgery, the development of epidemics, as well as the monitoring of

sports activities. This sensor can be read up to 35 cm, under constant conditions (represented by the curve in the upper left, and the rest) is shown in (Figure 29), and by dynamic conditions (represented by the curve of figure in the lower left, during voltage), with an accuracy of about 0.25 ° C Compared with reference measurements. In order not to influence the temperature measurement, the substrate was chosen to be biocompatible and waterproof

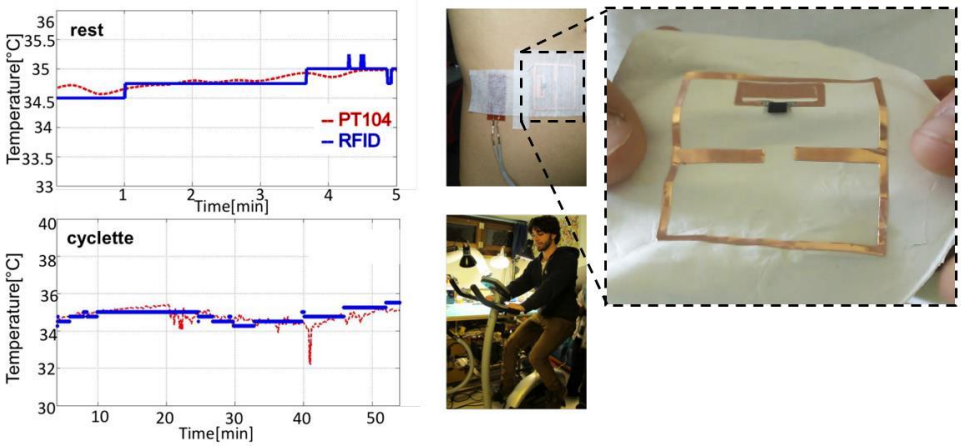

Figure 29: Prototype of the Epidermal RFID Temperature Sensor on a Flexible Substrate and Results of Temperature Measurements on the Body

2.8.2.1.2 External Sensor RFID UHF Tag Antenna

From an application point of view, an external sensor can connected to the RFID chip in three different ways [67].

- The first solution is based on using a digital sensor or microcontroller connected by serial access communication bus (SPI or I2C), this solution increases the capacities of the chip by adding expanded sensors and memory extensions. This method has the disadvantages of greatly increasing the power consumption and considerably reducing the performance of the RFID tag sensor.

- The second solution is based on the use of the analogic to digital conversion interface (ADC). This interface is able to program and controll an external Sensor, an example, is the SL900A chip that has two enbled analog inputs to witch one can connect other sensitive elements, capacitive, resistive or optical sensors (diodes).
- The table below presents the various RFID chips, and the ports through which they can be connected to other sensors, through tight and accurate connections, using their serial communication buses; we also see that the SL900a chip contains the most inputs, and therefore is the ablest to connect with other device

Table 5: Comparison of Commercial RFID Chips with External Sensor Inputs

Reference	Manufacturer	input external sensor	Possibility to connect with µcontroller
SL900A [64]	AMS	2 input dedicated to external resistive, capacitive or optical type sensors (diode)	SPI Protocol
EM4325 [63]	EM Microelectronic	No sensor input but possibility of extraction detection	SPI Protocol
PE3001 [68]	Productivity Engineering	x	SPI Protocol
WM72016-6 [69]	Cypress		
ANDY100 [70]	Farsens		
ROCKY100 [71]			
MONZA X 2K Dura [72]	Impinj	x	I2C Protocol
MONZA X 8K Dura [73]			
UCODE I2C			

[74]	NXP		
EM4324 [75]	EM Microelectronic	No sensor input but possibility of extraction detection	x
UCODE G2iM, G2iM+ [76]	NXP		

2.8.2.2 RFID Sensor with Analog Communication

To provide low-cost technology solutions, for specific applications, this second family of RFID sensors is most used, as this RFID sensor works, through analog communication, which is named because the sensor information is in the representative parameters of the EM wave that the reader receives, in this type of sensor, the physical variables work to be measured by modifying the resistance of the antenna, which affects the power radiated in the direction of the reader,(Figure 30) summarizes the sensitive elements of the parameter to match the resistance of the RFID tag antenna [77], they are represented by four sensitive elements.

- Substrate
- Structure of the antenna
- Deposit on the antenna
- External element used as a 'second' substrate

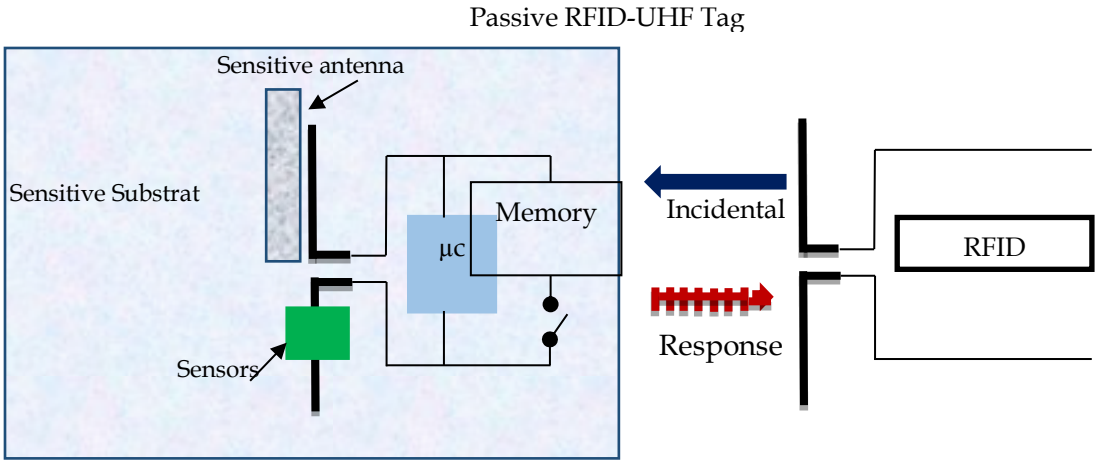

Figure 30: RFID Sensors with Analog Communication

There are several types of RFID sensors, which differ according to the type of their function. We have classified this type of RFID sensor according to four principles, which depend on the position of the sensitive element influencing the impedance matching:

- The first principle is simply based on the effect of the surrounding environment on the antenna of the tag. In this case, a simple unmodified RFID tag is sufficient. For example, the physical masking of an RFID tag makes it possible to detect a passage [78]. The soil hygrometry rate is measured using a simple buried tag [79].
- The second principle requires making the substrate on which the antenna is placed sensitive to a physical parameter. For example, a paper substrate sees its dielectric constant change as a function of the absorbed humidity [80].
- The sensitive element could be the antenna itself. The structural modification of the conductive deposit constitutingthe antenna allows the detection of humidity [81].
- Finally, transforming a tag into an RFID sensor can done by depositing a sensitive element on the antenna [82].

For example [83], we take study describing the dielectric properties of cork, and introduces the cork as a possible substrate for the implementation of antennas at high frequencies and explores its use in humidity sensing (Figure 31-(a)), where the electrical properties of two types of cork samples have been studied. Tolerance and loss factor for a sample of natural cork and a sample of compact pressed cork is extracted in two methods for characterization for comparison purposes. In addition, different antennas are designed to include negative RFID tags in barrels or stockpiles of stocks and their impact due to the permittivity shift with the variation of humidity

and the possibility of applying a negative humidity sensor based on RFID using cork as a sensitive mechanism appears (Figure 31-(b)).

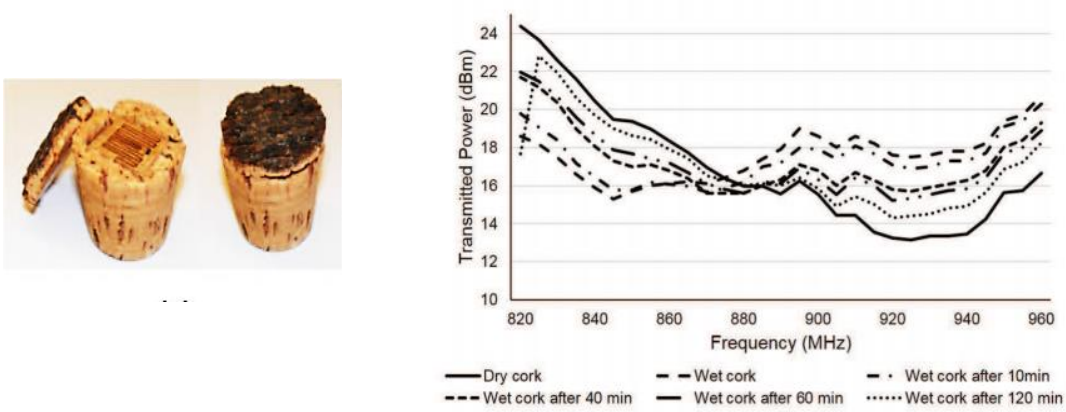

(a) ***(b)***

Figure 31:(a) Prototype of the Implemented On Cork Substat. (b) Minimum Transmitted Power to Activate the Prototype Tag with Different Wetting Conditions

This communication is considered to be more complicated in the implementation and application, to be in line with the principles of the work, as the sensor provides by following the differences in the transmission energy needed to activate the mark or in the energy that is reflected in the mark (RSSI: signal strength received signal) in proportion to the reader. Therefore, it is necessary to make sure of these differences, that come from the physical parameter under study and not from the measurement environment, the RFID sensors play an effective role in the industrial societies as well as the research community to work on developing these sensors and linking them to all physical variables of the things and for their low-cost fabrication.

2.9 Conclusion

In this chapter, we have introduced the general operation of RFID technology. Then, we made a technological progress report on the existing RFID sensor, from a commercial and academic point of view. The first objective allows validating the

functioning of the antenna in initial condition, the second allows us to validate the RFID Sensor operation in a controlled environment.

Chapter 3

Development of Automatic Platform Measurement for RFID Tag Characterization

3.1 Introduction

Before starting to the characterization of RFID-UHF Tag antennas, it is important to describe to devolvement a new platform for the performances characterization of RFID Tags. The envisioned elements of this platform: The hardware part consists of a programmable reader equipped with General Purpose Input Output (GPIO) ports to run a stepper motor to change the orientation of the tags. The software part controls the hardware and executes the test algorithms based on the theoretical part to draw the resulting graphs characterizing the tag. The our platform provides some solutions such as allowing drawing the graphs and characterization of the tags, meeting the needs of scientific research and developing of RFID-UHF tags. The software allows to switch the power (030-dBm) and the frequency (865-928-MHz) emitted by the reader in order to evaluate all the characteristics of an RFID tag, with variation in the orientation between the tag and the reader antenna by 1.8° each step. The platform results (power activation, read range, read pattern, and radiation pattern) validated by comparison with LCIS lab-INP results, Valence, France. The results of our developed system were in good agreement with the classical platform measurement systeme.

3.2 Theoretical Formulas Necessary for UHF RFID Tag Characterization

3.2.1 Recovery Energy at the Terminals of the Tag Antenna

This is one of the most important aspects of RFID applications, because simply of the costs involved, widely used labels for traceability applications … and must to remotely power by incident radiation from the station (antenna). The quality of the remote power supply and, therefore, the operating distance depends to large extent on the amount of energy or power that the label can recover from the base station to operate. Here we meet one of the main antenna label features RFID- UHF [84].

3.2.2 Recovering the Transmitted Radiated Power

The antenna (isotropic) of the station base radiates energy that travels towards the tag at the speed of light in all directions. At any given moment, this energy is distributing evenly over the entire surface of a sphere ($4\pi r^2$) whose center is the antenna of the station base and whose radius is equal to the travel time multiplied by the speed of light. As the surface of a sphere quadruples each time its radius doubles, the density of *EIRP* energies is dividing by four each time the radius doubles. The transmission system driving electrical power can provide station $P_{conduitbs}$, the power P_{ERIP}(watts) by it through the gain of its antenna G_{bs}, and thus the surface density of power at one point of space, since, by definition, for an isotropic antenna the surface density of isotropic power S_{iso} is:

$$s_{EIRP} = \frac{P_{EIRP}}{4\pi r^2} \qquad (W_{mean\ peak}.m^{-2}) \text{ (3.1)}$$

3.2.3 Effective surface antenna tag $\boldsymbol{\sigma_e}$

In order to be able to carry out the energy supply of the electronics on board, the tag must collect the energy that passes over a certain surface around its antenna, which "effective surface" σ_e of tag antenna.

$$\sigma_e = \frac{P_l}{s} \quad (3.2)$$

The incident field arriving at the antenna terminals in receiving mode considered to be from a distant source. The incident wave is therefore flat, and the electric field of effective value E_{eff} from the station base is present around the antenna of the tag. The tag antenna, consider it as dipole, has an effective length associated with I_{eff} . When the antenna is empty, a difference in $V_{equieff}$ potential created at its terminals ($V_{equieff} = E_{eff} I_{eff}$) by having a Z_l charge at the antenna terminals, and a difference in potential (ddp) (V_{reeeff}) it is developing at its terminals.

3.2.4 Equivalent Circuit of the Tag

The complex impedance $Z_{ant\,Tag}$ of the antenna in reception mode is also the same as the equivalent electric model for the antenna in broadcast mode. Those points condition the validity of this reciprocity. The whole tag is represented by the equivalent scheme are given in (Figure 32).

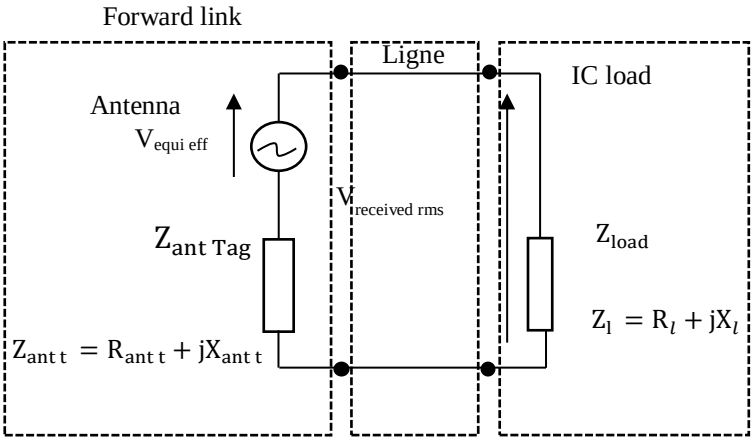

Figure 32: Equivalent Electrical Diagram the Tag

A cause the equivalent generator to the entire tag antenna:

- Composed of a source of tension delivering, vacuum an equivalent voltage$V_{equieff}$, this voltage is therefore independent of the load of the receiving antenna.

  If the load is adjusted$R_l = R_{ant}$, therefore, $P_{ant} = P_1$

  $$V_{equi\ rms} = 2V_{received\ rms} = 2\sqrt{P_t R_l} \quad (3.3)$$

- Whose internal impedance (impedance of the tag antenna) is equal to $Z_{ant\ Tag} = (R_{ant} + R_{loss}) + jX_{ant}$. Equation in which $R_{an\ t}$ is the radiation resistance of the transponder antenna, $R_{loss}$the ohmic loss resistance, $X_{an\ t}$ is the reactance of the tag antenna.

This equivalent generator represents the global conglomerate, medium-induced mitigation, surface-to-power density in which transmission takes place, and finallyG_{antt}. The impedance of an external load $Z_l = R_l + jX_l$ is the impedance equivalent to all the circuits present at the antenna terminals (integrated circuit of the tag).

3.2.4.1 Power in Load Rl

As for the study of the antenna in broadcast, we can write the expression of the total power received (or captured) available at the terminals of the antenna load of the tag. $P_t(\ w_e)$ is proportional to the module of the surface power density which radiates an efficient average s ($\mathrm{w_e m^{-2}}$) and the actual surface of the maximum power capture of the tag receiving antenna $\sigma_e(\ m^2)$ (Eq.3. 4).

$$P_{te} = \sigma_e . s(\mathrm{w}) \quad (3.4)$$

During the illumination of the tag by the incident electromagnetic wave, the $V_{reçue}$voltage creates an I current in the charge ($Z_l = R_l + jX_l$)

$$I = \frac{V_\mathrm{r}}{R_l + jX_l} \quad (3.5)$$

It therefore travels the entire circuit equivalent to the assembly composed of the load arranged in series with the antenna (Figure 1).

$Z_{ant\ t} = R_{ant\ t} + jX_{ant\ t}$.so V_{equi} the tension is therefore equal to $V_{equi} = [(R_{ant\ t} + jX_{ant\ t}) + (R_l + jX_l)]I$ or, by deferring the value of I. Then

$$V_\mathrm{r} = \frac{R_l + jX_l}{(R_{ant} + jX_{ant}) + (R_l + jX_l)} V_\mathrm{equi} (3.6)$$

Whatever the values of impedances involved, the complex form of the general equation of the current radiofrequency I circulating in the circuit will have the value of (Equation .3.7) (in the case of short lines without losses):

$$I = \frac{1}{(R_{ant} + R_l) + j(X_{ant} + X_l)} V_\mathrm{equi\ eff} \quad (3.7)$$

From this equation, the effective value $I_{eff}$of the current is equal to:

$$I_{eff} = \frac{1}{\sqrt{(R_{ant} + R_l)^2 + (X_{ant} + X_l)^2}} V_{\text{equi eff}} \quad (3.8)$$

We can encrypt the actual power delivered by the generator (the antenna) to the load R_l arranged at its terminals. The general equation of this one is equal to:

$$P_{l\ eff} = R_l {I_{eff}}^2 \quad (3.9)$$

$$P_{l\ eff} = R_l \frac{{V_{\text{equi eff}}}^2}{(R_{ant\ t} + R_l)^2 + (X_{ant\ t} + X_l)^2} \ (w) \ (3.10)$$

By deferring in the equation (3.1):

$$\sigma_e = \frac{R_l \,.\, {V_{\text{equi eff}}}^2}{s[\ (R_{ant\ t} + R_l)^2 + (X_{ant\ t} + X_l)^2]} \ (w) \ (3.11)$$

Between any torque generator/load, the maximum power provided in the load will be achieved when the combined adjustment condition between the impedances of source Z_{antt} and Z_l charge, (Figure 1) i.e. $R_l = R_{antrayounnemnt} + R_{loss}$, $X_l = -X_{antt}$, $R_{loss} = 0$,$P_{antt} = P_{charge}$.

In this specific case, it comes:

$$P_{l\ eff\ max} = \frac{R_{ant\ t}}{(R_{ant\ t} + R_{ant\ t})^2} {V_{\text{equi eff}}}^2 = \frac{1}{4R_{ant\ t}} {V_{\text{equi eff}}}^2 = \frac{1}{4R_l} {V_{\text{equi eff}}}^2 \ (3.12)$$

Then the equation (3.11) becomes:

$$\sigma_{\ e} = \frac{{V_{\text{equi eff}}}^2}{s \times 4R_l} ou \ \ \sigma_{e\ t} = \frac{{V_{\text{equi eff}}}^2}{s \times 4(R_{ant\ t})} (m^2) \ (3.13)$$

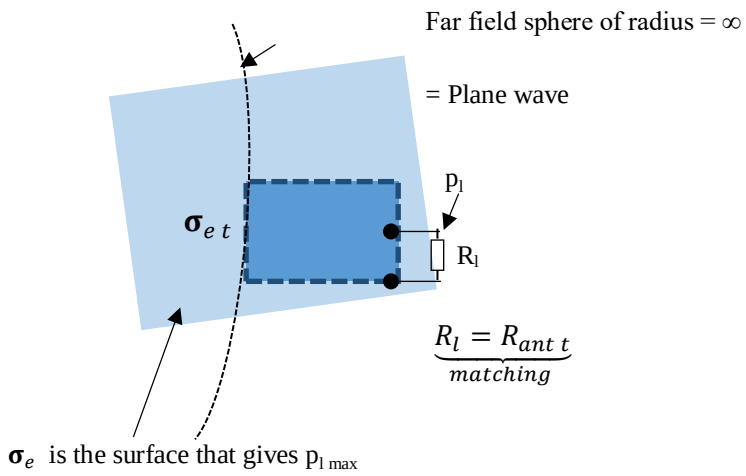

Figure 33: Effective Area of Receiving the Power of the Tag

Note: $R_l = R_{antt}$,

$$V_{equieff} = 2V_{reff} = 2\sqrt{p_{teff}R_l}$$

The maximum power for $R_l = R_{ant\,t}$:: you have the current

$$I = \frac{V_l}{R_{ant\,t} + R_l} \qquad (3.14)$$

The PD at the terminals of the load resistance R_l is therefore

$$V_l = R_l \frac{V_l}{R_{ant\,t} + R_l} \qquad (3.15)$$

The power dissipated in it has the expression:

$$P_{R_l} = V_l I \qquad (3.16)$$

For$R_{antt} = R_l$, and the function $P_{R_l} = f(R_l)$ goes through a maximum for this value, which has the value:

$$P_{R_l} = \frac{{V_l}^2}{4R_l} \qquad (3.17)$$

3.2.5 Friis Equation

Also within the framework of effective surfaces definitions (conjugate adaptation of impedance between antenna and charge→($P_l = P_{antt}$)), in order to obtain the maximum power value available at the tag antenna terminals, let us now postpone σ_{et} in the equation of the($P_t = \sigma_{et}.s$). By posing out of simplicity of writing $P_{ant} = P_t$,

By [84], it comes:

$$P_{t\,eff} = \sigma_{e\,t}.s_{eff} = \mathrm{P}_{bs\,eff}\mathrm{G}_{bs}(\frac{\lambda}{4\pi \mathrm{r}})^2\mathrm{G}_{ant\,t} = \mathrm{P}_{\mathrm{l\,eff}}(\mathrm{w}_{\mathrm{eff}}) \quad (3.18)$$

In case the load is not adapted during the introduction of power mismatch factor$q$, the general equation will become:

$$P_{t\,eff} = \mathrm{q}\ \mathrm{P}_{bs\ EIRP\ eff}(\frac{\lambda}{4\pi \mathrm{r}})^2\mathrm{G}_{ant\,t} = \mathrm{P}_{l\ \mathrm{eff}}(\mathrm{w}_{\mathrm{eff}}) \qquad (3.19)$$

Before examining in detail the relations between powers emitted, minimum operating distances, let us define in a few words what globally qualifies and characterizes the tag and integrated circuit that composes it.

3.2.6 Sensitivity of the Tag

Sometimes, the minimum effective power required (P_{min}) to allow the effective surface of the antenna $\sigma_{et}$to collect from the tag to start working properly, is called tag sensitivity. Due to the low impedance of the antenna, the power required to operate the circuit is a function of the voltage required by the integrated circuit and the impedance of the antenna. In fact, the minimum power $P_{min}, = P_{tmin}$, is defined as the minimum power required by the integrated circuit of the tag, so to allow the

adaptation to work properly, the following parameters in particular should be determining:

- The value of the maximum operating distance of a particular tag for a given powerP_{bsEIRP};
- Power $P_{bsEIRPmin}$ that the base station should be deliver to obtain a desired operating distance;
- Should be the minimum value of the electric field E_{min} to operate a given tag at a determined distance.

3.2.7 The Maximum Theoretical Distance for the Remote Power Supply and Operation of a Given Tag

This problem is certainly the most classic and the most frequent that opposes the user of tags in UHF. It is located in the frame in which the parameters of the base station imposed P_{bsEIRP}, and the consumption performance of the tag P_{tmin} necessary for its operation known. In this context, the theoretical maximum value of the Friis equation can written as follows:

$$r_{max} = \frac{\lambda}{4\pi}\sqrt{\frac{P_{bs\ cond}}{P_{t\ min}} G_{ant\ bs} G_{ant\ t}} \qquad (3.20)$$

3.2.8 Minimum Power Pbseirp That the Base Station Should Supply For Correct Operation of the Tag at the Distance R

Conversely, for the least efficient tag to operate correctly at a determined distance$r$, the base station must radiate a minimum power $P_{bs\ EIRP\ min}$ able to capture in order to deliver at least the minimum power $P_{t\ min}$ necessary for its proper functioning. Let us go back to Friss's equation:

$$P_{bs\ EIRP\ min} = \frac{P_{t\ eff}}{G_{ant\ t}}\left(\frac{4\pi r}{\lambda}\right)^2(w) \qquad (3.21)$$

The minimum value of the voltage ($V_{reçue\ min}$) is necessary for the proper functioning of the tag. In other words, the voltage applied to the pins/pads connection of the integrated circuit of the tag must exceed the minimum required threshold voltage ($V_{ic\ min\ eff}$; often noted$V_{ic\ threshold}$) indicated by the manufacturer. Let's take the LXMS31ACNA-010 circuit as an example; the data sheet of this product indicates that it requires the minimum operating threshold power of$P_{ic} = -8dBm$ @ 915 MHz, and at this frequency the complex value of its input impedance is equal to($Z_{ic} = R_{ic} - jX_{ic}$). This is the equivalent of a circuit consisting of a serial resistor arranged in series with a capacitance of $X_{ic} = \frac{1}{c_{ics}\omega}$ with c_{ics} (Figure 34).

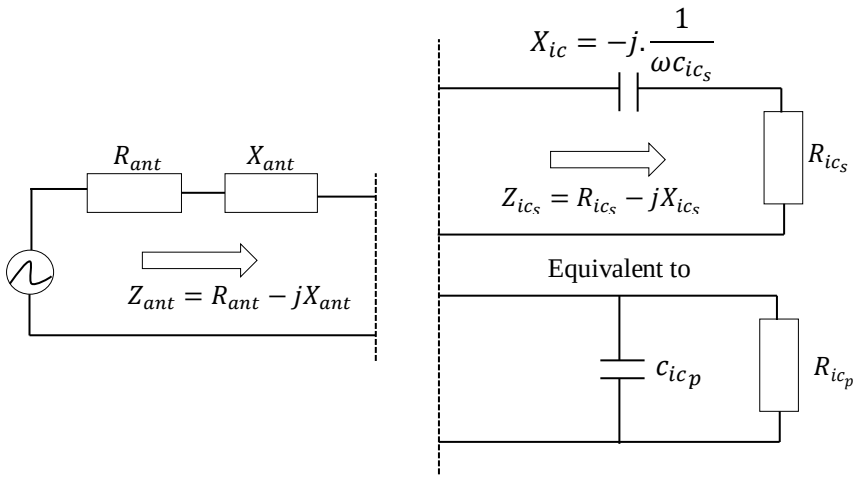

Figure 34: Equivalent Diagram of the Input Impedance of a UHF Integrated CircuitThe value of the quality coefficient $\boldsymbol{Q_{ic_s}}$ of the integrated circuit is equal to:

$$Q_{ic_s} = \frac{X_{ic_s}}{R_{ic_s}} \rightarrow Q_{ic_s} = \frac{1}{R_{ic_s} c_{ic_s} \omega} \qquad (3.22)$$

By definition, the effective power it is fully dissipating in the resistor. Knowing that $P_{ic} = R_{ic_s} {I_{ic_s}}^2$ is the equivalent current flowing through the resistor ($I_{iceff} = \sqrt{\frac{P_{ic}}{R_{ic_s}}}$).

Since this current flows in the series circuit R_{ic_s} , c_{ic_s}, the potential difference V_{iceff} developing at the terminals of this set will be equal to $V_{iceff} = |Z_{ic}|.I_{iceff}$. of course $||Z_{ic}| = \sqrt{R_{ic_s}^2 + X_{ic_s}^2}$, noting the strong predominance of the impedance of the capacitance $V_{iceff} = \sqrt{R_{ic_s}^2 + X_{ic_s}^2}.I_{iceff}$. If an equivalent parallel configuration of the integrated circuit input with the same wattage power that has been envisaged and dissipated in this one, would represent an equivalent parallel resistance:

$$P_{ic} = \frac{V_{ic}^2}{R_{ic_p}} \rightarrow R_{ic_p} = \frac{V_{ic}^2}{P_{ic}} \quad (3.23)$$

3.2.9 The Back Scattering Technique

The receiving antenna of the base station (which is often the same as that of transmission) detects the power reflected or reradiated P_s by the tag via the value of the powers surface density s_s. It can thus serve as a concrete signal that informs about the presence or absence of an object/tag in the electromagnetic field. Moreover, during its illumination, considering the provided tag modulated to answer in a precise way by means of a specific modulation, we could reinvent a communication device called back scattering modulation. It is therefore interesting to analyze how to vary/modulate the RCS and to quantify the value of its variation ($\Delta\sigma_{es}$s) according to a possible coding and a particular modulation, which will make it possible to characterize its aptitude to understand correctly from the base station.

Generally, with exceptions, the communication model according to how the standardized RFID-UHF systems works, resides in the principle of RTF (Reader Talk First) and in half-duplex mode (alternative link between base station and tag). The decomposition of all the phases of operation of the transmission can examined in the following paragraph.

3.2.9.1 The Forward Link: Communication from the Base Station to the Tag

The base station transmits the carrier frequency to tele-feed the tag. Simultaneously, during this phase of operation, the carrier is modulated (ASK - Amplitude Shift Keying) to ensure the transmission of command and interrogation codes to the tag. During this phase, the tag illuminated by the incident electromagnetic wave may, depending on the state of its antenna/load impedance matching, absorb the maximum possible power (thus "non-existence of standing waves"), or re-radiate part of the received power according to its "structural" aspect. This is effective in order to achieve the best possible remote power supply, and thus to obtain the greatest possible operating distance, as shown in (Figure 35).

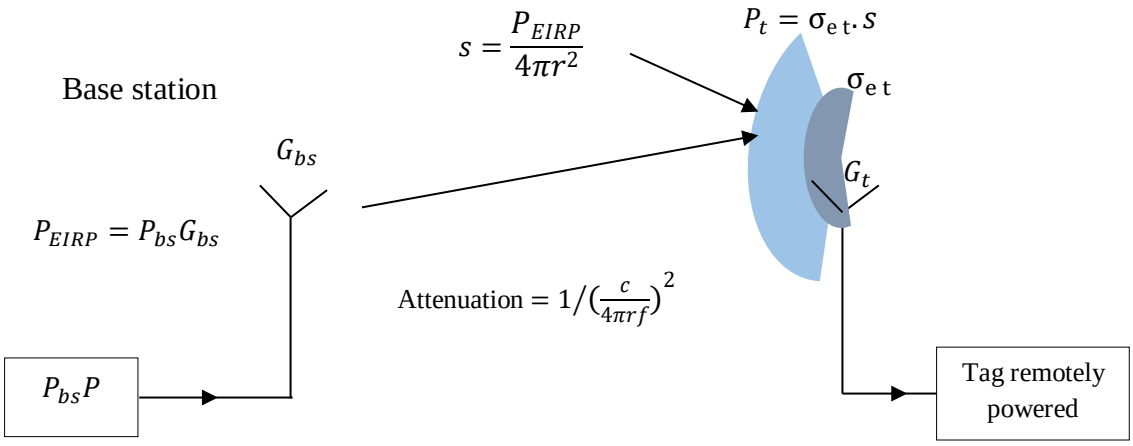

Figure 35: Back Scattering, Forward Link

3.2.9.2 The Return Link: Communication from the Tag to the Base Station

During the second phase of the so-called return link half-duplex coming from the tag, the base station provides or maintains the pure (unmodulated) carrier frequency to provide physical support for the tag response, following previous query commands. During this downlink phase, two sub-phases of operation may occur depending on the binary information transmitted from the tag to the station base: (i) either the sending of any useful information or even the sending of a logical "1"

(uplink) is the sending of a logic "0" (adapted tag descendant). In this case, the electronics present on board the tag will perform a modulation of the value of the load impedance ($Z_l = R_l + X_l$) of the tag antenna at the rate of a corresponding modulation to the logical data to be transmitted. At the tag level, there will be an impedance mismatch between the source (antenna tag) and its load, which produces the standing waves and a new effective radar surface value. Therefore, a variation of the surface RCS, which will have the immediate effect on modifying the amount of power (Figure36).

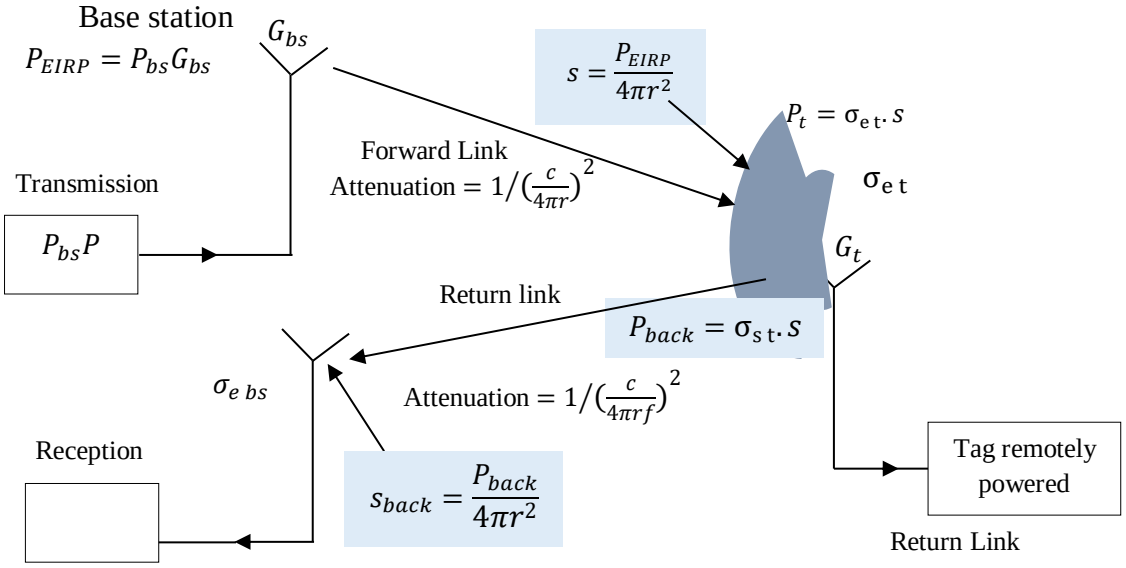

Figure 36: Back Scattering, Return Link

The phenomena produced by the tag during the downlink (the phase of modulation of the return wave such as the transmission of a logical "0" datum from the tag) starting from the conditions of optimal adaptations quoted previously. When we change the value of the impedance of the load out of the conditions of optimal adaptations. As already indicated, the fact of deliberately modulating the impedance of the tag load *(Z_l)* will causes a mismatch of impedances between source and load, as well as, emerging a phenomenon of wave radiation. Accordingly, the problem of

impedance modifications could be also inspecting within the aspect of "distributed constant line" by quantifying this mismatch using the reflection coefficient.

3.3 Realization of a Platform Measurement for UHF RFID Tags Characterization

The important parameter for evaluating the performance of a UHF tag along with radiation properties is describe in the previous section. Knowing the properties of UHF tags is of great importance. In this section, a basic validation of the theoretical definition will be describing. To this end, a radio propagation model for passive UHF RFID system is proposed (Figure 37). This system is consist of tag and reader antennas placed along a straight horizontal line at a "d" distance, large enough to guarantee the far-field condition.

3.3.1 Tag Sensitivity

By using the Friis equation, the power reaching the RFID chip given by [86]:

$$P_{chip,friis}(\theta,\varphi) = P_{tx}.G_{tx}.G_{tag}(\theta,\varphi).\tau\left(\frac{\lambda}{4\pi d}\right)^2.\eta_{plf}.A_{cable} \quad (3.24)$$

Where; P_{tx} is the power transmitted from the reader, G_{tx} is the maximum gain of the reader antenna. $G_{tag(\theta,\varphi)}$ is the tag antenna gain. λ is the wavelength. d is the distance between RFID tag and reader. η_{plf} is the polarization loss factor depending on the tag antenna structure. A_{cable} is the attenuation due to the cable connecting reader and antenna. τ is power transmission coefficient between tag antenna and RFID chip.

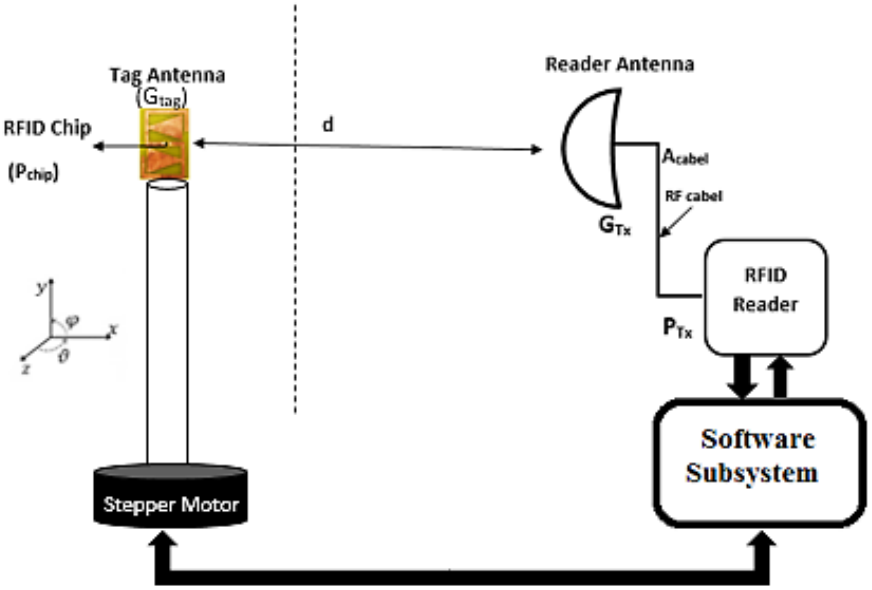

Figure 37: Radio Propagation Model for a Passive UHF RFID System Using Friis's Equation

From equation (3.24), the important parameter quantifying the performance of the RFID tag can be deriving. In particular, by gradually increasing the reader emitted power. It is possible to experimentally determine the so-called tag activation power threshold, $P_{txON(\theta,\varphi)}$, which represents the minimum power emitted by the reader at which the tag starts working. When a power as large as $P_{txON\ (\theta,\varphi)}$ it is emitting, power at the chip terminal becomes the chip sensitivityS_{chip}. This later is constant and represents an intrinsic characteristic of the RFID chip, hence, (3.24) becomes:

$$S_{chip} = P_{tx,ON}(\theta,\varphi).G_{tx}.G_{tag}(\theta,\varphi).\tau\left(\frac{\lambda}{4\pi d}\right)^2.\eta_{plf}.A_{cable} \quad (3.25)$$

Where; $P_{txON\ (\theta,\varphi)}$, is an angle dependent parameter, because if the interrogation angle changes, the minimum reader emitted power activating the tag change. S_{chip} is not adequate to quantify the goodness of the assembled tag, which definitely depends also on the quality of the tag antenna and on the quality of the conjugate matching between antenna and chip. A significant metric, already introduced in literature, is the sensitivity of the whole tag, S_{tag}, which defined as:

$$S_{tag}(\theta,\varphi) = \frac{S_{ship}}{\tau.G_{tag}(\theta,\varphi)} \quad (3.26)$$

Note that the lower the tag sensitivity is the better is the tag. Starting from (3.24), the tag sensitivity can derived as a function of the tag activation power threshold, $P_{\text{txON}(\theta,\varphi)}$,

$$S_{chip} = \frac{S_{ship}}{\tau.G_{tag}(\theta,\varphi)} = P_{tx,ON}(\theta,\varphi).G_{tx}.\left(\frac{\lambda}{4\pi d}\right)^2 = \eta_{plf}.A_{cable} \quad (3.27)$$

It is worth highlighting that the tag sensitivity evaluated in (3.24) is an angle-dependent parameter. Nevertheless, it could also be a useful performance evaluation when varying the frequency, in order to verify the capability of a tag to work properly worldwide. By keeping the angle constant, the frequency-dependent tag sensitivity can be writing as:

$$S_{tag}(f) = \frac{S_{ship}}{\tau(f).G_{tag}(f)} = P_{tx,ON}(f).G_{tx}.\left(\frac{\lambda}{4\pi df}\right)^2.\eta_{plf}.A_{cable} \quad (3.28)$$

3.3.2 Maximum Tag–Reader Range

In this part, we calculate the maximum read range that can be detecting when the reader antenna emits the maximum power by using the equation (3.29).

$$d_{max} = \frac{\lambda}{4\pi}\sqrt{\frac{P_{tx,max}(f).G_{tx}.\eta_{plf}.A_{cable}}{S_{tag}(f)}} \quad (3.29)$$

Where; $P_{tx,ON,min} = \min\{P_{tx,ON(\theta,\varphi)}\}$ is the minimum reader power activation on RFID tag antenna, when among all the minimum reader power values with variation of θ and φ.

3.3.3 The Calculation of Radiation Pattern

The radiation pattern can be calculate for a generic RFID tag using the formula (3.30):

$$RP = \frac{G_{tag}(\theta, \varphi)}{G_{tag,max}} \tag{3.30}$$

From formula (3.24), it follows that:

$$G_{tag}(\theta, \varphi) = \frac{S_{chip}}{\tau . S_{tag,min}(\theta, \varphi)} \tag{3.31}$$

$$G_{tag,max} = \frac{S_{chip}}{\tau . S_{tag,min}} \tag{3.32}$$

Then, the radiation pattern formula obtained:

$$RP = \frac{S_{tag,min}}{S_{tag}(\theta, \varphi)} = \frac{P_{tx,ON,min} . G_{tx} . (\frac{\lambda}{4\pi d})^2 . \eta_{plf}}{P_{tx,ON}(\theta, \varphi) . G_{tx} . (\frac{\lambda}{4\pi d})^2 . \eta_{plf}}$$

$$= \frac{P_{tx,ON,min}}{P_{tx,ON}(\theta, \varphi)} \tag{3.33}$$

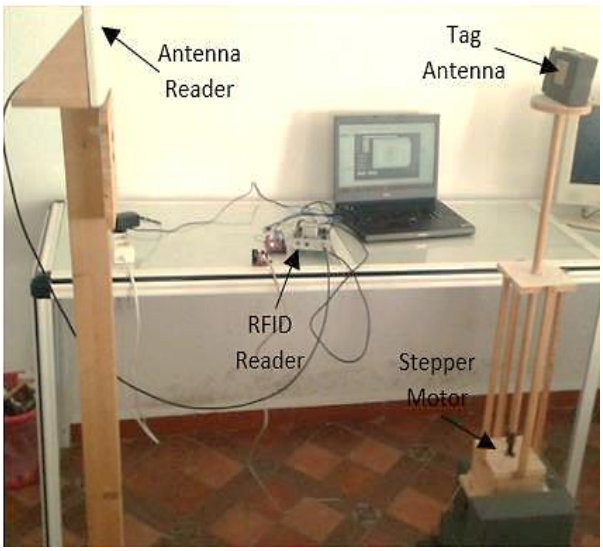

Figure 38: Implemented Tag System Measurement

Figure 38 shows the architecture of the proposed platform for measuring the performance and evaluation of the RFID tag sensor in the real condition. This system consists of two main blocks:, a software system where it is able to conduct RFID tag with automatic marking position, and a device system where the measurement procedure coordinates and calculates the required measurements.

3.4 Description of the Platform Measurement System.

3.4.1 Hardware Subsystem

In this research, we have used a subsystem, which mainly consists of a programmable and updated reading board known as ThingMagic Mercury 6e (M6e) [85]. This panel consists of 4 ports GPIO connected to other controllers, and a suitable USB interface port for programming and controlling, as well as 4 RF ports where the front end of the RF input capacity ranges from 5 to 31.5 dBm by 0.5 dBm for each port and at each step.

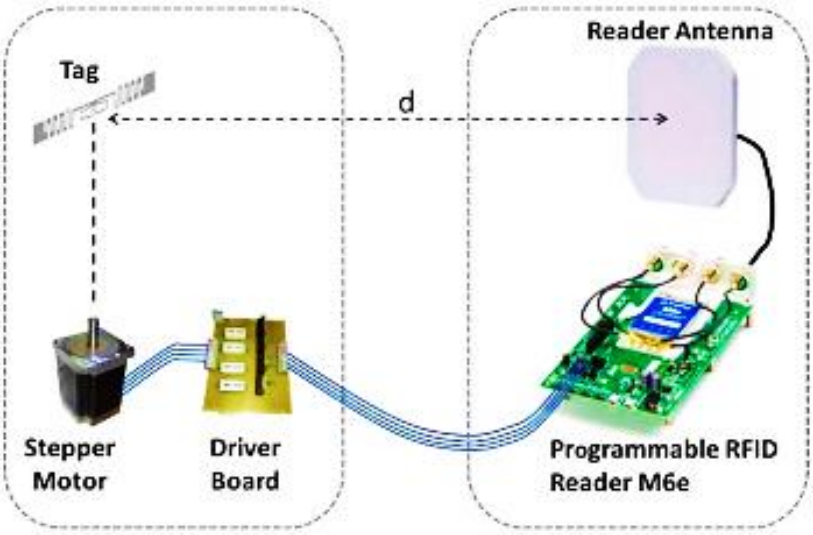

Figure 39: Hardware Subsystem

M6e Reader works in the European frequency bandwidth RFID (865-863 MHz), by implementing the established standards for ETSI systems to work, and also the American frequency bandwidth FID (902-928 MHz) prescribed by the FCC standard with a capacity to change the frequency by 1 MHz in each used system.

From (Figure 39), the architecture of the designed hardware subsystem connected to the RF port of the M6e reader with a circular polarized patch antenna a gain of 5.1 dB over connected by 1.8 m of coaxial cable model 50 CNT-195-FR. The driver, specially designed based on the MOSFETs, connected via GPIO interface, the last is necessary to rotate off the motor stepper in separate steps accurately and at a constant pace.

To achieve precision and control its mechanical properties, the Brother model unipolar motor KE58KM2-032 was selected. The minimum angular step of this rotating motor is only 1.8 degrees, so you can get a satisfactory number of 200 measurement points per whole cycle

3.4.2 Software and Control Subsystem

As theorized and asserted in Section I, the proposed measurement platform for evaluating the performance of UHF RFID tags is based on the individuation of the tag activation power threshold. This power threshold is the minimum power emitted by the reader in correspondence of which the RFID tag, therefore, capable of sending back its EPC code as feedback. In order to implement an algorithm that iteratively detects such a power threshold, specific software was designed to drive the hardware subsystem in terms of emitted power, frequency, stepper motor angular position, and so on.

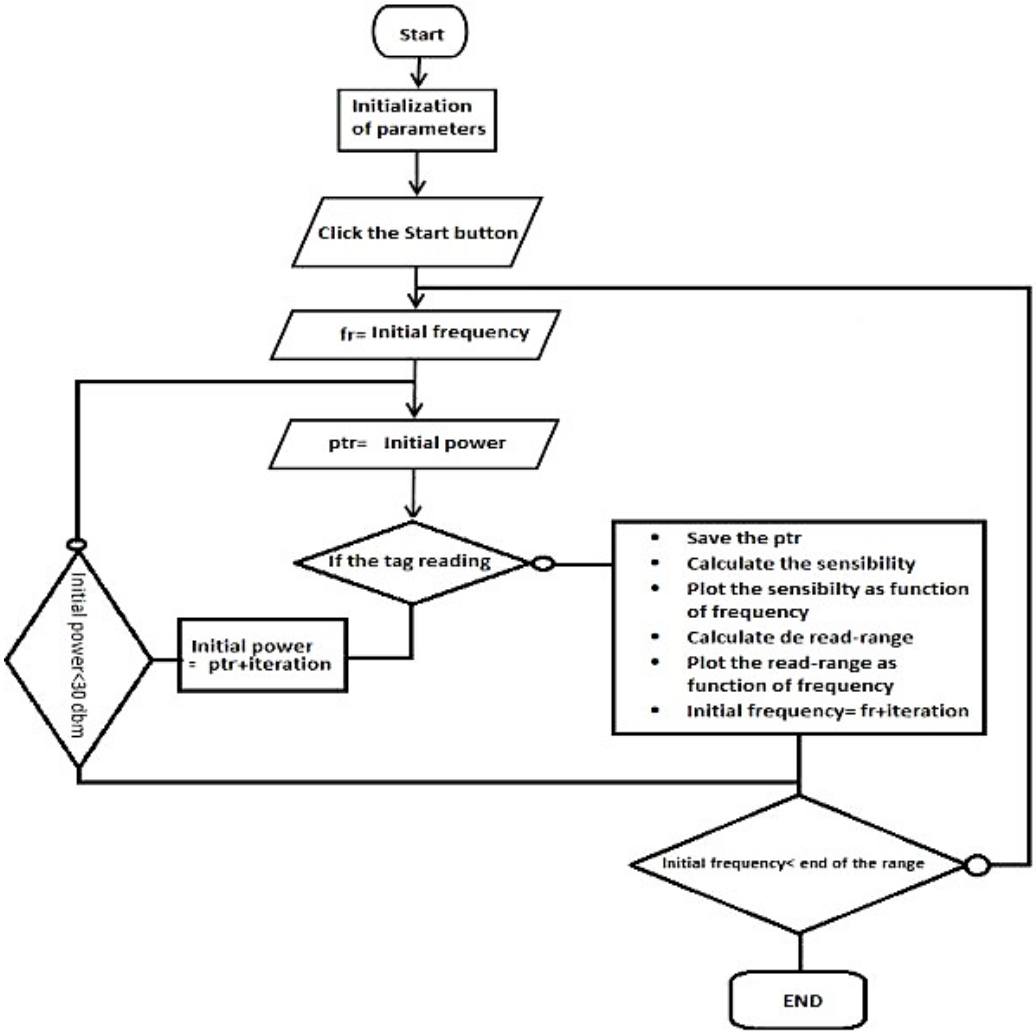

Figure 40: Organization Chart of the Proposed RFID Tag Characterization Platform

In practice, to measure the effectiveness of the control and rotation system, the activation limit of the RFID tag should be assigned to linear scanning of all reader's power values (from 5 to 31.5 dB) in incremental steps of 0.5 dB until the minimum activation is reached (Figure 39). The tag starts working despite this simplicity in the scaling ratio; this approach is computationally complex and takes a long time due to the large number of iterations, changing the ratios of reader values that may occur at every angle. In fact, to obtain a comprehensive characterization of the mark, the algorithm must be repeated for each angle step (corresponding to the minimum stepping of the stepper motor at a fixed angle of 1.8 degrees).

The Organization chart of the proposed RFID tag characterization platform presented in (Figure 40). The algorithms based on probabilistic consideration of the expected energy value were achieved, which reduce the number of times it is repeated to detect the threshold of mark activation. In fact, there are always very close ratios of angular steps, and also the frequency steps are smaller. For instance, let us assume that the values of the activation power of the mark and the angular steps or adjacent frequency are proportional. This assumption can lead us to the idea that the proposed algorithms or adjacent frequencies are proportional. The proposed algorithms can retain the activation of the observed mark at any stage of the measurement, whether it is an angle step or a frequency step, they store this value and use it as the starting value of the step. Next in measurement, this strategy allows us to quickly explore the starting energy value using the minimum mark activation capabilities at each step of measurement.

In order better understand the reader operation mode; the pseudo-code of the proposed algorithm is set out in (Figure 41). The maximum available range (equivalent to 30 dB) in the second stage is function of the connection made. In the case of the marker detection, the reader works to reduce the energy ratio until the inferior energy is reached to make the mark in that band. Then either the frequency value or angular position determine by user interface graphic had been developed to see the radiation pattern, read range, read pattern, in real-time (Figure 42). The same procedure is applied iteratively by setting the energy value of the marker activation in a given step as the starting value for the next value. Finally, once the activation threshold is detected for all measurement steps, all the individual metrics in Section II are calculated directly according to Formulas (3.28), (3.29), (3.31) and (3.32).

```
set power =30 dBm
set flag= false
try to read
     if ( not read)
         {
           power= power+0.1
           try to read the tag
            if ( read)
            {
             flag= true
             calculate metrics
             save
             }
            }
        }
elseif (read)
       {
          while (flag== power)
          {
          power=power-0.1
           try to read the tag
 if (not read)
 flag= true
 calculate metrics
 save
   }
 }
}
```

Figure 41:Pseudo-Code of the Implemented Algorithm

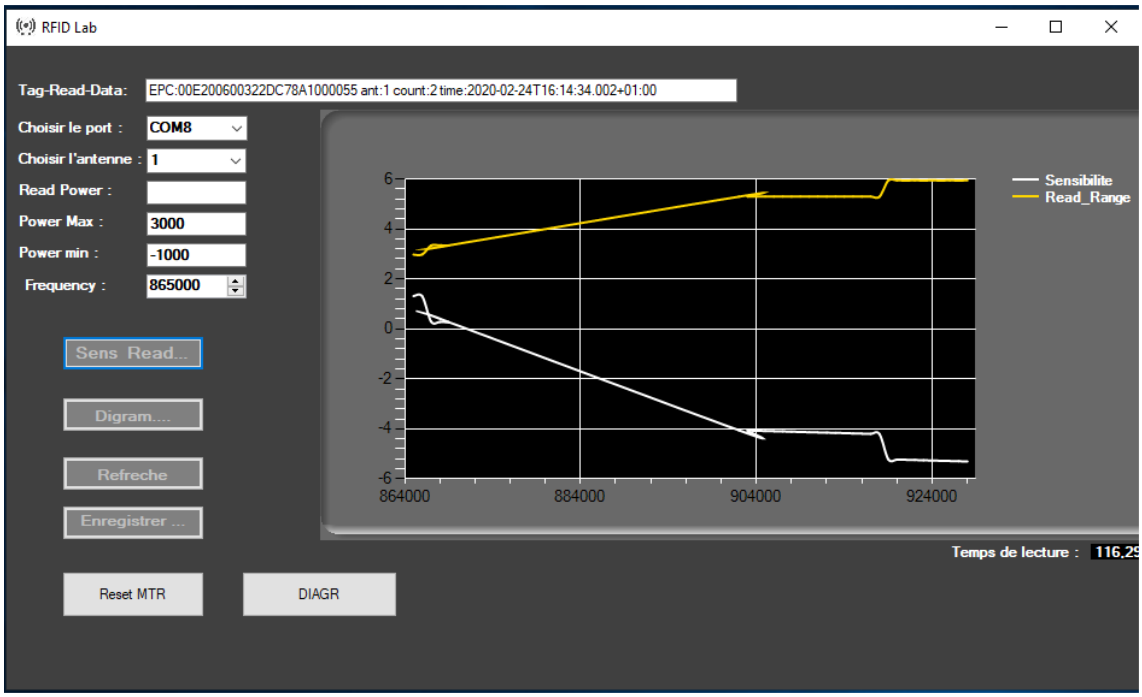

Figure 42: Interface Graphic

3.5 Validation Measurement Platform in Real Condition (Real Condition)

In this section, the performance of the proposed system was checked by comparing the measurements with the results obtained through the Brand Configuration Tool and the electromagnetic simulator (CST). These tests are based on

the ability of the system to perform the magnetic characterization of any RFID tags when placed in all directions. With the ease to use of this automated system, the results obtained by the reader were presented and compared with similar systems. In the next chapter, a detailed description of our system will be given and also the results obtained from the CST for the same RFID tag. The latter was set on the frequency of 915 MHz, the results (Figure 45) are in a perfect agreement, which shows the proposed system's ability to estimate the radiation pattern marks RFID properly. Alternatively, (Figure 44) indicates the same type of comparison that is made in terms of the sensitivity of the mark when changing the frequency in the entire RFID band. The very good compatibility between the results obtained again confirms the suitability of the proposed characterization platform in the case of sensitivity assessment as well as the vertical radiation pattern, which was calculated by equation (3.32). The pattern of radiation obtained by CST is then compared with measurement results. These results chart show that it is very compatible.

We compared the obtained results using our platform and the results obtained by the classical platform measurement system (LCIS lab-INP, Valence, France), regarding the sensibility (power activation de tag) and reading range. For measuring the effectiveness of the platform, an RFID tag antenna under test was used (Figure 43) which will be introduced in chapter 4.

Figure 43: Proposed RFID-UHF Tag Antenna

Figure 44 shows an optimal agreement between our platform measurement and the classical platform measurement system (LCIS lab-INP) around the sensibility and the reading range where the rate of convergence about to 90%.

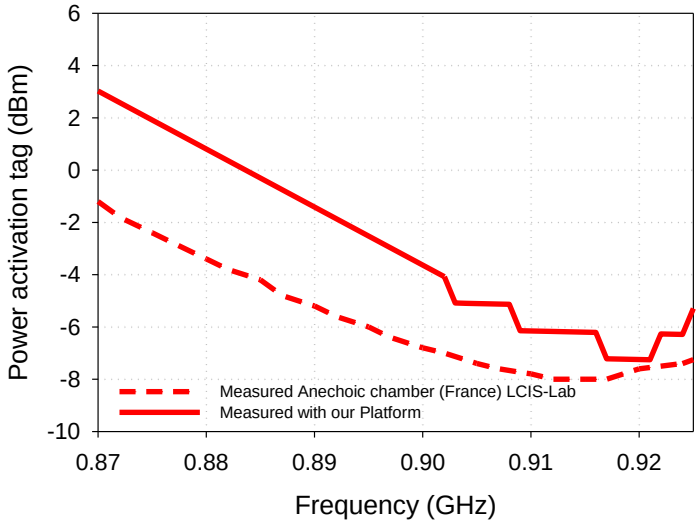

(a)

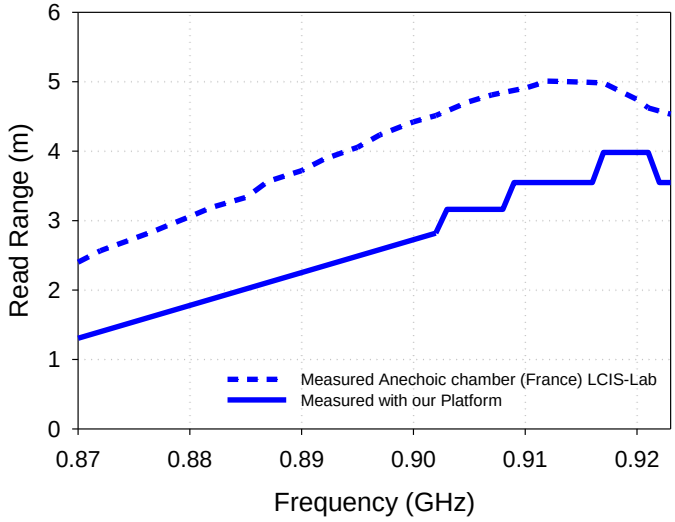

(b)

Figure 44: Comparison between the Classical Platform Measurement System (France) LCIS-Lab Instrumentation and Proposed Measurement System: (a) Sensitivity, (b) Read Range

Figure 45 shows the comparison between the radiation pattern of the tag in the Horizontal and vertical direction the platform in the free space at 915 MHz with that of the graph obtained with CST. A good similarity between the two diagrams is noted.

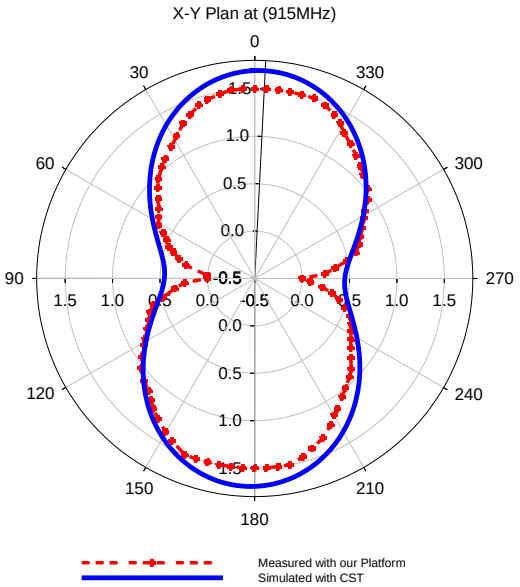

(a)

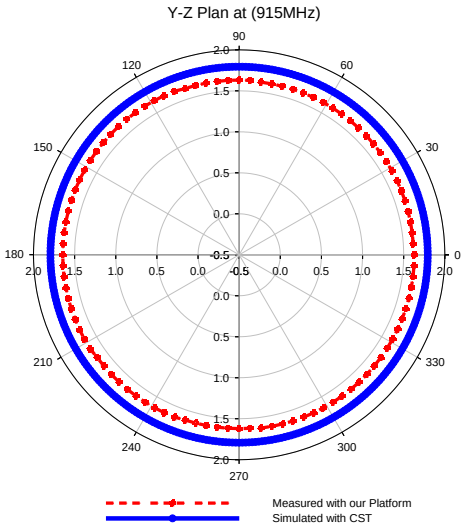

(b)

Figure 45: Measured and Simulated Radiation Patterns of Tag: (a) Vertical Radiation Pattern, (b) Horizontal Radiation Pattern

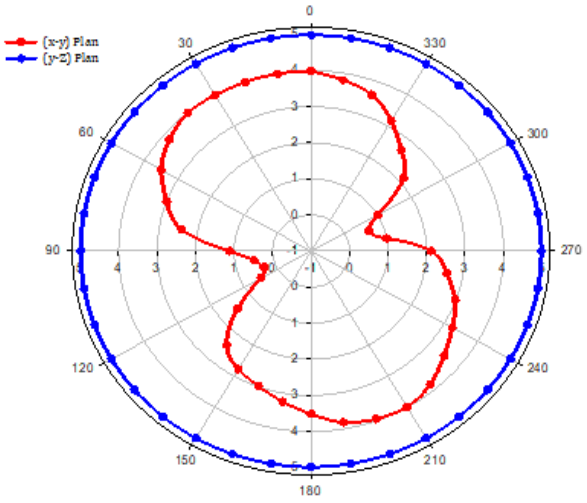

Figure 46: Measured Read Patterns of the Tag Using Our Platform

Figure 46 represents the measured read patterns of the tag using our platform of the mark in the vertical and horizontal direction in free space. We note that the results are very satisfactory for this tag.

3.6 Conclusions

In this chapter, a low-cost automated RFID tag antenna measurement was set-up based on UHF-RFID reader for UHF tags evaluation. The proposed approach uses a commercial multi-programmable UHF RFID reader and a computer developer environment that allowed us to program different metrics characterizing an RFID tag as sensitivity, read-range, radiation pattern, and read pattern with the plot of graphs. The results obtained are evaluated with the classical platform measurement system (LCIS lab-INP the laboratory France) which shows the validity of the proposed platform.

Chapter 4

Design and Characterization of a Compact Single Layer Modified S-Shaped Tag Antenna for UHF-RFID Applications

4.1 Introduction

The literature review showed that few RFID tag designs have proposed to tolerate a range of materials. To overcome this shortcoming, in this chapter we report the design of a new compact single layer modified S-shaped tag antenna for UHF-RFID applications. To achieve a compact size of 51×34 mm^2 for this tag antenna, the technique of using S shaped strip is applied, and by further adding a pair of equilateral triangular stubs into this structure, good impedance matching can be obtained at 915 MHz, which is the center frequency of the North-American UHF-RFID band (902 to 928 MHz). Besides exhibiting acceptable 5m read range in free space at 915 MHz, the proposed design shows a read range of about 4.5 m when mounted on a metallic object ($200 \times 30\, cm^2$) separated by spacer foam of thickness 1 cm. Furthermore, the proposed design shows a reasonable read ranges when it is mounted on different materials . The proposed design has a simple configuration, low cost, acceptable read range, and can work on various background materials.

4.2 RFID Tag Antenna Design and Equivalent Circuit Model

The physical structure of this proposed design is simple and consists of two meandered strips that have the form of S-shaped structure, connected in the middle by a chip (Figure 47). To keep the antenna size compact and to get a good matching with the chip, both meandered strips are loaded with equilateral triangular stubs. All the strips are coated on a FR4 substrate with thickness of h=1.58 mm, relative permittivity$\varepsilon_r = 4.4$, and loss tangent $\delta = 0.025$. The top antenna trace was made of copper having a thickness of the35 μm. The total area of the proposed structure is$51 \times 43\, mm^2$, which corresponds to $(0.155\, \lambda_0 \times 0.13\, \lambda_0)$, where λ0 is the free-space wavelength at 915 MHz.

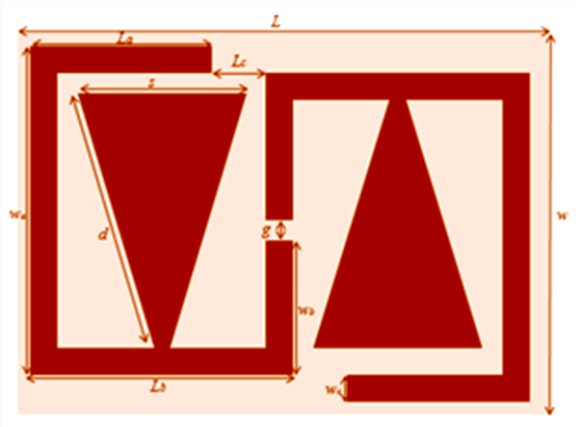

Figure 47: Structural Configuration of The Proposed RFID Tag Antenna

The proposed S-shaped modified tag antenna is designed to operate in the RFID-UHF band of 902– 928 MHz (North American Band). Murata LXMS31ACNA chip with an impedance of $Z_{Chip} = (17.6 - j100.9)\Omega$ at 915 MHz is selected for our design. The minimum threshold power to activate this chip is -8 dBm. Note that the impedance of the chip was measured using the same technique described in [87], which is a little different from the one ($Z_{Chip} = 12 - j107\ \Omega$) reported in the datasheet [88]. This discrepancy can be attributed to the accuracy of the method that we have used here

to evaluate the input impedance of the chip is different from the one used by the manufacturer. The input impedance of the antenna has to be $(17.6 + j100.9)\ \Omega$ to achieve a maximum power transfer. Thus, the final optimized geometrical parameters were obtained using a CST Microwave studio (Table 6).

Table 6: Dimensions of RFID Tag Antenna (mm)

L	La	L_b	L_c	w_a	w_b	w_c	W	D	g	s
51	*15.6*	*26*	*7.4*	*36*	*15.5*	*3*	*43*	*30*	*2*	*18*

4.2.1 Equivalent circuit model of the proposed tag antenna

The RFID chip used in this work exhibits a high capacitive reactance($Z_{Chip} = 12 - j107\ \Omega$), to overcome this issue, the technique of adding asymmetrical triangular stubs on both sides of the tag chip is introduced. In this case, the triangular stubs can be regarded as a short transmission line that is analogous to an inductive reactance connected in series to the tag, which in turn increase the inductive reactance of the antenna. Therefore, optimizing the parameters of the triangular stubs ($d\ and\ s$) appropriately can provide a good conjugate matching. To verify this conjecture, we have simulated the reflection coefficient of the proposed RFID tag antenna with and without the triangular stubs. The obtained results are presented in (Figure 48).

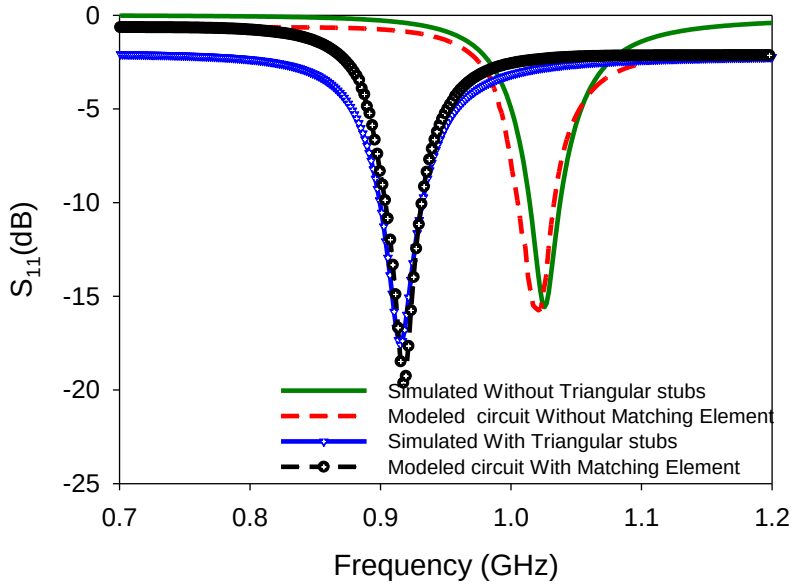

Figure 48: Modeled and Simulated Reflection Coefficient of The Proposed RFID Tag Antenna with and without The Triangular Stubs

One can see easily that without triangular stubs, a resonant frequency appears at 1.01 GHz. However, with the triangular stubs this resonant frequency shifts down to 915 MHz. This result reveals that the introduction of triangular stubs into the proposed structure has equivalent effect of increasing the electrical length of the antenna while keeping the same total size of the proposed design. Thus, we can conclude that the triangular stubs act as an inductor. To further explain the operating principle of the reactive matching of the proposed design, we have simulated the current distribution of the structure with and without the triangular stubs at 915 MHz which are displayed in (Figure 49) It can be clearly seen that adding triangular stubs increases the electrical length of the proposed structure, resulting in larger inductance effect in the structure.

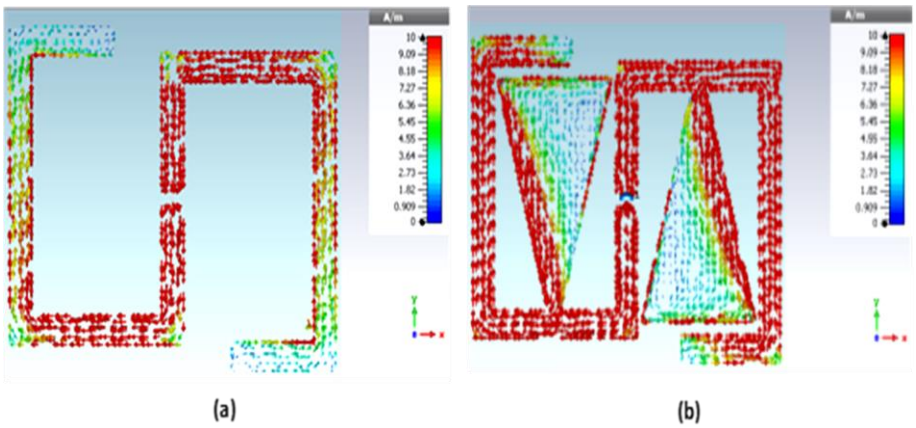

Figure 49: Simulated Distributed Current of The Proposed Structure with and without The Triangular Stubs at The Resonance Frequency.

Moreover, the reflection coefficient of the RFID tag antenna was modelled using a lumped elements circuit as shown in (Figure 50). For the sake of simplicity, the RFID chip and the antenna can be modelled as a series RC (R_{chip}, C_{chip}) and a series RLC circuit ($R_{ant}, L_{ant}, C_{ant}$), respectively. The lumped elements values have been obtained by using approximate equations, especially for the antenna. For example, according to [89], the radiation resistance for a small dipole can be approximated by

$$R_a = 80\pi^2\alpha^2\left(\frac{l}{\lambda}\right) \qquad (4.1)$$

Where $0.5 \leq \alpha \leq 1$ depending on how the current is distributed along the antenna, and l is the length of the antenna. By considering the working frequency of the antenna at1.01 GHz, the radiation resistance is supposed to be $R_{ant} = 15.9\ \Omega$ when α is equal to 0.6 and the length of the antenna is 93 mm. To find the inductance of the antenna, we can use the approximated formula given in [90]:

$$L_{ant} = \frac{\mu_0}{2\pi} l\left(\ln\left(\frac{l}{w}\right) + \frac{\pi}{2}\right) \qquad (4.2)$$

Where l and w are respectively the length and width of the conductive strip. The antenna capacitance can be obtained by using the self-resonant frequency of the

proposed antenna $f_c = \frac{1}{2\pi\sqrt{L_{ant}C_{ant}}}$ where Lant and Cant are the equivalent inductance and capacitance of the antenna structure respectively. Therefore the capacitance is given by:

$$C_{ant} \approx \frac{1}{\pi^2 f_c^2 L_{ant}} \qquad (4.3)$$

The value of Lant is then found to be $25.6\,nH$. From Eqs.4.1,4.2 *and* 4.3 we have approximate values for a series RLC circuit model of the proposed antenna (Figure 4). The equivalent circuit for MURATA RFID chip is a 17.6 Ω resistor in series with a $1.64\,pF$ capacitor. The two triangular stubs used as matching network can be modelled as a series inductance (L_{serie}). To demonstrate the validity of this lumped circuit model, the reflection coefficient ($S_{11}dB$) obtained by using a circuit simulator (Agilent's Advanced Design System) is compared with the 3D full wave simulation as shown in (Figure 50). The modelled results are in good agreement with the simulated data, confirming that the proposed equivalent circuit model is acceptable and accurate.

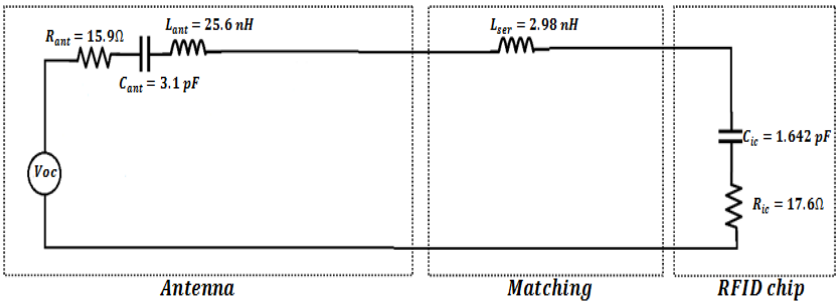

Figure 50: Equivalent Circuit Model of The Proposed RFID Tag Antenna

The slight different between circuit model and 3D full wave results. Especially after and before the resonance, can be ascribed to the fact that the circuit model proposed here is a simplified circuit model which allows an easy design of the proposed RFID

tag antenna near to the operating frequency band and doesn't take into account the behavior of the structure outside the operating band.

4.2.2 Parametic Study

4.2.2.1 Influence of The Parameter"d"

To find out the effect of the line width of the triangle "d" on the antenna resistance, we changed this parameter from 26 mm to 30 mm at step of 1 mm while preserving the other dimensions of the mark antenna described in Table 7.

According to (Figure 51), the increase in g value slightly changes the input resistance value and increases the antenna reaction value, making the imaginary part of the antenna more independent. The maximum power transfer between the antenna and the chip is achieved when$d = 30\ mm$.

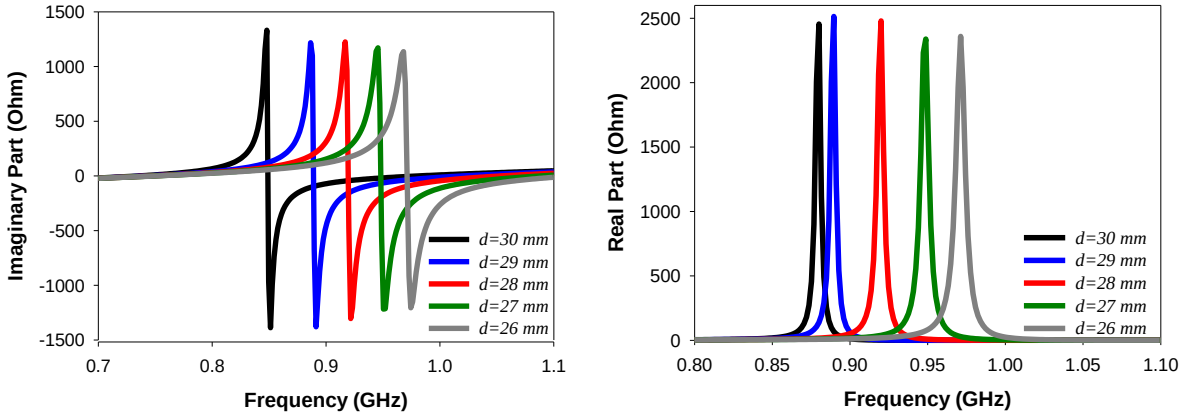

Figure 51: Influence of The Parameter "d" On The Input Impedance

The values of the real and imaginary part of the input impedance at 915 MHz are reported in Table 7.

Table 7: Simulation Results of The Influence Parameter "d"

Antenna Parameter (mm)	*Real Part (Ohm)*	*Imaginary Part (Ohm)*
d=26	*0.4488*	*-48.6916*
d=27	*7.6075*	*-185.7445*
d=28	*25.0612*	*155.6601*
d=29	*29.9558*	*226.1332*
d=30	*16.7238*	*154.3618*

4.2.2.2 Influence of The Parameter "S"

In this part, we propose to analyze the effect of the" S"parameter on the antenna input impedance. (Figure 52) illustrates its different values based on frequency. Note that in the $902-928\ MHz$ band, the actual part of the impedance increases, on the other hand the imaginary part increases. The values of the real and imaginary portion of the input impedance at 915 MHz are shown in Table 8. From this Table, we can see clearly that a better matchning between the antenna and the chip it is achieving in the case of $S = 18\ mm$.

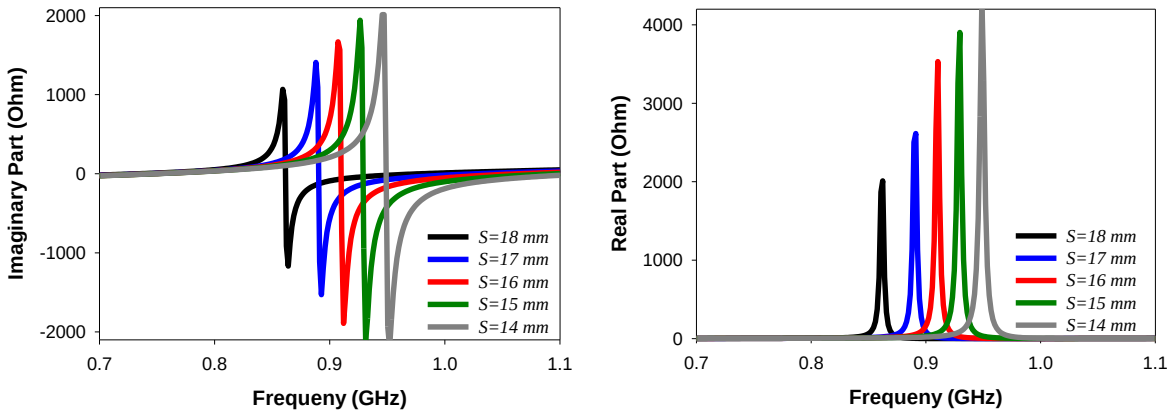

Figure 52: Influence of The Parameter "S" on The Input Impedance

The values of the real and imaginary part of the input impedance at 915 MHz are reported in Table 8.

Table 8: Simulation Result of The Influence Parameter "S"

Antenna Parameter (mm)	*Real Part (Ohm)*	*Imaginary Part (Ohm)*
S=14	*14.6*	*76*
S=15	*17.5*	*115.98*
S=16	*22.76*	*402.6*
S=17	*29.87*	*205.42*
S=18	*27.76*	*-80*

4.2.2.3 Influence of The Parameter "La".

In this part, we continue our parametric study, this time looking for the effect of the "La" parameter on the antenna input impedance. The obtained results plotted in (Figure 53) as a function of frequency. The values of the real and imaginary portion of the input impedance at 915 MHz are shown in Table 9. From this table, we note that better matching between the antenna and the chip was obtained in the case of $La = 15.5\ mm$.

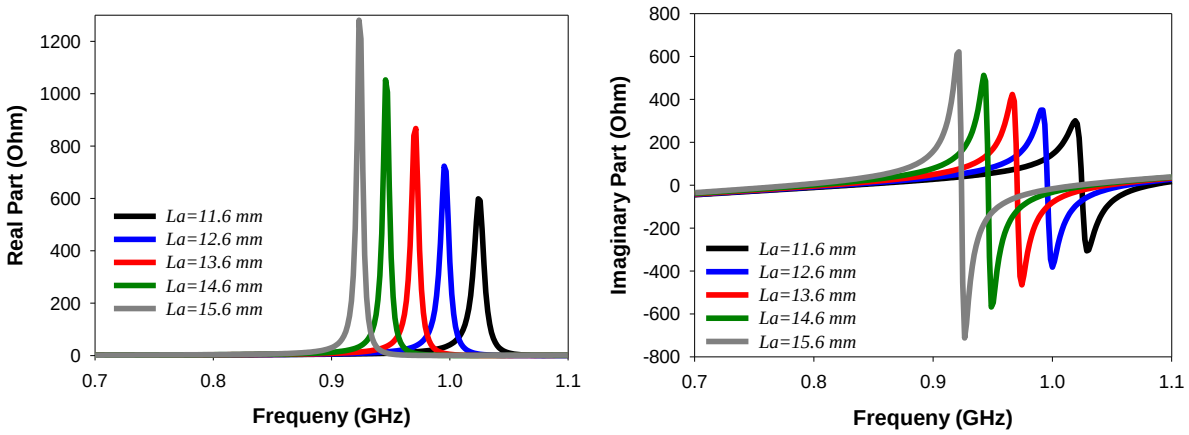

Figure 53: Influence of The Parameter "La" on The Input Impedance

The values of the real and imaginary part of the input impedance at 915 MHz are reported in Table 9.

Table 9: Simulation Result of The Influence Parameter "La"

Antenna Parameter (mm)	*Real Part (Ohm)*	*Imaginary Part (Ohm)*
La=11.6	*104.5*	*46.5*
La =12.6	*107.2*	*65.99*
La =13.6	*87.76*	*82.3*
La =14.6	*39.88*	*100.2*
La =15.6	*18.6*	*120.3*

4.3 Measurements Results and Discussion

4.3.1 Characterization of UHF RFID Chip Passive

Knowledge of the activation power and the input impedance of the RFID chips is necessary in design of RFID tag antenna to get a good conjugate matching and to guarantee a good communication with the reader. These RFID chips fabricated using various packages. A tiny unpackaged chip is frequently appling directly on a label-type tag. This makes the fabrication process easier and faster but it requires sophisticated fabrication appliances. An alternative packaging type is a tiny chip applied to conductive strip ready to implement inside the antenna. Another kind of packaging is SOT-323, which is bigger than the other kinds and has an acceptable area around5 mm^2. This kind of packaging is appropriate for prototype designs and lab works, which also used in the designs proposed in this thesis. Nowadays, there is another class of RFID chips in the market based on Quad Flat No-leads (QFN) package with integrated sensors to enable users to capture data such as temperatures, strain or weight, using a standard UHF RFID reader. The main groups of RFID chips packaging are depicted in (Figure 54).

Figure 54: Different Types of RFID Chip Packages

In this part, we introduce different techniques for measuring the input impedance of the RFID-UHF chip and the antenna. Initially, our study will focus on the characterization of the input impedance of the RFID-UHF chip using the technique described in [91]. Details of this technique will be given in the following section and the model of the chip used is LXMS31ACNA-010 [88]. Table 10 illustrates the impedance values provided by the manufacturer.

MAGICSTRAP® P/N / Parameter			LXMS31ACNA - 009 / LXMS31ACNB - 019	LXMS31ACNA - 010 / LXMS31ACNB - 020	LXMS31ACNA - 011 / LXMS31ACNB - 021	LXMS31ACNA - 012 / LXMS31ACNB - 022
Impedance value	@866.5 MHz	R	15	12	25	80
		X	-45	-107	-200	-405
	@915.0 MHz	R	25	12	25	80
		X	-45	-107	-200	-420
	@953.0 MHz	R	30	9	20	60
		X	-48	-105	-195	-425

Table 10: Impedance Value LXMS31ACNA-010 IC Chip

4.3.1.1 Electrical Model of RFID IC Chip Passive

The RFID-UHF chip has a complex input impedance composed of a real part and a negative imaginary part due to the capacitive input effect of the RFID reader detector. In general, the RFID-UHF chips can be modeled electrically by a circuit consisting of a resistor and a capacitor connected either in parallel by R_p and C_p or in

series R_s and C_s. Thus, the characteristic impedance of the RFID-UHF chip can be defined by:

$$Z_c = R_c - jX_c(\Omega) \tag{4.4}$$

From where we deduce the expression of resistance and reactance series and parallels of the RFID IC chip

$$R_s = R_e(Z_C), C_s = \frac{1}{(2\pi f I_m(Z_c))} \tag{4.5}$$

$$R_p = \frac{R_e(Z_C^2)+I_m(Z_c^2)}{R_e(Z_c)} \quad , \quad C_p = \frac{I_m(Z_c)}{2\pi f[R_e(Z_C^2)+I_m(Z_c^2)]} \tag{4.6}$$

The values of the LXMS31ACNA-010 chips at 915 MHz are reported in Table 11 as below.

Table 11: Impedance Value of The LXMS31ACNA-010 IC Chip

Frequency	*915 MHz*
Component	*LXMS311CN1-010*
$\boldsymbol{Z_c}$	$12 - j107(\Omega)$
$\boldsymbol{R_p, C_p}$	*697Ω, 1.61pF*
$\boldsymbol{R_s, c_s}$	*12Ω, 1.62pF*
$\boldsymbol{P_{min}}$	*-8dbm*

4.3.1.2 Experimental Description of The RFID IC Chip Platform Measurement

The measurement set-up used to characterize the impedance of the RFID-UHF chip is illustrated in Figure 11. The measurement is conducted using a two-port vector network analyzer (Agilent N5224A) and a SMA connector. The RFID chip is soldered on the inner and outer conductor of the SMA connector to form a test fixture without special matching. Before connecting this test fixture to the VNA, a classical calibration was done using thee electronic calibration module (ActECal) as shown in (Figure 55)

Figure 55: Calibration Kit Agilent ECAL Kit

After calibration, an analyzer check was carried out using a fixed weakens, adapted and unsuitable air lines based on known and calibrated values. It is a question of being able to completely characterize module and phase, reflection and transmission. First, the chip RFID (LXMS31ACNA-010) is connected to an SMA Connector as shown in (Figure 56).

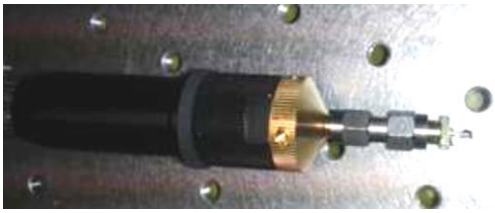

Figure 56:LXMS31ACNA-01 Chip Connected by SMA Connector

Second, and after de-embing, which eliminates the influence of the SMA connector when the chip is connected to the PNA network analyzer, the impedance of the chip was measured. (Figure 57) Shows the result plotted on a Smith chart.

Figure 57: Measured Impedance of The LXMS31ACNA Chip

4.3.1.3 Results and Discussions

Based on the results of the Smith diagram, the variation of the impedance of the LXMS31ACNA-010 IC chip is function of the frequency (Figure 58), ranging from 800 to 1000 MHz. The table 12 summarizes the values of impedance, resistances and reactance of the LXMS31ACNA-010 Chip at the measured resonance frequency 915 MHz for serial and parallel connection.

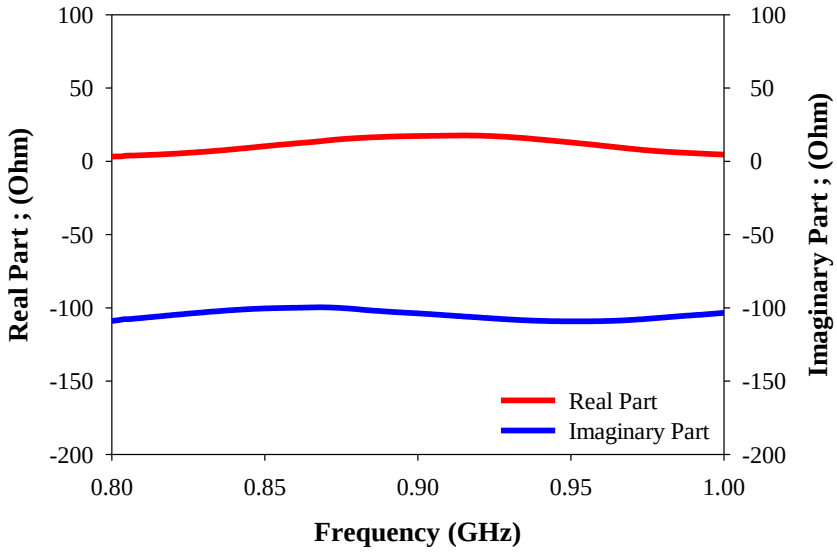

Figure 58: Variation Impedance of The LXMS31ACNA-010 IC Chip Depending as Frequency

Table 12: Measured Value Impedance of IC Chip RFID-UHF LXMS31ACNA-010

Frequency	*915 MHz*
Component	*LXMS311CN1-010*
$\boldsymbol{Z_c}$	$17.6 - j100.9(\Omega)$
$\boldsymbol{R_p, C_p}$	*597Ω, 1.72pF*
$\boldsymbol{R_s, c_s}$	*17.6Ω, 1.72pF*

In the above paragraph, the process of measuring the input-impedance of the RFID-UHF LXMS31ACNA-010 chip for a frequency range between 800 and 1000 MHz is presented. Comparing the values given in the data sheet (Table 11) and those obtained experimentally (Table 12), we notice a small discrepancy that is due to the choices of impedance measurement techniques and the tolerances of chip manufacturing. (Figure 12) shows a significant variation in the chip input impedance depending on the frequency. The frequency interval is also observed that the reactance always takes negative values indicating a capacitive behavior of the chip. These measurements are a starting point for the design of the RFID-UHF tag antennas.

4.3.2 Characterization of Passive UHF Tag S-Shape Antenna

4.3.2.1 Impedance Measurement: Differential Probe Technique.

The next step in designing the RFID tag antennas rely on the measurements of the Input impedance of the proposed antenna. The reflection coefficient and input impedance of the proposed RFID tag antenna was measured through a differential probe as shown in (Figure 59).

Figure 59: Differential Probe

This technique, adopted to determine the input impedance of the proposed antenna, involves the use of a test fixture probe. The impedance of a symmetrical antenna cannot be measured directly using asymmetrical ports, such as coaxial ports. When a balanced antenna is connected to an asymmetric test port, the currents on the antenna are not equal, and therefore it is necessary to use a balun and avoid leak currents. However, on a wide range of frequencies, the balun is not ideal and the measurement results may not be imprecise. The impedance of the balanced antenna can be expressed using the S parameters of the equivalent network. Using a coaxial device and port extension technique, the impedance of balanced antennas, seen as a two-port circuit, can be extracted directly from the measurement of S parameters. (Figure 60) shows an asymmetrical equivalent network of dipole antenna.

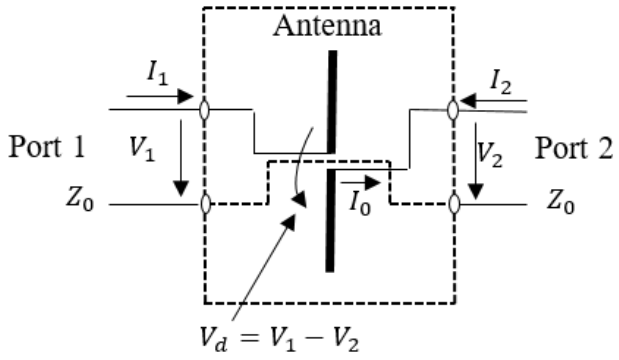

Figure 60: Asymmetrical Equivalent Network of Dipole Antenna

For the sake of clarity, we describe below the method proposed in [92].

The differential impedance of the antenna can be expressed as follows:

$$Z_d = \frac{V_d}{I} = \frac{(V_1 - V_2)}{I} \tag{4.7}$$

Based on the definition of Z parameters, port tensions can be expressed as follows:

$$\mathrm{V}_1 = Z_{11}I_1 + Z_{12}I_2 \tag{4.8}$$

$$V_2 = Z_{21}I_1 + Z_{22}I_2 \tag{4.9}$$

The differential impedance of the antenna is:

$$Z_d = \frac{V_d}{I} = \frac{(V_1 - V_2)}{I} = (Z_{11} - Z_{21} - Z_{12} + Z_{22}) \tag{4.10}$$

Differential impedance can be expressed based on S settings (after converting Z to S parameters):

$$Z_d = \frac{V_d}{I} = \frac{2Z_0(1 - S_{11}^2 + S_{21}^2 - 2S_{12})}{(1 - S_{11})^2 - S_{21}^2} \tag{4.11}$$

Where S_{11} and S_{21} are the S parameters of the antenna, considered a two-port network, and Z_0 the reference impedance. the S matrix is given by:

$$S = \begin{bmatrix} \frac{Z}{Z + 2Z_0} & \frac{2Z_0}{Z + 2Z_0} \\ \frac{2Z_0}{Z + 2Z_0} & \frac{Z}{Z + 2Z_0} \end{bmatrix} \tag{4.12}$$

When S_{11} and S_{12} can be replaced by S_{22} and S_{12}, respectively, due to the symmetry of the two-port circuit, equations 4.11 and 4.13 lead to an indefinite form (4.7). This

indeterminacy can be avoided by factoring the numerator of (Equation 4.11) as $2Z0\ (1-S_{11}-S_{21})(1\ -S_{11}-S_{21})$ and its denominator as $(1-S_{11}-S_{21})(1-\ \ S_{11}-S_{21})$ Therefore, (Equation 4.11) may simply be in the following form:

$$Z_d = 2Z_0\frac{1+S_{11}-S_{21}}{1-S_{11}+S_{21}} \qquad (4.14)$$

4.3.2.2 Measurement Results

To verify the above results, a prototype of the proposed RFID tag antenna was fabricated and its parameters were measured. The reflection coefficient and input impedance of the proposed RFID tag antenna was measured using a Rohde & Schwarz ZVB 20 Network analyzer through a differential probe as shown in (Figure 61).

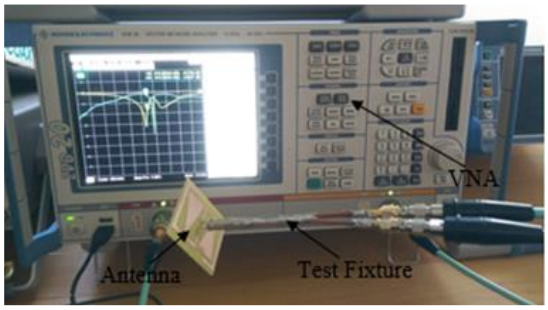

Figure 61: Measurement Setup using Rohde & Schwarz ZVB 20 VNA with Test Fixture Soldered to the Antenna

The antenna reflection coefficient is then extracted from the measured S-parameters over the frequency band of interest using the same method reported in [92]. (Figure 62) shows the measured and simulated reflection coefficient of the RFID tag antenna. There is a good agreement between the measured and simulated results. The measured -10dB bandwidth is ranging from 900 MHz to 928 MHz for a total bandwidth of 28 MHz and is centered at 0.914 MHz, which can cover totally the North-American UHF RFID band.

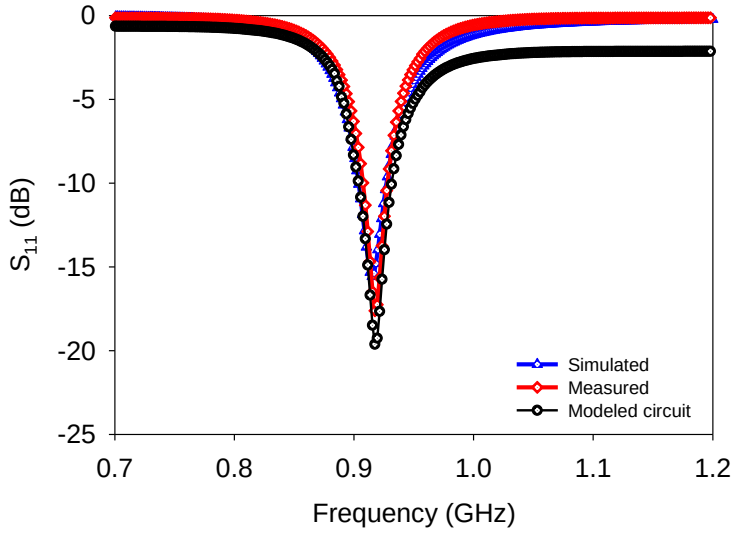

Figure 62: Reflection Coefficient of From The Simulated, Equivalent Circuit Model, and The Measured Impedance

(Figure 63) shows the measured and simulated input impedances of the prototype in free space. From measurement, the impedance of the antenna is approximately $(16.43 + j112.3\Omega)$ at 915MHz, which is very close to the measured conjugate impedance of the used chip $(17.6 - j100.9\Omega)$.

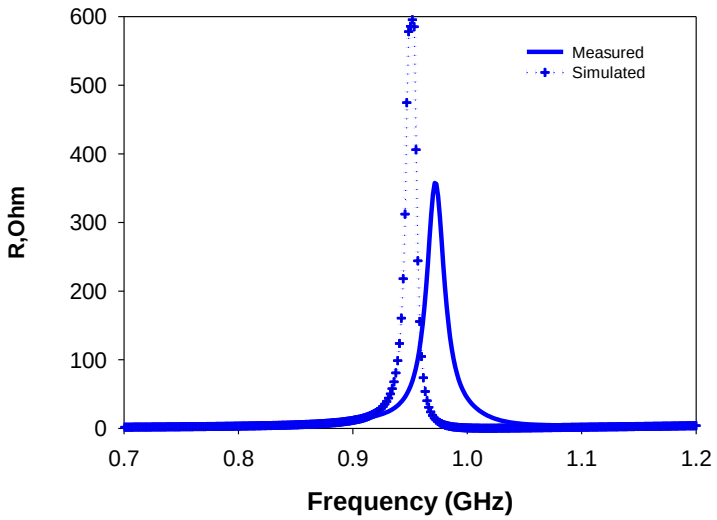

(a)

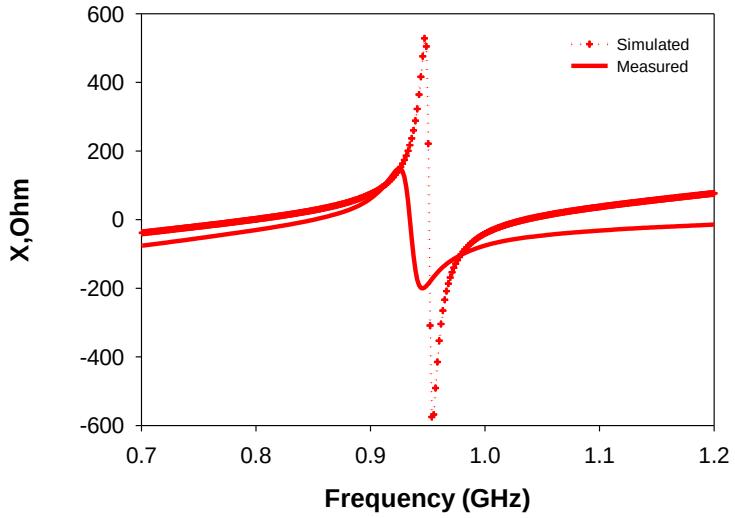

(b)

Figure 63: Measured and Simulated Input Impedances of The Prototype RFID Tag Antenna, (a) Resistance, (b) Reactance.

The measurement and simulation values of the proposed tag antenna at 915 MHz are reported in Table 13.

Table 13.Impedance Results of The Proposed Antenna Tag

@915 MHz	*Real Part (Ohm)*	*Imaginary Part (Ohm)*
Measured	*16.43*	*+j112.3*
Simulated	*17.5*	*+j115.98*
Measured IC chip	*17.6*	*-j100.9*

4.4 Measurmrnt of the Performances the RFID Tag Antenna in (Anechoic Chamber)

4.4.1 Sensitivity Measurement

The tag sensitivity of the (Minimum power activation) of the proposed design was also investigated using the backscatter measurement setup depicted in (Figure 64). This system consists of two horn antennas, a digital oscilloscope (Agilent DSO91204A), a pulse generator (Picosecond Pulse Labs Model 3500). The whole

system is controlled by homemade software based on Matlab. The transmitter and the receiver horn antennas (SAS-571) have very large bandwidth (700 MHz up to 18 GHz) and provide a flat 13 dBi gain over the frequency range from 860 to 960 MHz.

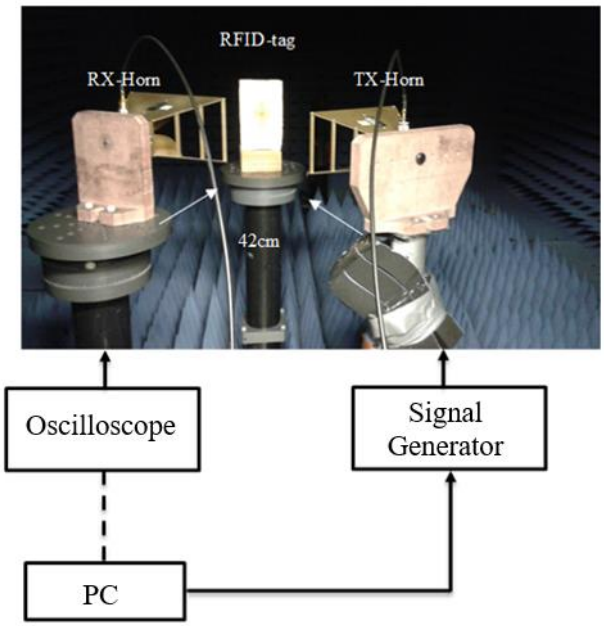

Figure 64: Measurement Setup

One horn antenna collects the backscatter signal produced by the tag and a digital oscilloscope (Agilent Infiniium) is connected to the other horn antenna and allows the measurement of the tag power activation. In this setup, the horn antenna is placed 0.42m away from the RFID tag antenna. It is worthwhile to note that the measurements were performed in an anechoic chamber, as shown in (Figure 64), at LCIS lab, Valence, France. The minimum power activation is presented in (Figure 65). It can be clearly seen that the measured minimum power to activate the tag at 915 MHz is −7 dBm. Next, we have measured the read range, which is considered as the main parameter that characterize an RFID system.

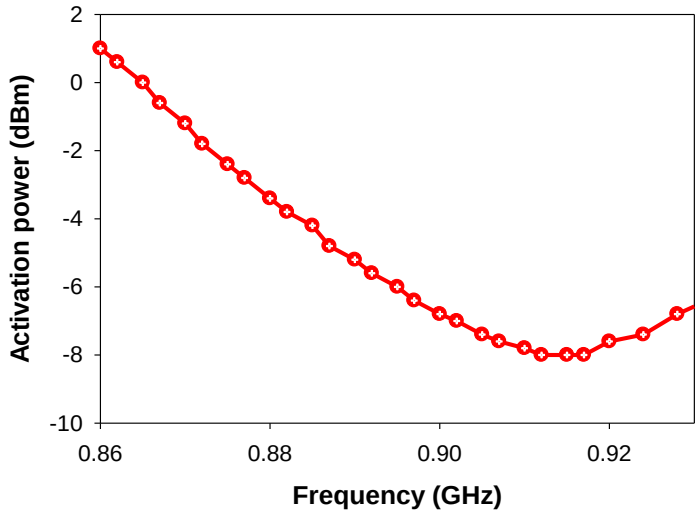

Figure 65: Measured Activation Power as a Function of Frequency in Anechoic Chamber

4.4.2 Read Range Measurement

From the measured results of the activation power presented in (Figure.66), the read range of the RFID tag antenna can be determined using the following formula [89]:

$$r_{\max} = d\sqrt{\frac{P_{EIRP}}{G_t P_{th}}} \qquad (4.15)$$

Where d is the distance between the RFID tag antenna and the transmitter antenna of the measurement system. P_{th} is the minimum transmitted power obtained from the measurement system to activate the tag, G_t is the gain of Transmitting antenna, and PEIRP is the maximum output allowed transmitted power.

The measured read range versus the frequency over the 902-928 MHz band is presented in (Figure 66) for the EIRP = 4W. The results reveal that within the operation bandwidth (902-928 MHz) the read range is above 4.5 m, confirming that

the proposed structure is capable to operate at North-American band with a good performance. At 915 MHz, the maximum read range was found to be 5.25 m in free space, which is very close to the calculated one. This value of the read range indicates that a good conjugate matching between the antenna and the RFID tag is obtained. It is worth noting that when compared to the read range of the RFID tags reported in [93], the proposed design has higher read range value.

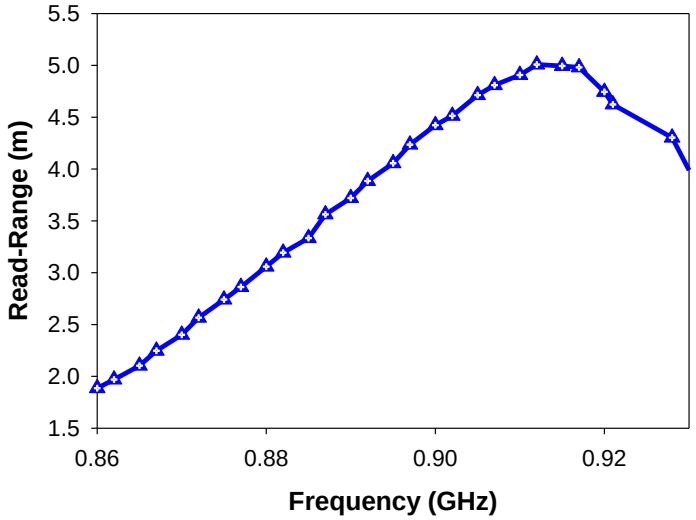

Figure 66: Measured Read Range as a Function of Frequency in Anechoic Chamber

4.4.3 Delta Radar Cross Section Measurement

The differential radar cross section (ΔRCS) is also an important parameter, which measures the strength of the modulated backscattered signal reradiated by the tag. It is expressed as the ratio of backscattered power of the modulated signal reflected from the tag to the incoming power received by the tag from the reader. It can be obtained from the following relationships [94]:

$$\Delta\text{RCS} = \frac{P_{tag}(4\pi)^3 d^4}{P_r\, G_r^2\, \lambda_0^2} \qquad (4.16)$$

Where Ptag is the power of the modulated signal received by the reader from the tag, $d = 0.45\,m$ is the distance between the tag and the reader antenna. Also, P_r, G_r and λ_0^2 were defined in (Equation 4.16). The measured differential radar cross section obtained of the proposed tag in the frequency range from 0.8 GHz and 0.9 GHz is shown in (Figure 67). The peak value is ΔRCS = 0.0015 dBsqm at the resonant frequency of 915 MHz. Again, as the value of ΔRCS is considerably decreasing to about 0.00025 dBsqm at 868 MHz, we should note that the very small values of the differential cross section are an indication that it will be difficult to detect the tag, especially in real conditions with non-negligible values of ΔRCS noise floor level. However, the strong backscattered signal at the resonant frequency 915 MHz leads to a maximum reading range and allows the reader to detect the backscattered signal more easily. As indicated, this may be useful in traceability applications, where important information can be collected.

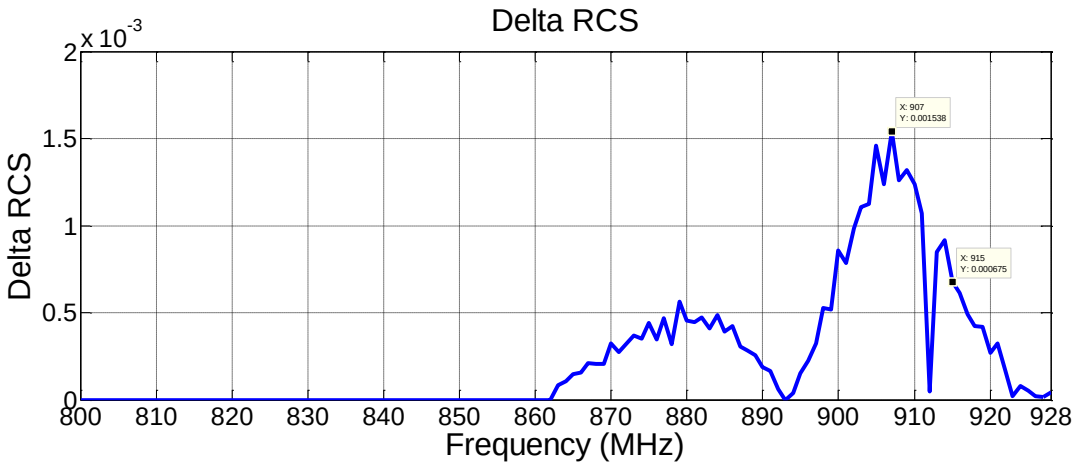

Figure 67: Measured Differential Radar Cross Section of The Proposed Tag as Frequency

4.5 Measurmrnt of the Performances the RFID Tag Antenna on Different Object (Real Condition)

In the above paragraph, we have measured the read range in free space,, however, in the real world, RFID tags antennas are often mounted on different materials (e.g., Glass, Metal, liquid, plastic, wood, cardboard…). In this situation, the antenna properties such as radiation pattern, impedance and radiation efficiency may be drastically affected especially in UHF band. Thus, we have measured the read range of the proposed design mounted on different materials in an ordinary room as shown in (Figure 68). The measurement setup used here is similar to the one reported in [86] and include Thing Magic Micro (M6e-M) UHF RFID development kit [85] , the stepper motor (Brother model KE58KM2-032), a driving board and a single circularly polarized patch antenna having the gain of 6 dBi at the frequency range of 800-1000 MHz. The reader is connected to the antenna via 1.8 m of 50 ohm coaxial cable model CNT-195-FR to generate 36 dBm at 915 MHz. Hence, the total transmitted power was approximately 4W EIRP (effective isotropic radiated power)., the obtained read range was found to be 0.5 m, 2 m, and 4 m, respectively ,using the foam spacer of 2 mm, 6 mm, and 8 mm thickness. These obtained results showed that the read range decreased with decreasing thickness of the foam layer.

This is owing to the fact that the proposed structure was designed and optimized without a ground plane which can deteriorate drastically the performance of the RFID tag antenna. Note that, here we have used a low-cost foam dielectric (polyethylene) which is attractive owing to its easy integration into the roll-to-roll process. Therefore, the proposed design is suitable to be installed in a recessed cavity in metallic objects such as vehicles, and metallic containers. It is worthwhile to mention that the proposed structure can demonstrate farther read ranges on different objects because of the RFID chip used in this study has Pth= -8 dBm and this value is certainly very

high if compared to other chips like NXP G2XL, and Alien Higgs. For example, if an NXP G2XL IC chip with P_{th}= -17 dBm is used in the design of this RFID tag antenna the calculated read range would be 12.43 m.

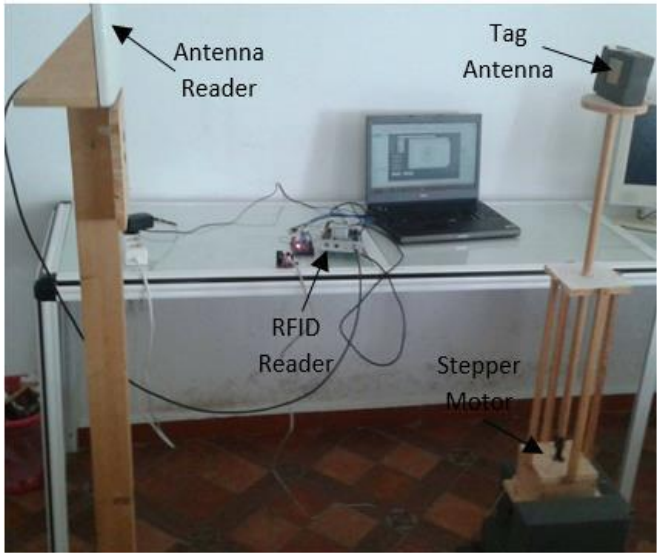

Figure 68: RFID Tag Read Range Measurement Setup in Real Conditions.

4.5.1 Read Range Mesurment

The RFID tag antenna attached on a foam substrate was oriented in the line of sight direction of the RFID reader, as shown in (Figure 68). Both of them are kept fixed and of the distance separation between them is 0.5m. Note that the measurements of the read range of the proposed structure mounted on different objects were carried out at our laboratory .The obtained results are presented in (Figure 69). It can observed that the RFID tag antenna has an acceptable read range when it is mounted on glass, plastic, wood, and cardboard. For the case where the tag antenna is mounted on a 1 cm thin foam spacer for use on a metallic object, the maximum read range was found to be 4.52 m. We have also investigated the effect of the foam spacer thickness on the read range.

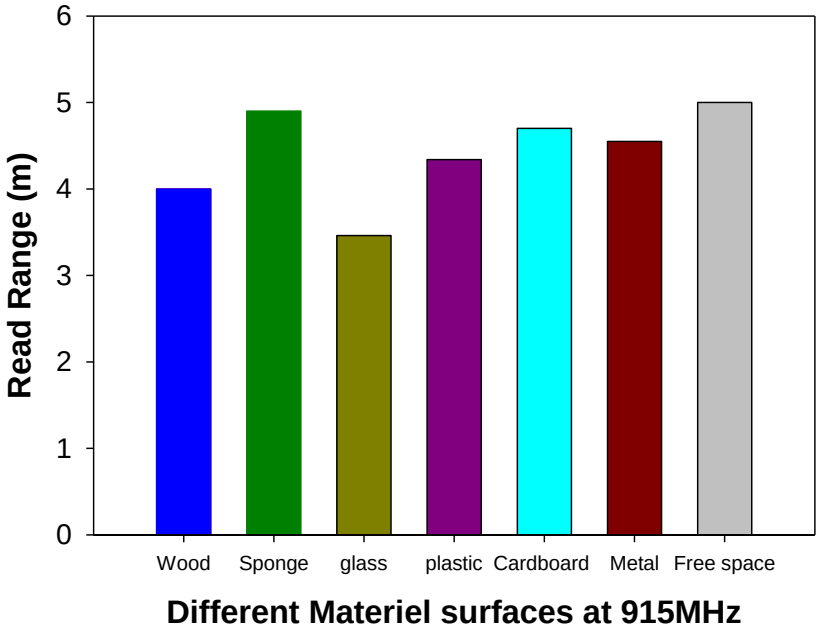

Figure 69: RFID Tag Read Range Measurement Setup in Real Conditions on Different Objects.

4.5.2 Read Pattern Mesurment

Finally, we have measured the 2-D reading patterns of the RFID tag antenna in the (x-y) and (y-z) planes at 915 MHz by using the same measurement set-up described above. The reading range patterns of the proposed structure were measured in an ordinary room. To measure the read range pattern at the operation frequency of 915 MHz in the x-y and y-z planes, the RFID tag antenna was rotated from 0° to 360° stepped by 10°. Here, we have used a stepper motor (Brother Model KE58KM2-032) with 4 GPIO ports and minimum angular step of 1.8° to rotate the rotating platform. The connection between the stepper motor and the RFID reader is realized using Arduino Mega 2560 as shown in (Figure 68). The obtained results are presented in (Figure 70), which shows that the reading pattern, is omnidirectional radiation pattern in the y-z plane with the maximum read range of 5 m. However, the reading pattern in the x-y plane reveals that the maximum read range has decreased to 3.8 m and the pattern is quite close to a more mono-directional.

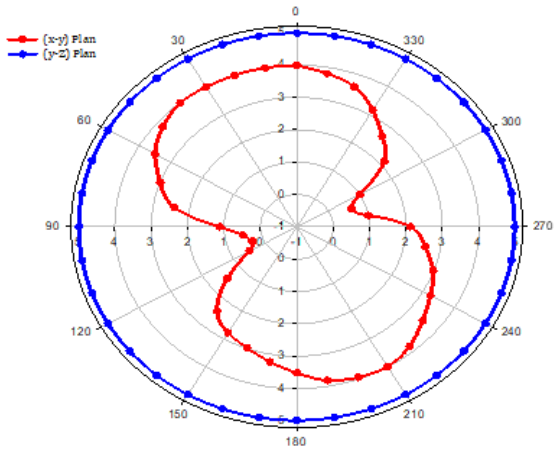

Figure 70: Read Pattern Measurement of the RFID Tag

For both planes, slight variation (0.3 m) of the read range is observed specially between the back and the front read ranges. Additionally, it is found that the maximum read range in the x-y plane is tilted by 15° which may be caused in particular by the effect of the surface current distribution around the triangular stubs.

4.6 Conclusions

This chapter comprises of two sections. In the first section, methods of chip and antenna impedance mesaurements have been presneted. It is found that the the differential probe provides better agreement with simulated results. In the second section, a compact modified S-shaped tag antenna for UHF-RFID applications it is studing numerically and experimentally. The antenna is one single layer and designed using a low-cost substrate (FR4) with a total size is $51 \times 43 \times 16\ mm^3$. Two triangular stubs are used to achieve conjugate matching for the desired input resistance and reactance. The measured 10-dB impedance bandwidth of the proposed design is 28 MHz which covers the entire 902-928 MHz band designed for North America. The maximum read range measured in free space was to be 5.2 m. The experimental results show also that the proposed design can have a maximum read range of 4.2 m

when separated by a 1 cm thin foam spacer from a large metallic plate (200 × 30 cm2). In addition the experimental results reveal that the proposed design has demonstrated acceptable read range when mounted on different materials which make it suitable for general UHF-RFID applications, except for liquid bottles.

Chapter 5

Design and Characterization of a Broadband Flexible Polyimide RFID Tag Sensor for Detection of Liquid Concentration

5.1 Introduction

Over the past decades, radio frequency identification (RFID) technology has been developing rapidly. It is considred as a promising technology for future connectivity. It has been a real competitor to bar code technology and has found many applications beyond monitoring and tracking applications. Despite their indisputable advantages, passive RFID tags antenna working in the ultra-high frequency (UHF) band (860-960 MHz) are sensitive to the surrounding medium (liquids, plastic, paper, wood, and so on) which affect their performance. The motivation of this research is to exploit and value this sensitivity to nearby medium, in order to extend its field of application to sensing applications, which is nowdays, one of the hot competitive topics.

To this end, this chapter presents a broadband flexible RFID sensor tag antenna to detect the concentration of aqueous solutions. The proposed RFID tag antenna sensor with T-matching network is based on a printed dipole whose arms are loaded with circular disk patch. The structure is printed on Kapton polyimide flexible substrate. The sensing mechanism of the RFID tag antenna is based on the change of the RFID

tag antenna sensitivity which occurs when the aqueous solution concentration change. The proposed sensor is designed using CST Microwave studio, and its various parameters are optimized in order to have a broadband impedance that covers all the RFID band (860-960 MHz). The experimental set-up is small, rapid, contactless, and inexpensive. Results are presented for NaCl, sugar and Alcohol aqueous solutions with concentrations ranging from 0% to 80%.

5.2 Operating and Working Principles of RFID Tag Antenna as Sensor

The working principle of the proposed sensor is based on the use of the RFID technology. In this technique, the liquid under test is introduced into a glass beaker filled with the liquid solution (Sucrose or NaCl) on which we pasted an RFID tag antenna. The beaker is then placed near the RFID reader to ensure a backscatter communication.

In general the sensitivity of the RFID-UHF tag antenna can be written as:

$$S_{tag} = P_{tx,ON}.G_{tx}.\tau.(\frac{\lambda}{4\pi d})^2.\eta_{plf}.A_{cable} \qquad (5.1)$$

Where $G_{\text{tx}}$the gain of the reader is, η_{plf} is the polarization mismatch, τ is the transmission coefficient of the RFID tag, $P_{tx,ON}$ the minimum power emitted by the reader at which the tag starts working, and A_{cable} is the attenuation of the cable.

Depending on the matching between the antenna and the chip, only a fraction of this power is transferred to the latter and is given by [95]:

$$S_{chip} = (1-\left|\Gamma_{tag}\right|^2).G_{tag}.S_{tag} \qquad (5.2)$$

All the irrelevant parameters excluded and from (5.1) and (2.5) we obtain:

$$S_{tag}\alpha\frac{1}{(1-\left|\Gamma_{tag}\right|^2).G_{tag}} \tag{5.3}$$

Since the reflection coefficient is dependent on the dielectric characteristics of the surrounding medium, any change in the latter will affect the sensitivity, hence the underlying measurement principle. The dielectric dependence of the permittivity of the sucrose and sodium chloride solutions concentration have been established respectively by Buchner et al. [96] and by CG Malmberg et al. in [97] for the working frequency and for T=298 K through the fitting equations:

$$\varepsilon_{NaCl}(c)=78.45-15.45c-3.76c^{3/2} \tag{5.4}$$

$$\varepsilon_{Succ}(c)=\varepsilon_w-0.226c-6.75(10^{-4})c^2-1.09c^3 \tag{5.5}$$

Where c is the weight percent and ε_w is the permittivity of the pure water.

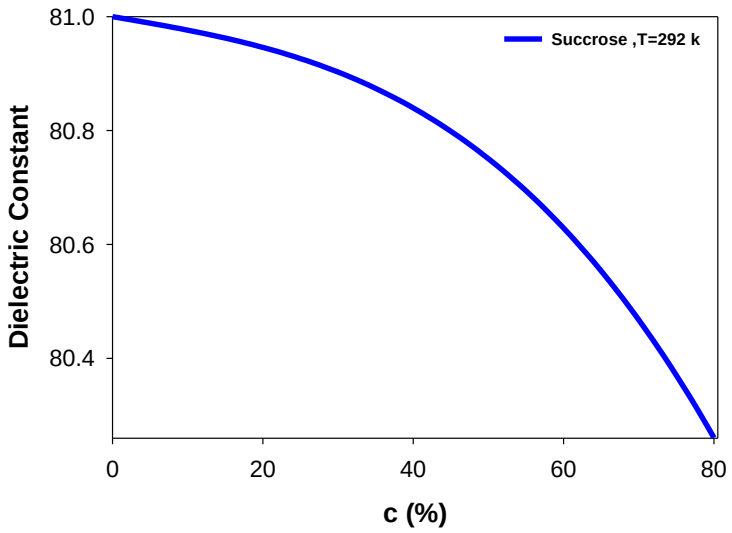

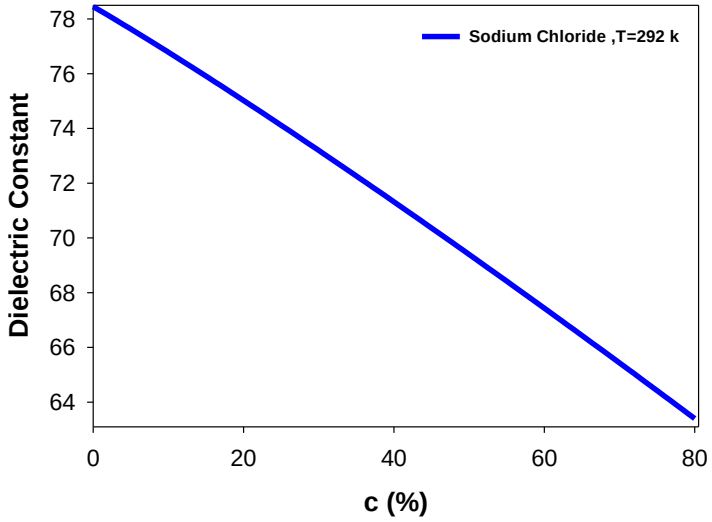

Figure 71: Concentration Dependence of the Dielectric Constant of Nacl Electrolyte Solution and Sucrose Solution at T = 298.15 K from the Measurements of Buchner et Al. [18] (Eq. (1)) And Cg Malmberg Et Al [19] (Eq.(2)).

Figure 71 shows that as c increases, the static permittivity decreases, and thus changing the RFID-tag reflection coefficient ¸Γ́ $_{tag}$andG_{tag}. This change can be measured through S_{tag}, which explains the underlying sensing mechanism of the RFID tag antenna.

5.3 RFID Tag Antenna Sensor: Analysis and Design

The main part of the proposed sensor structure is an RFID tag antenna configuration shown in (Figure 72). The proposed tag antenna is of a simple design. It is based on a printed dipole whose arms are loaded with circular disk patch with a T matching network. The proposed design is printed on 127 µm (Kapton) polyimide flexible substrate, with a dielectric constant of 3.5 and a loss tangent of 0.002. The top antenna trace was made of copper having a thickness of 35 µm. The overall size of the substrate is $100 \times 32\ mm^2$.

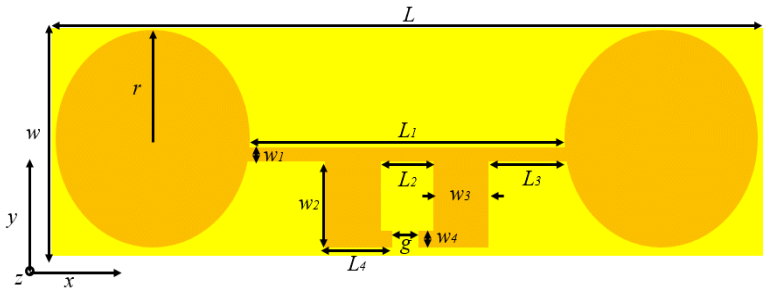

Figure 72: The Geometry of The Proposed RFID Tag Antenna

Table 14: Dimensions of RFID Tag Antenna [mm]

L	L_1	L_2	L_3	L_4	W	w_1	w_2	w_3	w_4	g	R
100	*36*	*6*	*10.14*	*7*	*32*	*1.25*	*12.4*	*4.8*	*2*	*2*	*15.5*

The proposed RFID tag antenna is designed to operate in the RFID-UHF band of 860–960 MHz. Its covers the whole global UHF RFID frequency band. The Murata LXMS31ACNA chip with an impedance of $Z_{Chip} = (17.6 - j100.9)\ \Omega$ at 915 MHz was selected for our design. The minimum threshold power to activate this chip is -8 dBm [88]. Note that the impedance of the chip was measured using the same method reported in [91]. Therefore, the input impedance of the antenna has to be $17.6 + j100.9\ \Omega$ so that a maximum power transfer can be achieved. The optimized geometrical parameters obtained by using CST Microwave studio are listed in Table. 14.

To demonstrate the operating principle of the reactive matching of the proposed design, we proposed the equivalent electrical model shown in (Figure 73). For the sake of simplicity, the RFID chip and the antenna are modelled as a series RC (R_{chip},C_{chip}) and a series RLC circuit (R_{ant},L_{ant}, C_{ant}), respectively. The radiation resistance for a small dipole can be approximated by [89]:

$$R_a = 80\pi^2\alpha^2\left(\frac{l}{\lambda}\right) \qquad (5.6)$$

Where $0.5 \leq \alpha \leq 1$ depending on how the current is distributed along the antenna, and l is the length of the antenna. By considering the working frequency of the antenna at 1.1 GHz, the radiation resistance is 43.39 Ω when α is equal to 0.7 and the length of the antenna is 93 mm. The inductance of the antenna is found to be 35.43 nH by using the following approximated formula given in [90]:

$$L_{ant} = \frac{\mu_0}{2\pi} l\left(\ln\left(\frac{l}{w}\right) - \frac{\pi}{2}\right) \quad ; \mu_0 = 4\pi \times 10^{-7}\frac{H}{m} \qquad (5.7)$$

Where l and w are respectively the length and width of the conductive strip.

Next, the antenna capacitance C_{ant} found to be 0.71pF by using equations (5.8) and (9) given below. By using the self-resonant frequency of the proposed antenna where Lant and Cant are the equivalent inductance and capacitance, respectively, of the proposed antenna. Therefore the capacitance C_{ant} found to be:

$$f_c = \frac{1}{2\pi\sqrt{L_a C_a}} \qquad (5.8)$$

$$C_{ant} \approx \frac{1}{4\pi^2 f_c^2 L_{ant}} \qquad (5.9)$$

where f_{c} , L_{ant}, C_{ant} are respectively the self-resonant frequency ,the equivalent inductance and the capacitance, of the proposed antenna.

The equivalent circuit for MURATA RFID chip is an 17.6 Ω resistor in series with a 1.64pF capacitor. The T-matching network can be modelled as series inductance (L_{series}) and (C_{Shunt}) (Figure 73).

With the lumped component values given above, the reflection coefficient S_{11}(dB) of the RFID tag antenna in free space can be obtained by using a circuit simulator (Agilent's Advanced Design System). The obtained results are plotted in (Figure 74) along with the S_{11}(dB) from the CST Microwave studio for easy comparison.

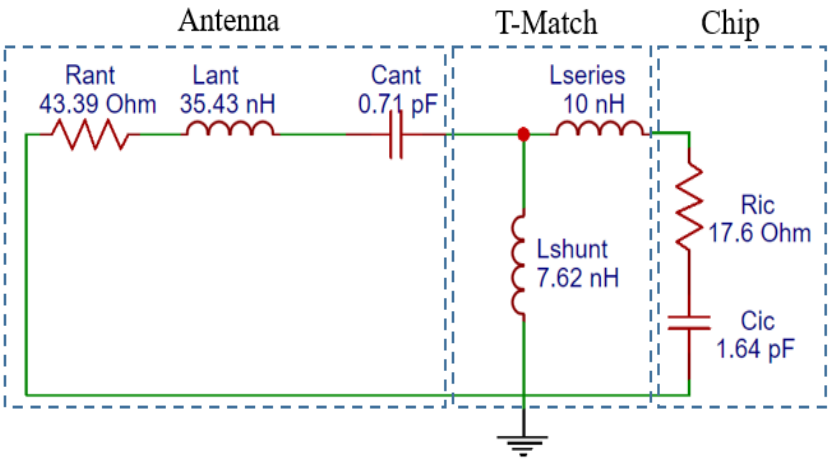

Figure 73: Equivalent Circuit Analysis of the Antenna Tag

Small discrepancy between full wave simulation and the equivalent circuit model can be observed. This can be ascribed to the use of the approximated equations to calculate all the lumped elements, even though, the proposed model can accurately predict the reflection coefficient. Furthermore, (Figure 74) shows the simulated -3dB bandwidth ranged from 820 MHz to 960 MHz for a total bandwidth of 140 MHz which can cover totally the UHF-RFID band.

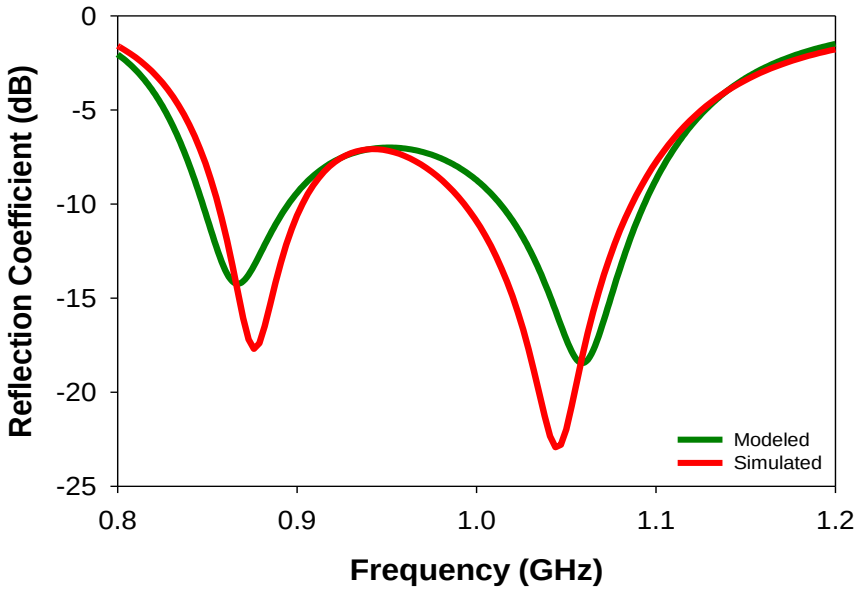

Figure 74: Comparison Results Between Full Wave Simulation and the Equivalent Circuit Model

5.3.1 Parametric Study of the Flexible UHF RFID Antenna

To design a dual band dipole antenna adapted to the MURATA-LXMS31ACNA-010, we have used the chip with the impedance $17.6 - j100.9\Omega$ at the frequency 915 MHz, this means that the antenna tag's impedance must be close to its conjugate $(17.6 + j100.9\Omega)$ to guarantee maximum power transfer. To do this, we varied the values of the parameters of the proposed RFID tag antenna such as r, w_2, l_4until satisfactory results were obtained. We tried to visualize the influence of the geometrical parameters of this antenna on its input impedance. We started with the diameter of the circular patch "r", change it from a minimum value of 11 mm to a maximum value of 15 mm taking 5 samples, while setting the value of "w_2" to 7 mm and "l_4" to 12.4 mm

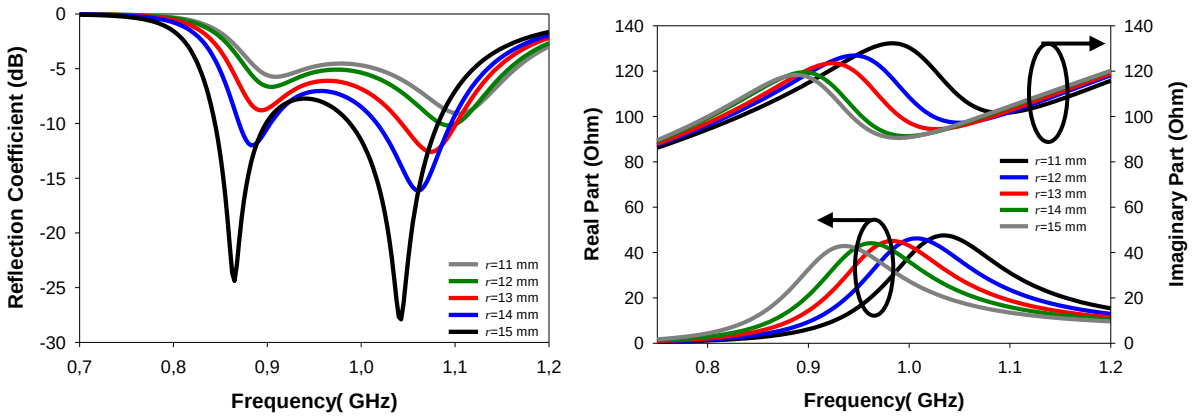

Figure 75: Influence of the Parameter "r" on The Input Impedance

In (Figure 75), it can be seen that a good impedance matching is obtained when the parameter "*r*" is 15 mm. Table 3.11 shows the impedance and coefficient reflection of the antenna for different "*r*" values and the maximum bandwidth is 520 MHz.

The values of the real and imaginary part of the input impedance at 915 MHz are reported in Table 15.

Table 15: Simulation Results of the Influence Parameter "r"

Antenna Parameter -@ (f_c=915 MHz)	*Real Part (Ohm)*	*Imaginary Part (Ohm)*	*Bandwidth (MHz) @-5dB*
r=11 mm	*7.7633*	*118.0069*	*127*
r=12 mm	*12.0856*	*122.1025*	*140*
r=13 mm	*15.4899*	*122.7429*	*272*
r=14 mm	*16.7954*	*117.4614*	*282*
r=15 mm	*18.1703*	*113.9536*	*520*

Then, we have studied the effect of the parameter "l_4" that we vary within the interval ranged from 9 mm to 13 mm, considering always 5 samples, and taking $r = 15$ mm. The obtained results summarized in Table 15 and plotted in (Figure 76).

Similarly, it is clear that a good impedance matching is obtained when the parameter $l_4 = 10\ mm$.

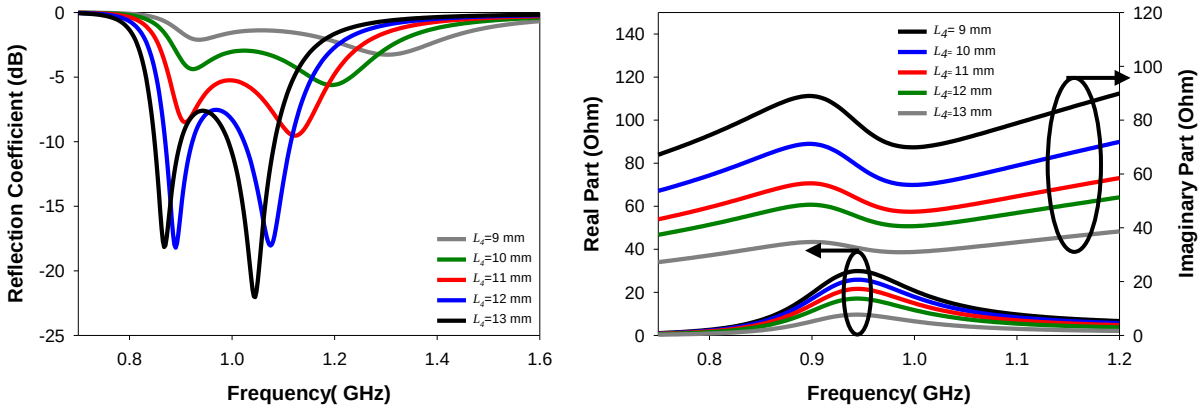

Figure 76: Influence of the Parameter "L_4" on The Input Impedance

The values of the real and imaginary part of the input impedance at 915 MHz are reported in Table 16.

Table 16: Simulation Results of the Influence Parameter "L_4"

Antenna Parameter -@ (fc=915 MHz)	*Real Part (Ohm)*	*Imaginary Part (Ohm)*	*Bandwidth (@-5dB)*
L_4=9 mm	*21.4244*	*24.6961*	*--*
L_4=10 mm	*17.9127*	*87.4294*	*12*
L_4=11 mm	*625.0612*	*69.5985*	*315*
L_4=12 mm	*14.2696*	*59.8927*	*300*
L_4=13 mm	*8.1180*	*43.0460*	*288*

Similarly, in this paragraph, we try to see the effect of the parameter "w_2" that we vary in the range of 7 mm to 11 mm. Five samples were considering with fixed values of $r = 15\ mm$ and $l_4 = 15mm$.

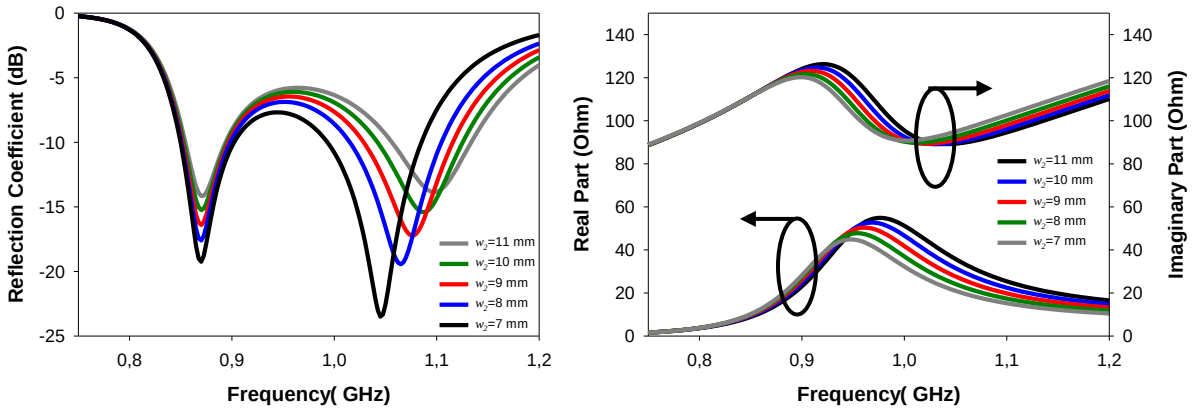

Figure 77: Influence of the Parameter "w_2" on The Input Impedance

The values of the real and imaginary part of the input impedance and cover bandwidth at 915 MHz are reported in Table 17.

Table 17: Simulation Results of the Influence Parameter "w_2"

Antenna Parameter -@(fc=915 MHz)	*Real Part (Ohm)*	*Imaginary Part (Ohm)*	*Bandwidth (@-5dB)*
w_2=7 mm	*35.8457*	*124.7159*	*287*
w_2=8 mm	*35.2453*	*122.7850*	*307*
w_2=9 mm	*33.9890*	*120.9320*	*322*
w_2=10 mm	*22.2822*	*120.7850*	*333*
w_2=11 mm	*18.3213*	*118.4231*	*208*

Figures 77 and Table 17 results in the deferent values of the antenna impedance at the variation of w_2, it is clear that the best adaptation of the tag antenna when the parameter$w_2 = 11mm$. From the study illustrated in the Figures above, we can see that at the desired resonant frequency, the "r" parameter has a significant influence on the real and imaginary parts of the input impedance of the dipole. We consider the values $r = 21.4$ mm,$l_4 = 7mm$ $w_2 = 12.4mm$ very convenient to obtain an impedance equal to $17 + 100j$.

5.3.2 Fabrication Process of the Flexible RFID Tag Sensor.

A prototype of the proposed flexible RFID tag antenna has been fabricated and tested to verify the above results. Note that the prototype shown in (Figure 78) was fabricated using an integrated process divided into several steps. First, the proposed antenna is fabricated on a thin adhesion layer as a mask by using a board laser cutting machine 1390 triumph [98], then the mask is pasted on a thin sheet copper layer. The removal of the copper in the unwanted region is done by a Cu etchant to get the designed top layer of the proposed antenna. The latter is cleaned with isopropyl alcohol and deionized water, and then directly attached to the Kapton polyimide flexible substrate.

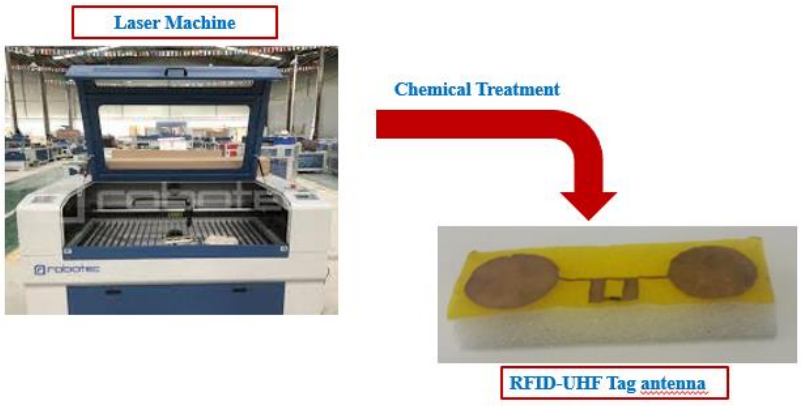

Figure 78: Fabrication Process using Chemical Treatment

5.3.3 Impedance Measurement of the Proposed Flexible RFID Antenna

The performance of a UHF RFID tag depends on the conjugate matching between the chip and the antenna. The design of such device therefore requires the measurement of its impedance. In the literature, there are few works that describes the input impedance measurement of RFID tag antennas, the major problem lies on the power supply of the antenna. After having made the UHF RFID tag antenna prototype (Figure 79), it is necessary to measure its input impedance in order to be

compared with that of the used chip. To this end, we have implemented measurement methods to characterize the impedance of the proposed antenna.

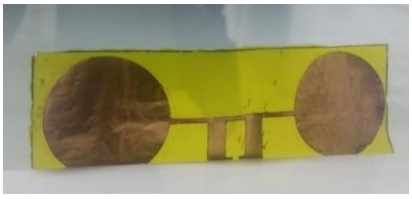

Figure 79: Prototype of the Proposed Flexible Tag Antenna

The measurement of antenna impedance is a major problem, each type of cable connection between the antenna and the network analyzer generally disturbs the near field in the vicinity of the antenna. Such a disturbance is very severe in the case of antennas with non-traditional power supply (RFID tag) by means of the input of direct chip at the center of the proposed antenna. This is because of the appearance of an electrical current leakage generated by the antenna and circulating on the SMA connector and which creates additional radiated fields that could damage the network analyzer. Therefore, specific measures are necessary to obtain a sufficiently accurate experimental verification of the tag antenna. There are two effective methods to address this problem. The first consists in implementing a balun of length λ /4 which makes it possible to eliminate the leakage current. The second technique, valid only for symmetric structures, uses Babinet's principle (Image theory) (Figure 80)[99].

Figure 80: Proposed Half RFID Antenna

This measurement technique (Image Theory) that we have implemented is based on the method introduced in reference [99]. This method uses the image theory, with an measurement of a half-antenna on a conductive plane.

In our case, the symmetry of the plane E was used to determine the impedance of the antenna (Figure 81). Instead of measuring the complete antenna, half of its structure was deposited on a large electrical metal plate replacing the symmetry of the plane E. The impedance of a half antenna with an metal plate is equivalent to half of the complete antenna impedance. The measuring device set up is illustrated in (Figure 83). It is composed of one half of the antenna connected to a conductive plane and powered by a coaxial probe (SMA Connector) having an impedance of 50 ohm. The complete structure is connected to the network analyzer via a coaxial line. The mass-metal plane that we used in practice is a double-sided plate, connected by conducting wires, made of FR4 materials, of an relative permittivity $\varepsilon_r = 4.4, tan\,\delta = 0.025$ and dimension (160 x 100) mm^2. Measurements were made with the Rohde & Schwarz ZVB 20 network analyzer with the standard previously calibrated.

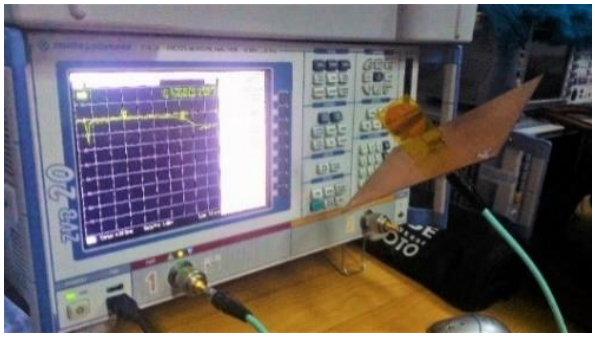

Figure 81: Measurement Set-Up Using Rohde & Schwarz ZVB 20 VNA

The measured input impedance of the proposed design obtained is plotted in (Figure 82). The input impedance was measured using a Rohde & Schwarz ZVB 20 Network analyzer as shown in (Figure 81).

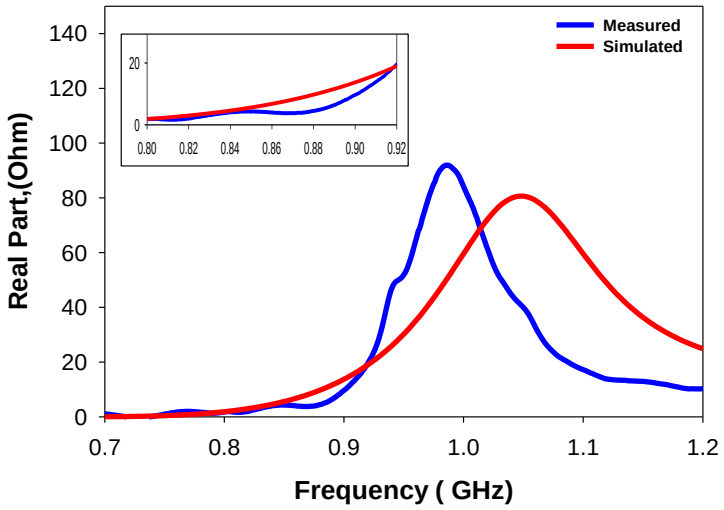

(a)

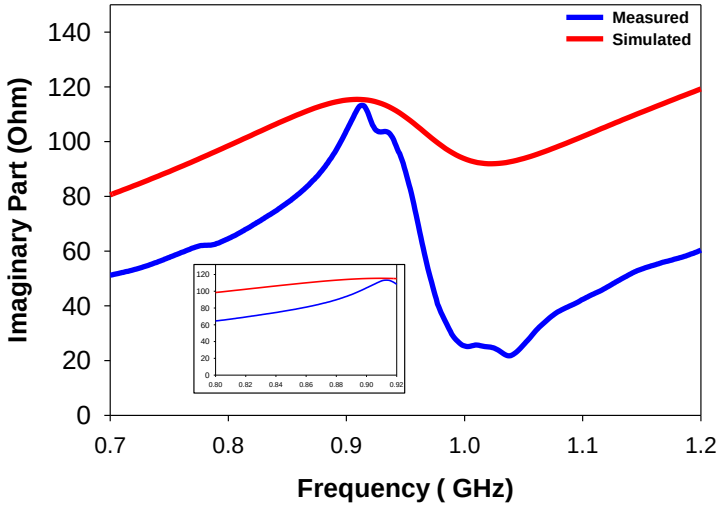

(b)

Figure 82: Input Impedances of the Prototype in Free Space. (a) Real Part; (b) Imaginary Part.

The measured and simulated input impedances of the proposed RFID tag antenna in free space are plotted in (Figure 82). From the measurement, the impedance of the antenna is approximately (16.43+j112.3Ω) at 915MHz, which is good enough to guarantee a maximum power transfer between the Murata chip (17.6-j100 Ω) and the antenna at this frequency.

5.3.4 Reflection Coefficient

Figure 83. Shows the reflection coefficient generated from the equivalent circuit model, the CST microwave studio simulation, and the image theory measurement. Good agreement can be observed between the three sets of data. The measured results show a bandwidth (-3dB) 100 MHz ranging from 860 to 960 MHz which can cover totally the UHF RFID band.

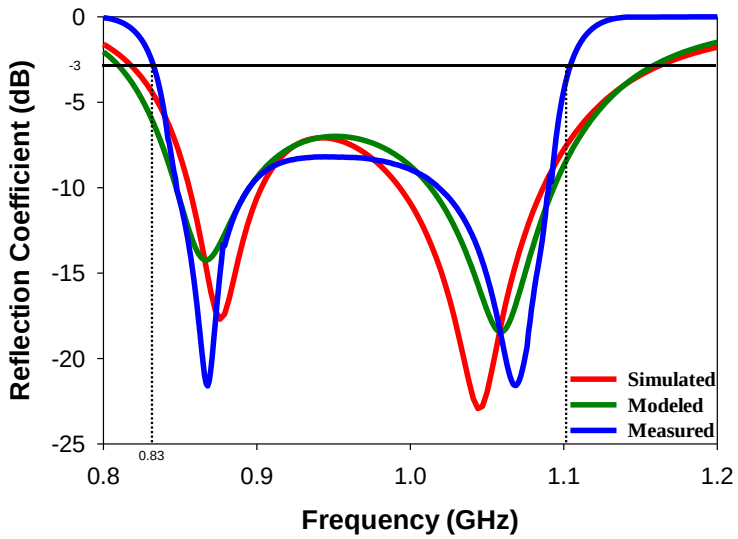

Figure 83: Simulated and Measured Reflection Coefficient of the Proposed RFID Tag Antenna

5.4 Measured Performance of RFID Tag Antenna

5.4.1 Reading Range and Sensitivity Measurement

Another more practical feature of the RFID tag antenna is the read range. This important characteristic can be calculated using the Friis equation:

$$S_{tag} = P_{tx,ON}.G_{tx}.\tau.(\frac{\lambda}{4\pi d})^2.\eta_{plf}.A_{cable} \qquad (5.10)$$

$d_{\max}$ can be expressed as follow :

$$d_{max} = \frac{\lambda}{4\pi}\sqrt{\frac{P_{tx,ON}.G_{tx}.\eta_{plf}.A_{cable}}{S_{tag}(f)}} \qquad (5.11)$$

Where $P_{tx,ON}$ is the power transmitted from the reader, G_{tx} is the gain of the reader, $\eta_{\text{plf}}$is the polarization mismatch, τ is the transmission coefficient of the RFID tag, and Acable is the attenuation of the cable. The measurement setup has been deployed in an ordinary room to measure the maximum read range. This measurement setup used here is similar to the one reported in [100]. It consists of a Thing Magic Micro (M6e-M) reader connected to a single circularly polarized patch antenna, with a gain of 6 dBi at the frequency range of 800-1000 MHz.The RFID reader is connected to the polarized patch antenna via 1.8 m of 50 coaxial cable model CNT-195-FR. Hence, the total transmitted power was approximately 4W EIRP (effective isotropic radiated power). The whole system is controlled by a homemade software installed in a computer to plot the measured activation power and read range. The distance between the polarized patch antenna and the RFID tag antenna in this setup, which are aligned in parallel is 1m to meet far field requirement.

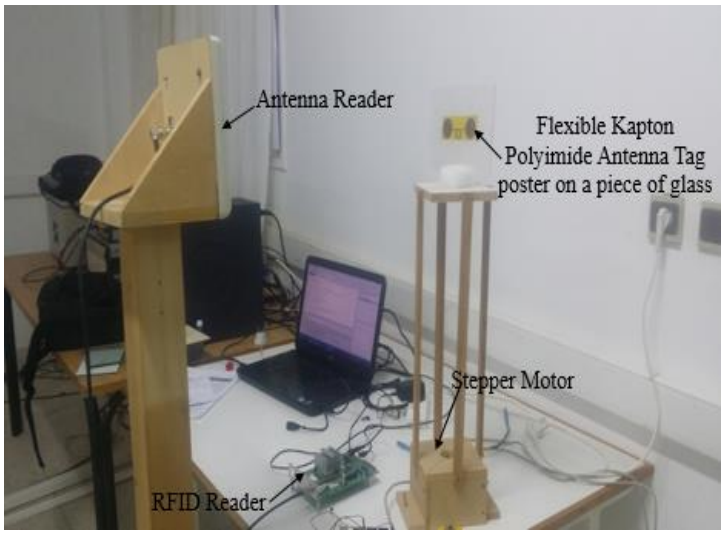

Figure 84: Measured Setup Read Range of the Proposed RFID Tag Antenna in Ordinary Room

The Figure 84 represents the measured setup of the read range when the RFID tag antenna is placed on a glass piece of dimension $20 \times 20\ mm^2$. The RFID tag antenna has a read range more than 4.8 m across the whole band allowed for RFID technology (860-960 MHz). In addition, (Figure 85) shows that the best activation power of -7.5 dBm can be achieved near to 915 MHz. It is worthwhile to mention that the proposed structure can demonstrate farther read ranges on different objects because the RFID chip used in this paper has $P_{\text{th}} = -8$ dBm and this value is certainly very high if compared to other RFID chips like NXP G2XL, and Alien Higgs. For example, if an NXP G2XL IC chip with $P_{\text{th}} = -17$ dBm is used to design this RFID tag antenna, the calculated read range would be more than 12 m in free space.

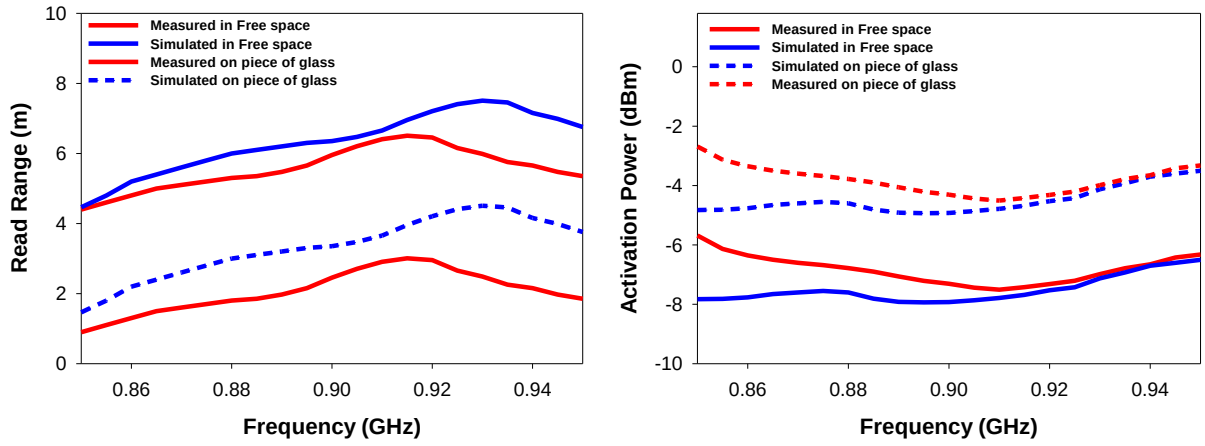

Figure 85: Read Range and Activation Power of the Proposed RFID Tag Antenna as a Function of Frequency in Free Space and on Piece of Glass

5.4.2 Read Range Patterns Measurement

We have also measured the read range patterns in free space on a foam curved (with a dielectric constant ≈ 1) of the proposed design for the two planes at 868 and 915 MHz respectively. The obtained results are plotted in (Figure 86) (Figure 87).. We can see that the read range pattern is similar for both frequencies. In the (y-z) plane (Horizontal position), a maximum read range of 8 m in the 30° direction at 915 MHz and 7.5 m at 868 MHz is measured. As can be seen clearly in (x-y) plane (Vertical position), a maximum read range of 7.5 m at 915 MHz and 7m at 868 MHz, with a good unidirectional read range pattern is obtained.

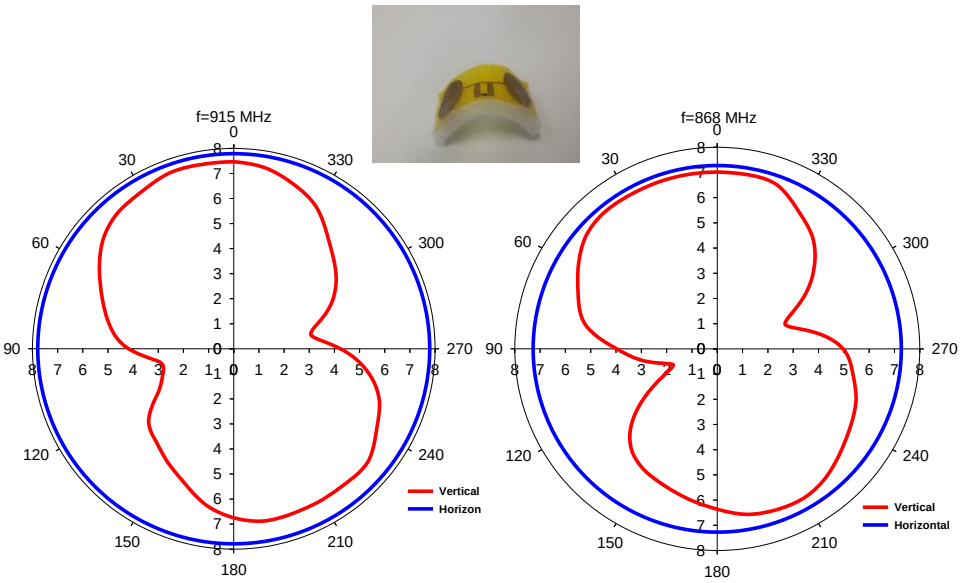

(a) (b)

Figure 86: Measured Read Range Patterns of the Proposed RFID Tag: (a) 915 MHz, (b) 868 MHz in Free Space on a Foam Curved.

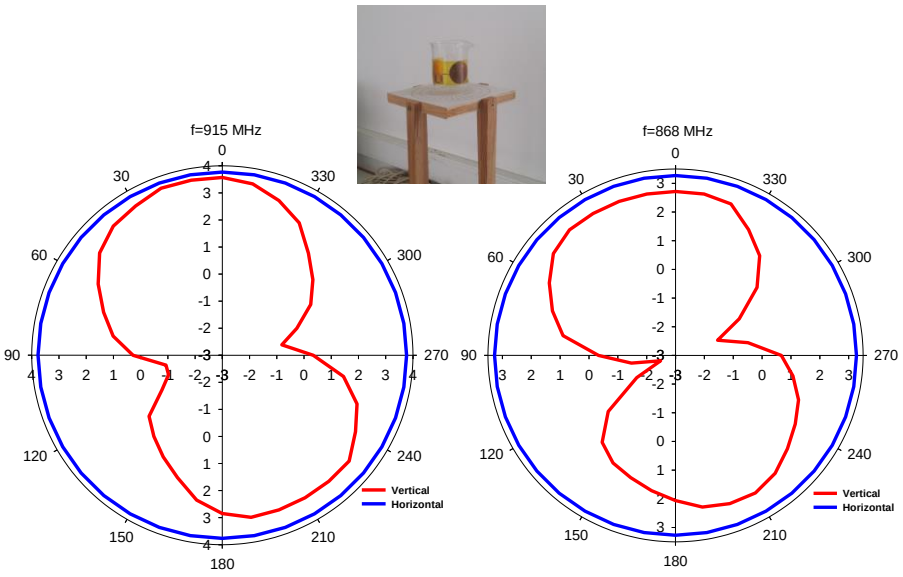

(a) (b)

Figure 87: Measured Read Range Patterns of the Proposed RFID Tag: (A) 915 MHz, (B) 868 MHz on a Glass Beaker Empty.

5.5 RFID Tag Sensor Application

5.5.1. Preparation Solution and Results

In this part, we studied the RFID tag antenna numerically and experimentally in the previous paragraph as sensor to detect both ionic (Sodium Chloride) and nonionic (Sucrose) concentrations. The experimental set-up used in this work to measure the concentration of both aqueous solutions is described in (Figure 88). It consists of an RFID reader, a glass beaker filled with the liquid solution under test, on which we pasted an RFID tag antenna. The RFID Reader and the RFID tag antenna are positioned in line of sight disposition and are positioned at 0.3 m away from each other.

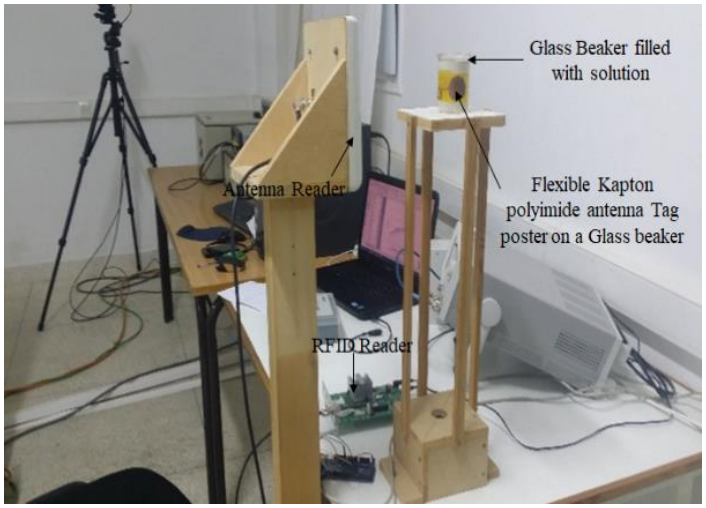

Figure 88: Photograph of the Experimental Set-Up for The Measurements of The Concentration of Aqueous Solutions

5.5.2 Concentration Sensing of Nacl and Sucros Solution

For validation purposes, we have prepared two aqueous solutions separately. The first one is made of distilled water and sodium chloride (NaCl). The second solution investigated in this work is made of distilled water and sucrose (C12H22O11). For the experiment, NaCl and sucrose are dissolved individually in

water to prepare concentrations ranging from 0 to 80% with a step of 20%. For each concentration, the sensitivity of the RFID tag antenna is measured by stepped increasing Ptx until successfully reading the RFID tag. It is worthwhile to mention that all the measurements are performed in an ordinary room equipped with an air conditioner temperature that has been set to 28 degrees Celsius.

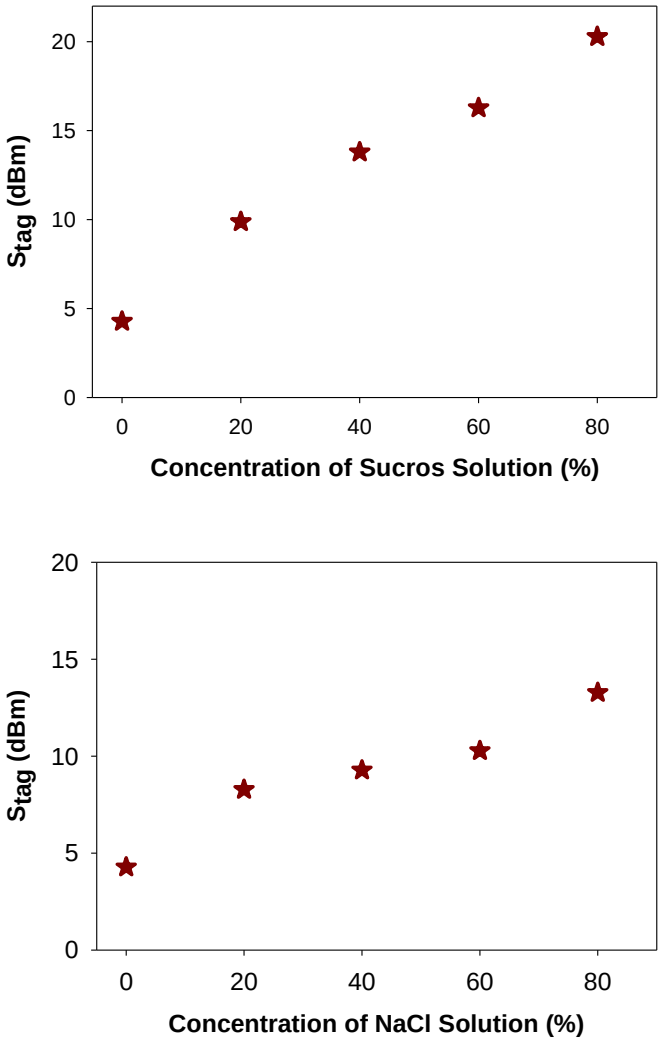

Figure 89: Sensitivity of the RFID Tag Antenna Variation with the Different Percentage of the Sucrose Solution at 915 MHz

From (Figure 89) and (Figure 90), the sensitivity of the RFID tag antenna increases with the increase in the percentages of NaCl and sucrose in water. Furthermore, we have measured the sensitivity of the RFID tag at 864, 868, 915 and 926 MHz, respectively, with the same concentrations of the NaCl and Sucrose solutions. The obtained results are presented in (Figure 18) and (Figure 19), respectively. The obtained results show that for all frequencies the sensitivity of the RFID tag increases as the frequency increases. It is found that the best performance of the RFID sensor corresponds to an operating frequency of 864 MHz that ensures the highest sensitivity of the proposed RFID sensor with a change of S_{tag} (6.72 /20%) and (9.25/20%) for 864MHz and 926MHz, repectively.The enhancement of the sensitivity of the RFID sensor is about 37%. Hence, the sensor is more likely to detect small concentration variations at the lower bound of the RFID-UHF band.

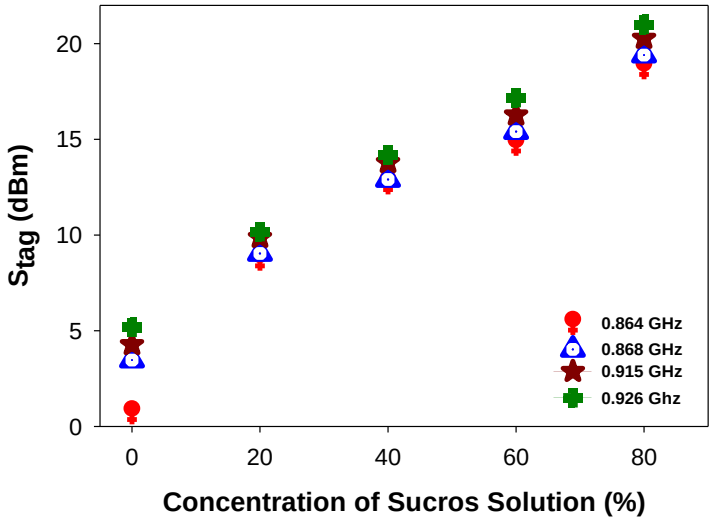

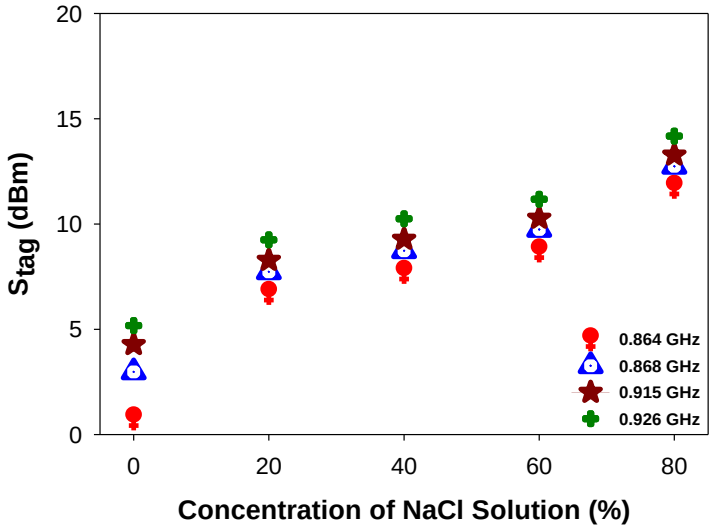

Figure 90: Sensitivity of the RFID Tag Antenna Variation with The Different Percentage of the Nacl Solution as the Different Frequencies.

5.5.2.1 Small Concentration Sensing of Nacl and Sucros Solution

In this section, we have checked the fiability of the proposed method to detect small concentration of NaCl and Sugar solutions. Therfor we have measured the sensitivity of those solutions with the concentration of 5 % at different frequencies. The obtained results depicted in (Figure 91). For the sodium chloride (NaCl) solution can be obiened to 2.5 dBm at 868 MHz and 4.1 dBm at 915MHz, and 0.6 dBm at 886MHz and 3.2dBm for the sucrose solution.

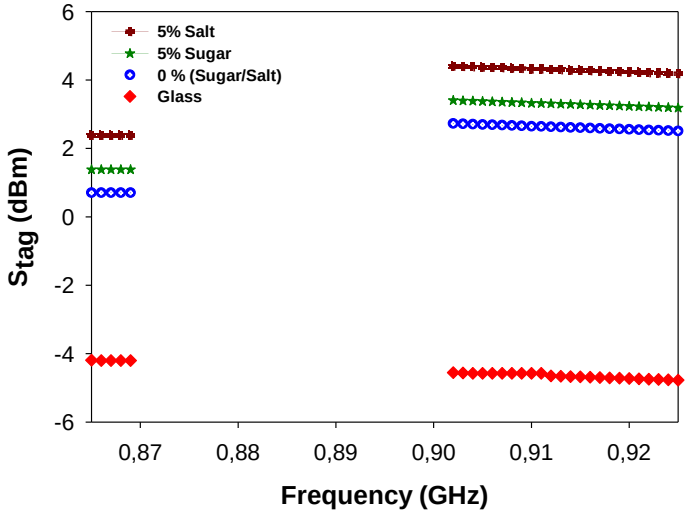

Figure 91: Sensitivity of The RFID Tag Sensor Variation as Small Percentage of the Nacl and Sugar Solution as the Different Frequencies.

5.5.3 Concentration Sensing of Alcohol Solution

Some industrial drinks depend on an important percentage of industrial Alcohol; this greatly affects human health [101]. Now, there are no effective ways to determine the concentration of alcohol in aqueous solutions and industrial drinks. In this part, we mainly focuse on detecting the concentration of Alcohol in liquid solutions. We used the RFID system to authentication of the sensitivity variation of this proposed tag sensor. From (Figure 92) one can see that the sensitivity of the RFID tag antenna increases with the increase in the percentages of Alcohol in water. Furthermore, we have measured the sensitivity of the RFID tag at 864, 868, 915 and 922 MHz, respectively, with the same concentrations of the alcohol solutions. The obtained results are presented in (Figure 93), respectively. The obtained results show that for all frequencies the sensitivity of the RFID tag increases as the frequency increases. It is found that the best performance of the RFID sensor corresponds to an operating frequency of 868 MHz that ensures the highest sensitivity of the proposed

RFID sensor with a change of Stag (20 /40%) and (6/20%) for 864 MHz and 926MHz,repectively.

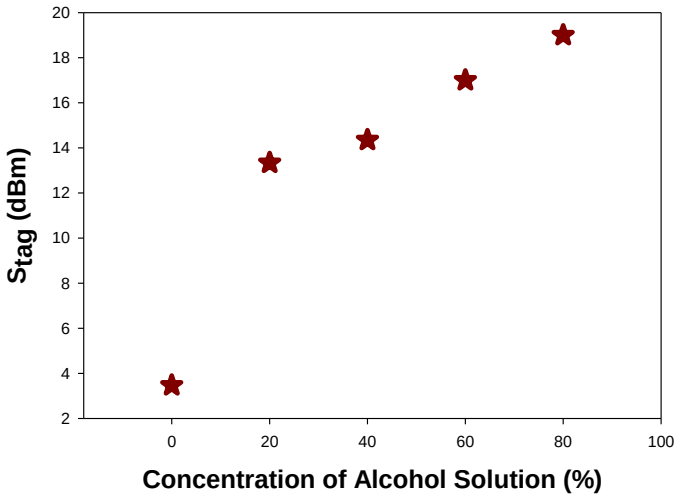

Figure 92: Sensitivity of RFID Tag Sensor Variation with Different Percentages of Alcohol Solution at 915 MHz

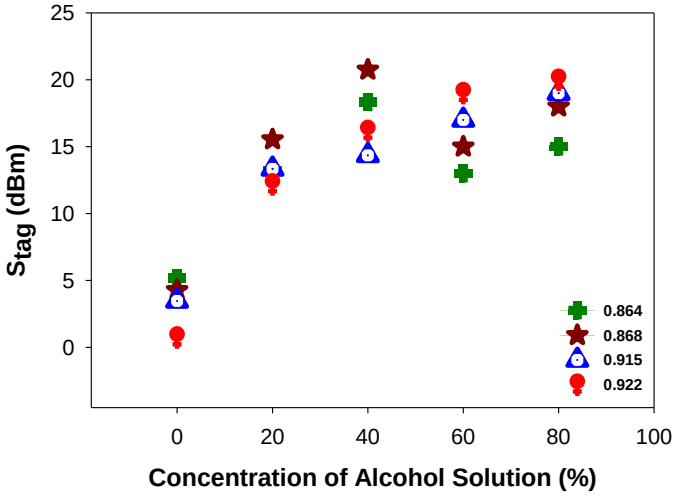

Figure 93: Sensitivity of The RFID Tag Sensor Variation with Different Percentages of Alcohole Solution as the Different Frequencies

5.6 Conclusion

In this chapter, we show the capability of RFID-UHF technology to detect the concentration of aqueous solutions such as NaCl and sucrose solutions. The proposed low cost flexible RFID tag sensor has a whole size of 100 × 20 mm2 and an read range of 5.8 m in free space. The tag sensor sensitivity has been measured and analyzed when there are changes in the concentrations of NaCl and sucrose in deionized water. The obtained results show that for all frequencies within the RFID-UHF band, the Stag increases with the increment in percentages of NaCl and sucrose concentrations in water. This behavior can be explained by the change in the dielectric constant. Furthermore, the experimental results show that the tag sensitivity is more likely to detect small variations in liquid concentration at the lower bound of the RFID-UHF band. The proposed technique has many features such as rapid measurements and lower cost.

General Conclusion and Future Directions

Nowadays there has been a growing interest in RFID technology, owing to its vast range of applications including security identification, retail item management, inventory, access control and tracking. An imperative element of this technology are the RFID tag antennas, which are the components that can besides tracking are sensitive to any change in their environment which allow to collect valuable data with low cost. Therefore, the correct design of those RFID tag antennas for different applications are crucial.

On that note, the research work developed during this thesis focused on the design and realization of UHF passive RFID tag antennas, which allowed us to deal with several aspects of RFID technology application. The main performances of these RFID-UHF tag antennas were evaluated numerically by using electromagnetic simulation and experimentally by using automated measurement platform developed in our laboratory.

All of the proposed RFID tag antennas presented in this thesis offer a low profile with acceptable performances, which are comparable to the most significant published works in the literature during the last decade. In addition to proposing new prototypes in this thesis, analysis and studies that was not covered in the literature before was conducted, including analysis of the effect of the background material of the proposed designs which make them suitable for different practical applications.

In the last part of this thesis, we have extend the field of application of this technology that until now has been limited to tracking information and identifying objects in different supply chains by designing a new low-cost flexible RFID tag antenna with sensing capability. This type of device was validated for the detection of molecules concentration such as sucrose, Alcohol and NaCl in deionized water.

In this thesis, we have also managed to develop a low-cost automated RFID tag antenna measurement set-up based on UHF-RFID reader for UHF tags evaluation. The developed kit uses a commercial multi-programmable UHF RFID reader and a computer developer environment (interface) that allow us to measure all the performances of the RFID tag antenna such as sensitivity, read-range, radiation pattern, read pattern.

Finally, the author believes that the current thesis has met all of the proposed goals and gave a small contribution to the world of RFID technology. The RFID tag antenna is the primordial element and represent the heart of this rapidly developing technology, and thus must be developed with precision to allow a good communication with the reader.

Future Research Directions

This thesis has provided some new configurations of RFID tag antennas. As a simpler project, those designs can be further optimized using new generations of the IC chips such as NXP or Higgs with low P_{th} to increase their reading range. Also, regarding the RFID tag antenna with sensing capability, which is now one of the hot topics in the last decade, it can be further studied in order to measure the permittivity as a function of the frequency (from 860 to 960 MHz) of the NaCl and sucrose in aqueous liquid.

With the fast growth of Internet of Things (IoT), this system can be easily integrated into mobile phones technologies/apps to monitor the measured data in real time.

Finally, and for more ambitious works, the proposed designs can be matched to other IC chips such as SL 900A or EM3425 chips that allow adding more sensors. There is no doubt an exciting future is waiting for this technology.

PhD. Publications

International Journals

1. **M.A. Ennasar**, M.kanjaa, O El Mrabet, M,Essaaidi "Design and Characterization of a broadband flexible polyimide antenna UHF RFID Tag Sensor for detection the concentration of salt and sugar contents in water "'Progress In Electromagnetics Research c", Vol. 94 , pp. 273-283,2019

2. **M.A. Ennasar**, I Aznabet, O El Mrabet, M,Essaaidi ''Advanced Electromagnetics journal", 2018 "Design and Characterization of a Compact Single Layer Modified S-Shaped Tag Antenna for UHF-RFID Application

3. M. El Khamlichi ,A.Alvarez Melcon ,O.El Mrabet, **M.A. Ennasar**, j.Hinojosa," Flexible UHF RFID Tag for Blood Tubes Monitoring" Journals Sensors ,Volume 19, Issue 22 10.3390/s19224903-2019 MDPI

4. I Aznabet, **M.A. Ennasar**, O El Mrabet, G Andia-Vera, M Khalladi, S Tedjni '' Progress In Electromagnetics Research C", 2017 A Broadband Modified T-Shaped Planar Dipole Antenna for UHF RFID Tag Applications P 137-144

International Conferences

1. **M.A. Ennasar** ,O. EL Mrabet, I. Aznabet, M.kanjaa, M.Khalladi, S,Tedjini, M.Essaaidi "18 th Mediterranean Microwave Symposium, October 31 to 2 November , 2018, Istanbul, turkey " subtopic" concentration measurement of aqueues liquid based on the RFID-UHF Technology; IEEE Explorer

2. L.Moutis, **M.A. Ennasar,** I. Aznabet, O. EL Mrabet, A. Farksi " International Conference on Multimedia Computing and Systems (ICMCS) , May 10-12 , 2018, Rabat, Morocco," A Low Cost Automated RFID Tag Antenna Measurement Set-Up Based On UHF-RFID Reader". IEEE Explorer

3. A,Abattoy, **M.A. Ennasar**, M,Douieb, O. EL Mrabet" International Conference on Multimedia Computing and Systems (ICMCS) , May 10-12 , 2018, Rabat, Morocco,"Desing of a low cost meander line RFID tag antenna using 3D printing Technology". IEEE Explorer

4. M.El Khamlichi, **M.A. Ennasar**,O. EL Mrabet " International Conference on Multimedia Computing and Systems (ICMCS) , May 10-12 , 2018, Rabat, Morocco," T-shaped Tag antenna for UHF RFID Applications ".IEEE Explorer

5. M.El Bakkali, **M.A. Ennasar**,O. EL Mrabet " International Conference on Multimedia Computing and Systems (ICMCS) , May 10-12 , 2018, Rabat, Morocco," Single-Layer UHF RFID Tag Antenna with Multi-functional Characteristics". IEEE Explorer

6. **M.A. Ennasar**, I. Aznabet, O. EL Mrabet, M. Essaaidi " International Conference on Computing wirless and communication Systems (ICCWCS), November 15-16, 2016,Settat , Morocco, " S shaped RFID UHF Tag Antenna with differents matching techniques"

7. **M.A. Ennasar,** I. Aznabet, O. EL Mrabet, M. Essaaidi " International Conference on Multimedia Computing and Systems (ICMCS) , 29 September to 1 October, 2016, Marrakesh, Morocco," A UHF RFID tag antenna with improved bandwidth". IEEE Explorer

8. I Aznabet, **M .A.Ennasar**, O El Mrabet, S Tedjini, M Khalladi" International Conference on Multimedia Computing and Systems (ICMCS) , 29 September to 1 October, 2016, Marrakesh, Morocco," Meander-line UHF RFID tag antenna loaded with split ring rersonator". IEEE Explorer

9. **M.A. Ennasar**, I. Aznabet, O. EL Mrabet, M. Essaaidi "5th Mediterranean Microwave Symposiun, November 30 to 2 December , 2015, Lecce, Italy " subtopic" A Compact modified S-Shaped RFID tag antenna for metallic applications '.IEEE Explorer

10. **M.A. Ennasar**, I. Aznabet, O. EL Mrabet, M. Aznabet, H. Berbia, S. Tedjini, and M. Essaaidi accepted for ieee conferences "4th Mediterranean Microwave Symposiun, December 12-14 2014, Marrakesh, Morocco" subtopic" A New Modified S-Shaped Compact Antenna for RFID-UHF Tag Applications '.

Patents

1. 2019: **Ennasar Mohammed Ali,** Essaaidi Mohammed, Otman El Mrabet ." Capteur RFID UHF-Tag-Flexible pour les Mesures des Concentrations de Sucre et de Sel dans les Solutions aqueuses (Deposit Date 25/03/2019)

2. 2018: **Ennasar Mohammed Ali**, Essaaidi Mohammed, "Antenne pour les puces d'identification Radiofréquence UHF, RFID UHF tag operant dans les environnement métalliques" .N° de publication MA39655 A1, IC international H01Q 1/8

Bibliography

[1] Finkenzeller, K., RFID Handbook, 2nd ed., New York: John Wiley & Sons, 2003.

[2] Banks, J., et al., RFID Applied, New York: John Wiley & Sons, 2007.

[3] Wikipedia, "Barcode," http://en.wikipedia.org/wiki/Barcode.[Accessed: 27-Mai-2019].

[4] Wikipedia, Magnetic Stripe Cardhttp://en.wikipedia.org/wiki/Magnetic_stripe_card. .[Accessed: 27-Mai-2019].

[5] Wikipedia, "Smart Cards," http://en.wikipedia.org/wiki/Smart_card. .[Accessed:27 Mai-2019].

[6] Landt, J., "The History of RFID," IEEE Potentials, November 2005, pp. 8–11.

[7] H. Tafekirt, A. Bouajaj, and M. R. Britel, "A Sensitive Triple-Band Rectifier for Energy Harvesting Applications," *IEEE Access*, vol. PP, p. 1, 2020, doi: 10.1109/ACCESS.2020.2986797.

[8] V. D. Hunt, A. Puglia, and M. Puglia, *RFID-A Guide to Radio Frequency Identification*. 2006.

[9] The History of RFID Technology, RFID Journal, 2005, http://www.rfidjournal.com/article/articleview/1338/1/129

[10] I. Korkmaz, C. Atay, and G. Kyparisis, "A mobile patient monitoring system using RFID," Int. Conf. Comput. - Proc., vol. 1, no. May, pp.726–732, 2010.

[11] E. Perret, Radio Frequency Identification and Sensors: From RFID to Chipless RFID, vol. 9781848217. 2014.

[12] T. Deleruyelle, P. Pannier, M. Egels and E. Bergeret, "An RFID Tag Antenna Tolerant to Mounting on Materials," in IEEE Antennas and Propagation Magazine, vol. 52, no. 4, pp. 14-19, Aug. 2010.

[13] V. D. Hunt, A. Puglia, and M. Puglia, RFID-A Guide to Radio Frequency Identification. 2006.

[14] J. T. Yee and S.-C. Oh, Technology Integration to Business. 2013.

[15] C. A. C. Erick C. Jones, RFID in Logistics: A Practical Introduction. 2008.

[16] D. M. Dobkin, *The RF in RFID Passive UHF RFID in Practice*. 2004.

[17] Landt, "The history of RFID," IEEE Potentials, vol. 24, no. 4, pp. 8–11, 2005.

[18] H. Stockman, "Communication by Means of Reflected Power," *Proc. IRE*, vol. 36, no.10, pp. 1196–1204, 1948.

[19] S.-H. Jeong and H.-W. Son,'UHF RFID tag antenna for embedded use in a concrete floor' IEEE Antennas Wireless Propag. Lett. vol. 10, 2011 pp. 1158–1161.

[20] RFID Forecasts, Players and Opportunities 2017-2027: IDTechEx." [Online]. Available: https://www.idtechex.com/research/reports/rfid-forecasts-players andopportunities-2017-2027-000546.asp. [Accessed: 25-Mai-2019].

[21] "Fonctionnement d'un système RFID." [Online]. Available: http://www.centrenationalrfid.com/fonctionnement-dun-systeme-rfid-article-17-fr-ruid 17.html. [Accessed: 25-Mai-2019].

[22] M. Schubler, C. Damm, M. Maasch, R. Jakoby, "Performance Evaluation of LeftHanded Delay Lines for RFID Backscatter Applications", IEEE MTT-S International Microwave Symposium (IMS2008), Atlanta, 15-20 June 2008.

[23] S. Hu, C. L. Law, W. Dou, "Measurements of UWB Antennas Backscattering Characteristics for RFID Systems", ICUWB 2007. IEEE International Conference on Ultra-Wideband, Singapore, 24-26 September 2007.

[24] Banks, J, et al., RFID Applied, New York: John Wiley & Sons, 2007.

[25] S.-H. Jeong and H.-W. Son,'UHF RFID tag antenna for embedded use in a concrete floor' IEEE Antennas Wireless Propag. Lett. vol. 10, , 2011 pp. 1158–1161

[26] R. Gonçalves, R. Magueta, P. Pinho and N. B. Carvalho, "RFID passive tag antenna for cork bottle stopper," IEEE Antennas and Propagation Society International Symposium (APSURSI), Memphis, TN, 2014, pp. 1518 - 1519,2014

[27] R. Colella, L. Catarinucci, P. Coppola, and L. Tarricone ‘‘Measurement Platform for Electromagnetic Characterization and Performance Evaluation of UHF RFID Tags’’,IEEE Trans Antennas Propag 65 (2016), 905-914

[28] Marrocco, G., L. Mattioni, and C. Calabrese, “Multiport sensor RFIDs for wireless passive sensing of objects — Basic theory and early results,” IEEE Transactions on Antennas and Propagation, Vol. 56, No. 8, 2691–2702, Aug. 2008.

[29] X. Qing, C. K. Goh and Z. N. Chen, "Impedance Characterization of RFID Tag Antennas and Application in Tag Co Design," in IEEE Transactions on Microwave Theory and Techniques, vol. 57, no. 5, pp. 1268 - 1274, May 2009

[30] L. Ukkonen, Ang Yu, L. Sydanheimo, Fan Yang, M. Kivikoski and A. Elsherbeni, ‘Analysis of bow tie array RFID tag antenna for paper reel identification systems,’ 2007 IEEE Antennas and Propagation SocietyInternational Symposium, Honolulu, HI, 2007, pp. 2745- 2748.

[31] H.-W. Son,’UHF RFID tag antenna for embedded use in a concrete floor’ IEEE Antennas Wireless Propag. Lett. vol. 10, , 2011 pp. 1158 – 1161.

[32] UHF Gen-2 System Overview,” Texas Instruments, September 2005, http://rfidusa.com/superstore/pdf/UHF_System_Overview.pdf.

[31] Interface Bus, NRZ Encodinghttp://www.interfacebus.com/NRZ_Definition.html. [Accessed: 25-Mai-2019].

[32] Banks, J., et al., RFID Applied, New York: John Wiley & Sons, 2007.

[33] Balanis, C., Antenna Theory, Analysis and Design, 3rd ed., New York: John Wiley & Sons, 2005.

[33] Balanis, C., Antenna Theory, Analysis and Design, 3rd ed., New York: John Wiley & Sons, 2005.

[34] Rida, A., et al., “Conductive Inkjet-Printed Antennas on Flexible Low-Cost Paper-Based Substrates for RFID and WSN Applications,” IEEE Antennas and Propagation Magazine, Vol. 51, No. 3, June 2009, pp. 13–23.

[35] « GS1 - Bienvenue chez GS1 France ». [En ligne]. Disponible sur:https://www.gs1.fr/.[Accessed: 25-Mai-2019].

[36] K. Finkenzeller, « RFID Handbook: Fundamentals and Applications in Contactless Smart Cards, Radio Frequency Identification and Near-Field Communication, Third Edition »,
p. 480.

[37] S Mukherjee, "Chipless radio frequency identifi cation by remote measurement of complex impedance", Proc. 10th European Conference on Wireless Technology, pp: 249–252, Munich, Germany, Oct. 2007.

[38] D. M. Dobkin, The RF in RFID Passive UHF RFID in Practice. 2004.

[39] H. Chu, B. An, F. Wu, Y. Wu, "RFID Tag Packaging with Anisotropically Conductive Adhesive, Electronic Packaging Technology", 7th International Conference on Electronic Packaging Technology, Shanghai, 26-29 August 2006.

[40] A. Ahson and M. Ilyas, RFID Handbook Aplications, Technology, Security, andPrivacy. 2008.

[41] A. Ahson and M. Ilyas, RFID Handbook Aplications, Technology, Security, andPrivacy. 2008.

[42] J. P. Curty, N. Joehl, C. Dehollain, and M. J. Declercq, "Remotely powered addressable UHF RFID integrated system," IEEE J. Solid-State Circuits, vol. 40, no.
11, pp. 2193–2202, 2005.

[43] R. K. Mod, "Mod ´ elisation comportementale en VHDL-AMS du lien RF pour lasimulation et l ' optimisation des syst ` emes RFID UHF et micro-ondes Rami KhouriTo cite this version :," 2009.

[44] Der Biometrie-Pass kommt - c't 13/2005 direkt im heise shop." [Online]. Available:https://shop.heise.de/katalog/der-biometrie-pass-kommt. [Accessed:25-Mai-2019].

[45] G. Fritz, "Simulation de fautes pour l'évaluation du test en ligne de systèmes RFID," p.158, 2012.

[46] O. Picon, Les Antennes: Théorie, Conception et Applications. 2009.

[47] A. Marzuki, "Advances in RFID Components Design: Integrated Circuits," Dev. Implement. RFID Technol., no. February, pp. 180–199, 2009.

[48] A. Vena, “Contribution au développement de la technologie RFID sans puce à haute capacité de codage,” 2012.

[49] B. Constantine A., Antenna Theory Analysis and Design Third Edition. 2005.

[50] D. M. Dobkin, The RF in RFID Passive UHF RFID in Practice. 2004.

[51] K. Finkenzelle, "RFID Handbook: Fundamentals and Applications in Contactless Smart Cards and Identification", John Wiley & Sons, Second Edition, 2003.

[52] P. Hauet, "L’Identification par Radiofréquence (RFID) Techniques et Perspectives", article invité, REE No.10, Novembre 2006.

[53] Landt, J., “Shrouds of Time—The History of RFID,” AIM Inc., ver. 1.0. October 2001.

[54] The History of RFID Technology,” RFID Journal, 2005,http://www.rfidjournal.com/article/articleview/1338/1/129. [Accessed: 25-Mai-2019].

[54] J. P. Curty, N. Joehl, C. Dehollain, and M. J. Declercq, “Remotely powered addressable UHF RFID integrated system,” IEEE J. Solid-State Circuits, vol. 40, no. 11, pp. 2193–2202, 2005.

[56] Baldwin, H., “How to Handle RFID’s Real-World Challenges,” Microsoft Corporation, 2006, http://www.microsoft.com/midsizebusiness/businessvalue/rfidchallenges.mspx. [Accessed: 25-Mai-2019].

[57] M. C. Caccami, C. Miozzi, M. Y. S. Mulla, C. D. Natale, et G. Marrocco, « An epidermal graphene oxide-based RFID sensor for the wireless analysis of human breath », in 2017 IEEE International Conference on RFID Technology Application (RFIDTA), 2017, p. 191- 195.

[58] Gao, Antenna-based passive UHF RFID sensor tags Design and application. Sundsvall: Mid Sweden University, 2013.

[59] « Decathlon Sees Sales Rise and Shrinkage Drop, Aided by RFID – 2015 12-07 - Page-RFIDJournal».[Enligne]. www.rfidjournal.com/articles/view?13815. [Accessed: 25-Mai-2019].

[61] « ASICS › Productivity Engineering ». [Accessed: 25-Mai-2019].

[62] « Magnus® S Product Family », RFMicron. [Accessed: 25-Mai-2019].

[63] «EM4325 /EMMicroelectronic». http://www.emmicroelectronic.com/products/rf-identification security/epc-and-uhfics/em4325. [Accessed: 25-Mai-2019].

[64] « EPC sensor tag and data logger IC - ams SL900A - ams ». https://ams.com/sl900a

[65] S. Amendola, G. Bovesecchi, A. Palombi, P. Coppa and G. Marrocco, "Design, Calibration and Experimentation of an Epidermal RFID Sensor for Remote Temperature Monitoring," in *IEEE Sensors Journal*, vol. 16, no. 19, pp. 7250-7257, Oct.1, 2016.

[66] S. Milici, S. Amendola, A. Bianco, et G. Marrocco, « Epidermal RFID passive sensor for body temperature measurements », in 2014 IEEE RFID Technology and Applications Conference (RFID-TA), 2014, p. 140- 144.

[67] Nadeen R. Rishani, Raed M. Shubair, Ghadah Aldabbagh, "On the design of wearable and epidermal antennas for emerging medical applications", Sensors Networks Smart and Emerging Technologies (SENSET) 2017, pp. 1-4, 2017

[68] X. Chen, L. Ukkonen, et T. Björninen, « Passive E-Textile UHF RFID Based Wireless Strain Sensors With Integrated References », IEEE Sens. J., vol. 16, n o 22, p. 7835- 7836, nov. 2016.

[69] S. Caizzone, C. Occhiuzzi, et G. Marrocco, « Multi-Chip RFID Antenna Integrating Shape-Memory Alloys for Detection of Thermal Thresholds », IEEE Trans. Antennas Propag., vol. 59, 7, p. 2488- 2494, juill. 2011

[70] D. Shuaib, L. Ukkonen, J. Virkki, et S. Merilampi, « The possibilities of embroidered passive UHF RFID textile tags as wearable moisture sensors », in 2017 IEEE 5th International Conference on Serious Games and Applications for Health (SeGAH), 2017,p. 1- 5.

[71] E. Sipilä, J. Virkki, L. Sydänheimo, et L. Ukkonen, « Experimental Study on BrushPainted Passive RFID-Based Humidity Sensors Embedded into Plywood Structures », Int. J. Antennas Propag., vol. 2016, p. 1- 8, janv. 2016.

[72] K. E. Belsey et al., « Switchable disposable passive RFID vapour sensors from inkjet printed electronic components integrated with PDMS as a stimulus responsive material », J. Mater. Chem. C, vol. 5.2015

[73] Q. Qiao, L. Zhang, F. Yang, Z. Yue, et A. Z. Elsherbeni, « Reconfigurable Sensing Antenna With Novel HDPE-BST Material for Temperature Monitoring », IEEE Antennas Wirel. Propag. Lett., vol. 12, p. 1420- 1423, 2013.

[74] Q. Qiao, L. Zhang, F. Yang, Z. Yue, et A. Z. Elsherbeni, « Reconfigurable Sensing Antenna With Novel HDPE-BST Material for Temperature Monitoring », IEEE Antennas Wirel. Propag. Lett., vol. 12, p. 1420- 1423, 2013.

[75]] S. Merilampi, H. He, L. Sydänheimo, L. Ukkonen, et J. Virkki, « The possibilities of passive UHF RFID textile tags as comfortable wearable sweat rate sensors », in 2016 Progress in Electromagnetic Research Symposium (PIERS), 2016, p. 3984- 3987.

[76] C. Occhiuzzi, A. Ajovalasit, M. A. Sabatino, C. Dispenza, et G. Marrocco, « RFID epidermal sensor including hydrogel membranes for wound monitoring and healing », n 2015 IEEE International Conference on RFID (RFID), 2015, p. 182- 188.

[77] Yassin Belaizi. Etude et conception d'un capteur-RFID passif en bande UHF : application à l'agroalimentaire. Electronique. Université Montpellier, 2018. Français. ⟨NNT : 2018MONTS061⟩. ⟨tel-02134586⟩

[78] G. A. Vera, A. Abdelnour, M. Sarkis, A. Georgiadis, D. Kaddour, et S. Tedjini, « Passive RFID-enabled proximity sensor », in 2016 IEEE MTT-S International Microwave Symposium (IMS), 2016, p. 1- 3.

[79] R. V. Aroca, A. C. Hernandes, D. V. Magalhães, M. Becker, C. M. P. Vaz, et A. G. Calbo, « Application of Standard EPC/GEN2 UHF RFID Tags as Soil Moisture Sensors », Proceedings, vol. 1, n2, p. 10, nov. 2016.

[80] S. Sajal, Y. Atanasov, B. D. Braaten, V. Marinov, et O. Swenson, « A low cost flexiblepassive UHF RFID tag for sensing moisture based on antenna polarization », in IEEE International Conference on Electro/Information Technology, 2014, p. 542- 545

[81] M. Akbari, J. Virkki, L. Sydänheimo, et L. Ukkonen, « The possibilities of graphenebased passive RFID tags in high humidity conditions », in 2016 IEEE International Symposium on Antennas and Propagation (APSURSI), 2016, p. 1269- 1270.

[82] J. S. Lee, J. Oh, J. Jun, et J. Jang, « Wireless Hydrogen Smart Sensor Based on Pt/Graphene-Immobilized Radio-Frequency Identification Tag », ACS Nano, vol. 9, n8, p. 7783- 7790, août 2015 .

[83] R. Gonçalves *et al*., "RFID-Based Wireless Passive Sensors Utilizing Cork Materials," in *IEEE Sensors Journal*, vol. 15, no. 12, pp. 7242-7251, Dec. 2015.

[84] D. Paret, RFID at Ultra and Super High Frequencies: Theory and Application. 2009.

[85] ThingMagicM6eRFIDM6eguide[online].Available: http://www.dpie.com/manuals/rfid/M6eHardwareGuide_Sept13.pdf. [Accessed: 25-Mai-2019].

[86] Riccardo Colella; Luca Catarinucci; Paolo Coppola; Luciano Tarricone Measurement Platform for Electromagnetic. Characterization and Performance Evaluation of UHF RFID Tags .IEEE Transactions on Instrumentation and Measurement.

[87] M. Daiki, H. Chaabane, E. Perret, S. Tedjni, T. Aguili, "RFID Chip Impedance Measurement for UHF Tag Design, " Progress in Electromagnetics Research Symposium (PIERS'11), Mar 2011, pp.679, 2011.

[88] http://www.murata.com/~/media/webrenewal/support/library/catalog/products/k70e.ashx [Accessed: 25-Mai-2019].

[89] D. B. Miron, Small Antenna Design, Burlington, MA, USA: Newnes, 2006

[90] F. E. Terman, Radio Engineer's Handbook. New York: McGraw -Hill, 1945

[91]] C. Liang, L. Li, and H. Zhai, "Variational stability form for the capacitance of an arbitrarily shaped conducting plate," Chinese J. Electron., vol. 13, no. 4, pp. 714–718,2004.

[92] X. Qing, C. K. Goh and Z. N. Chen, "Impedance Characterization of RFID Tag Antennas and Application in Tag Co Design," in IEEE Transactions on Microwave Theory and Techniques, vol. 57, no. 5, pp. 1268 - 1274, May 2009

[93] C. Cho, H. Choo and I. Park, "Broadband RFID tag antenna with quasi - isotropic radiation pattern," in Electronics Letters, vol. 41, no. 20, pp. 1091 - 1092, 29 Sept. 200

[94] K. She, Y. He, B. Li, Z. Hou, Y. Zhu and L. Zuo, "Theory and Measurement of Delta RCS for RFID Tag on Various Materials," *2010 6th International Conference on Wireless Communications Networking and Mobile Computing (WiCOM)*, Chengdu, 2010, pp. 1-4.

[95] Bhattacharyya, R., C. Floerkemeier, and S. Sarma, "Low-cost, ubiquitous RFID-tag-antenna-based sensing," Proceedings of the IEEE, Vol. 98, No. 9, 1593–1600, Sep. 2010.

[96] Buchner, R., G. T. Hefter, and P. M. May, "Dielectric relaxation of aqueous NaCl solutions," J. Phys. Chem. A, Vol. 103, 1–9, 1999.

[97] Malmberg, C. G. and A. A. Maryott, "Dielectric constants of aqueous solutions of dextrose and sucrose," Journal of Research of the National Bureau of Standards, Vol. 45, No. 4, Oct. 1950.

[98] http://www.triumphlaser.com/laser-cutting-system/ [Accessed: 25-Mai-2019].

[99] Qing, X., C. K. Goh, and Z. N. Chen, "Impedance characterization of RFID tag antennas and application in tag co design," IEEE Transactions on Microwave Theory and Techniques, Vol. 57, No. 5, 1268–1274, May 2009.

[100] M. A. Ennasar, O. El Mrabet, K. Mohamed, and M. Essaaidi, "Design and Characterization of a Broadband Flexible Polyimide RFID Tag Sensor for NaCl and Sugar Detection," Progress In Electromagnetics Research C, Vol. 94, 273-283, 2019.

[101] "Health risks and benefits of alcohol consumption." Alcohol research & health : the journal of the National Institute on Alcohol Abuse and Alcoholism vol. 24,1 (2000): 5-11